

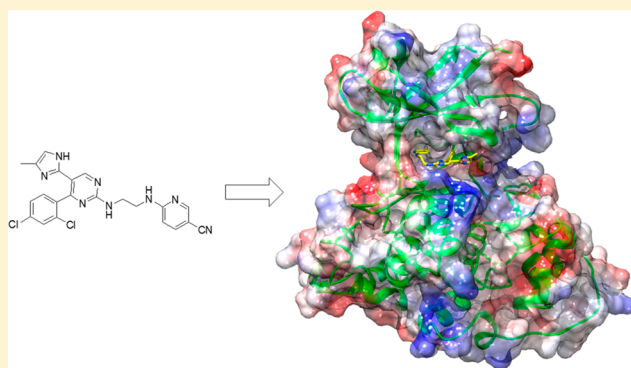
Synthesis, Binding Mode, and Antihyperglycemic Activity of Potent and Selective (5-Imidazol-2-yl-4-phenylpyrimidin-2-yl)[2-(2-pyridylamino)ethyl]amine Inhibitors of Glycogen Synthase Kinase 3

Allan S. Wagman,^{†,‡} Rustum S. Boyce,^{†,§} Sean P. Brown,^{†,||} Eric Fang, Dane Goff,^{†,⊥} Johanna M. Jansen, Vincent P. Le,^{†,#} Barry H. Levine,^{†,▽} Simon C. Ng,^{†,○} Zhi-Jie Ni,^{†,◆} John M. Nuss,^{†,¶} Keith B. Pfister, Savithri Ramurthy,^{||} Paul A. Renhowe,^{†,□} David B. Ring,^{†,●} Wei Shu, Sharadha Subramanian, Xiaohui A. Zhou, Cynthia M. Shafer, Stephen D. Harrison,^{†,◇} Kirk W. Johnson,^{†,■} and Dirksen E. Bussiere^{*||}

Global Discovery Chemistry, Novartis Institutes for BioMedical Research, 5300 Chiron Way, Emeryville, California 94608, United States

Supporting Information

ABSTRACT: In an effort to identify new antidiabetic agents, we have discovered a novel family of (5-imidazol-2-yl-4-phenylpyrimidin-2-yl)[2-(2-pyridylamino)ethyl]amine analogues which are inhibitors of human glycogen synthase kinase 3 (GSK3). We developed efficient synthetic routes to explore a wide variety of substitution patterns and convergently access a diverse array of analogues. Compound 1 (CHIR-911, CT-99021, or CHIR-73911) emerged from an exploration of heterocycles at the C-5 position, phenyl groups at C-4, and a variety of differently substituted linker and aminopyridine moieties attached at the C-2 position. These compounds exhibited GSK3 IC₅₀s in the low nanomolar range and excellent selectivity. They activate glycogen synthase in insulin receptor-expressing CHO-IR cells and primary rat hepatocytes. Evaluation of lead compounds 1 and 2 (CHIR-611 or CT-98014) in rodent models of type 2 diabetes revealed that single oral doses lowered hyperglycemia within 60 min, enhanced insulin-stimulated glucose transport, and improved glucose disposal without increasing insulin levels.



■ INTRODUCTION

The incidence of noninsulin-dependent diabetes mellitus (NIDDM) or type II diabetes mellitus (T2DM) is growing rapidly worldwide. It is estimated that NIDDM will be one of the leading causes of mortality and morbidity over next 25 years. In 2015, the International Diabetes Foundation (IDF) reports that there were 415 million diagnosed cases of diabetes worldwide. The IDF estimates that by 2040 the number of diagnosed cases will have risen to 642 million.¹ Currently, there are more than 44.3 million diabetics in North America and the Caribbean and 59.8 million diabetics in Europe.¹ Several factors have emerged which contribute to the spread of type II diabetes or impaired glucose tolerance (IGT), including an increasingly technological society, high calorie diets rich in fats and carbohydrates, and an ever more sedentary lifestyle. Increasingly, physicians have become aware of the health risks associated with diabetes, and health advocacy organizations are championing the education of the medical community and the public to the dangers of obesity and IGT. Stricter guidelines for monitoring and control of blood glucose levels, and a new

lower standard for normal fasting plasma glucose levels have helped to identify type II diabetics more readily.

Spurring the shift in the diagnosis and treatment of type II diabetes was the landmark United Kingdom Prospective Diabetes Study (UKPDS). This long-term study of multiple risk factors and treatment programs clearly showed that rigorous control of circulating blood glucose levels and hypertension significantly reduced the incidence and severity of related complications such as macrovascular disease, neuropathy, nephropathy, retinopathy, and cataract.² As the disease inevitably progresses, the task of managing blood glucose levels becomes increasingly difficult. Oral agents such as sulfonylureas, metformin, and thiazolidinediones in combination with exercise and diet can help control diabetes as measured by the amount of circulating glycosylated hemoglobin (HbA1c), but there are still 30–40% of patients who do not respond to such therapy. The UKPDS showed that

Received: June 27, 2017

combination therapies of insulin and one or more oral medications gave the best assurance of maintaining HbA1c levels near the target of 7% and gave an increased quality of life.³ There is an obvious need for new and better antihyperglycemic agents, especially those which target the underlying metabolic dysfunctions which progressively advance the disease. By treating the cellular targets responsible for insulin resistance, insufficient glucose disposal or inadequate β -cell function, new therapeutics may be developed that reliably reduce both morbidity and mortality. Because the typical type II diabetic patient is typically over 55 years old, they are likely to be treated for cardiovascular or other health problems and will need chronic treatment, so new hypoglycemic medications must be safe and compatible with a host of supplementary medications.^{4–6}

Insulin signaling controls blood glucose by increasing glucose uptake and expanding its storage as glycogen in muscle and liver. NIDDM, or its precursor state impaired glucose tolerance (IGT), is initially signified by higher than normal circulating levels of plasma insulin and glucose. Insulin secretion increases to overcome the emergent insulin resistance in the peripheral tissues. While the underlying cause or causes of cellular insulin resistance may be heterogeneous through the diabetic population, a pharmaceutical which increases the rate of glycogen synthesis should result in lower circulating blood glucose levels and thereby reduce the burden on pancreatic beta cells. Regulatory control of glycogen synthase (GS), the final enzyme in glycogen biosynthesis, is an obvious system to explore for antihyperglycemic control. GS is considered to be the rate-limiting enzyme for glycogen deposition in skeletal muscle and is responsible for building glycogen stores in the liver. GS activity in resting cells is maintained at minimal levels through phosphorylation and inactivation by the protein kinase GSK3.^{7,8} Constitutively active in resting cells, GSK3 is inhibited by insulin signaling through its phosphorylation by protein kinase B (PKB, also called AKT). Thus, in response to insulin, GSK3 is inhibited, allowing GS to be dephosphorylated and activated, which in turn increases the rate of glycogen synthesis. In diabetic muscle, GS activity is decreased and GSK3 expression is increased compared to normoglycemic muscle, suggesting a potential role for GSK3 in the etiology of insulin resistance.^{9–11} GSK3 has also been implicated in the negative regulation of glucose uptake into the cells of peripheral tissue. GSK3 has been found to phosphorylate insulin receptor substrate-1 (IRS-1) on serine residues which have been observed to block some insulin signaling events.^{12,13} It is unclear whether GSK3's activity toward IRS-1 is part of the pathology of diabetes or part of the complex insulin signaling cascade.^{14,15} Together, these observations suggest that inhibition of GSK3 might have a more profound effect on glucostasis than merely increasing the rate of glycogen synthesis. GSK3 inhibitors may act as insulin sensitizing drugs which could improve glucose disposal, suppress hepatic glucose output, and increase glucose transport in an insulin-sparing manner.¹⁶

Since its discovery in the early 1980s, GSK3's role in glucose control and various disease states has been extensively studied.^{17–26} However, the details of the signaling pathway linking insulin to GSK3 and GS activity were not fully understood until the mid-1990s. As a negative regulator among the kinases involved in insulin signaling, GSK3 is an attractive target for small-molecule drug therapy. Inhibition of this unique kinase has a direct effect on GS activation and on improving

glucose disposal into glycogen. As a kinase, GSK3 presents a well-defined starting point for the project using ATP-competitive kinase inhibitors as molecular tools to understand GSK3's role in cellular biology and for a structure-based design approach utilizing X-ray crystallography. We recognized that developing highly selective inhibitors would be a primary challenge for this project, particularly for the management of diabetes where chronic treatment would be required.

At the time this study was undertaken, natural products and known ATP-competitive kinase inhibitors were available that had activity against GSK3 but none were highly selective. For example, the indirubin dye indirubin-3'-monoxime and kenpauillone inhibit GSK3- β at ~ 200 nM IC₅₀s but are also active against LCK and CDK2/cyclin A among other kinases.^{27,28} Historically, lithium had been used to probe the biochemistry of GSK3. Unfortunately, lithium's potency (~ 2 mM IC₅₀) against GSK3 is relatively low and lithium also inhibits several other kinases such as CK2, which phosphorylates GS as a prerequisite for GSK3 activity.²⁹ Lithium also affects the levels of inositol phosphates through inhibition of inositol monophosphate phosphomonoesterases which could affect insulin signaling. Because the effects of lithium might not be due to direct inhibition of GSK3, the role of GSK3 in insulin resistance and glucose disposal would have to be confirmed once we had selective and potent compounds. Our approach was to utilize structure-guided drug design to produce novel kinase inhibitor structures which would likely have different kinase selectivity profiles compared to known GSK3 inhibitors and would distinguish our work from other programs in the field.^{30–32} To definitively answer questions about GSK3's role in diabetes and potential for side effects related to GSK3's other regulatory roles, we set our goal for potency against GSK3 in the low nM IC₅₀s and better than 500-fold selectivity against any other kinase in a broad screening panel which included closely related kinases such as CDC2 and ERK2. Exploiting our ability to quickly produce small focused libraries with known ATP-competitive kinase binding motifs,^{33–36} we identified the initial dihydropyrimidine **9c** and pyrimidine **11d** hits (Scheme 1), which led to our first generation lead series exemplified by the advanced preclinical compound **1** (also known as CHIR-911, CT-99021 or CHIR-73911^{16,37}) and by compound **2** (CHIR-611 or CT-98014^{16,37}) in Figure 1.

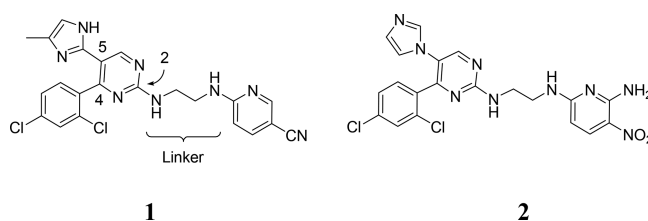
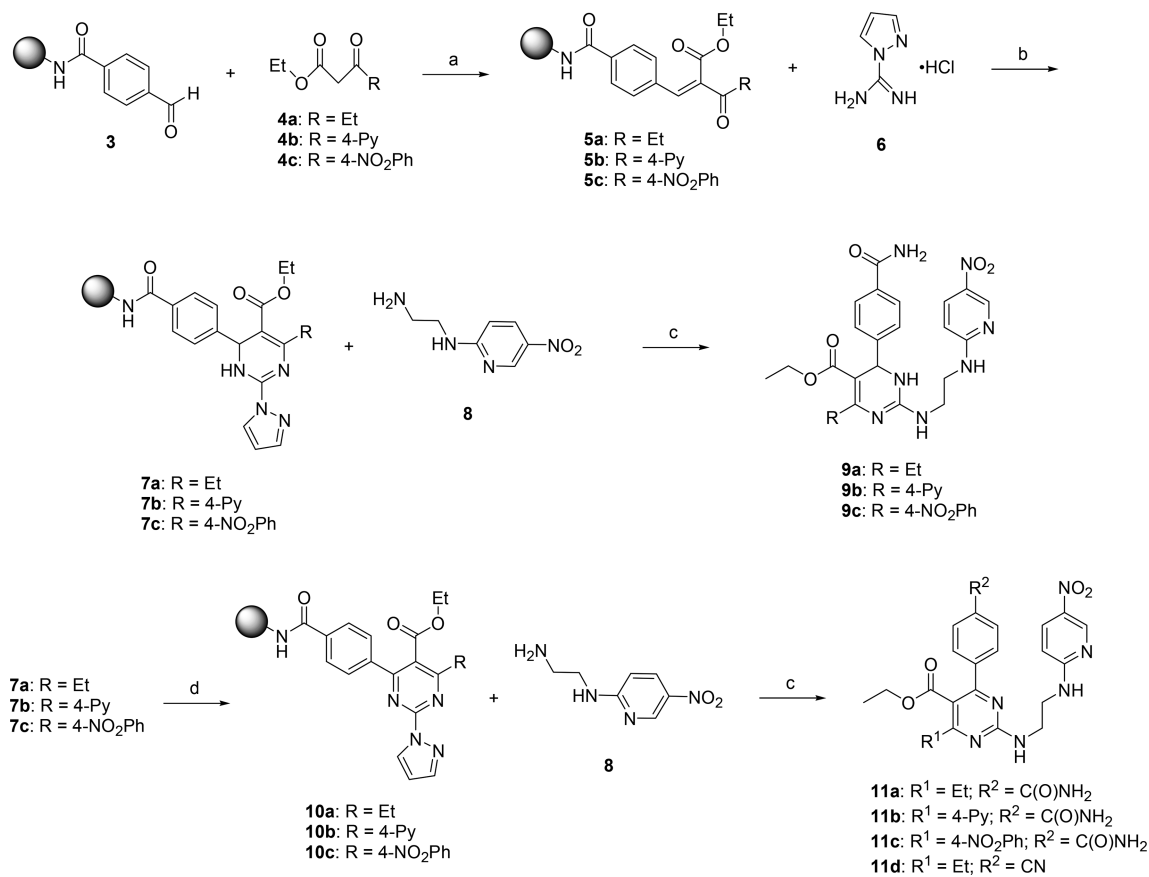


Figure 1. Potent and selective GSK3 inhibitors with oral antihyperglycemic efficacy.

RESULTS

Chemistry. GSK3 inhibitor activity was initially identified by screening small combinatorial libraries based on drug-like core scaffolds with moderate to low molecular weight and dense functionality. Libraries of novel pyrimidines and dihydropyrimidines were constructed by following the sequence shown in Scheme 1 which was derived from previous work used to produce dihydropyrimidine calcium channel

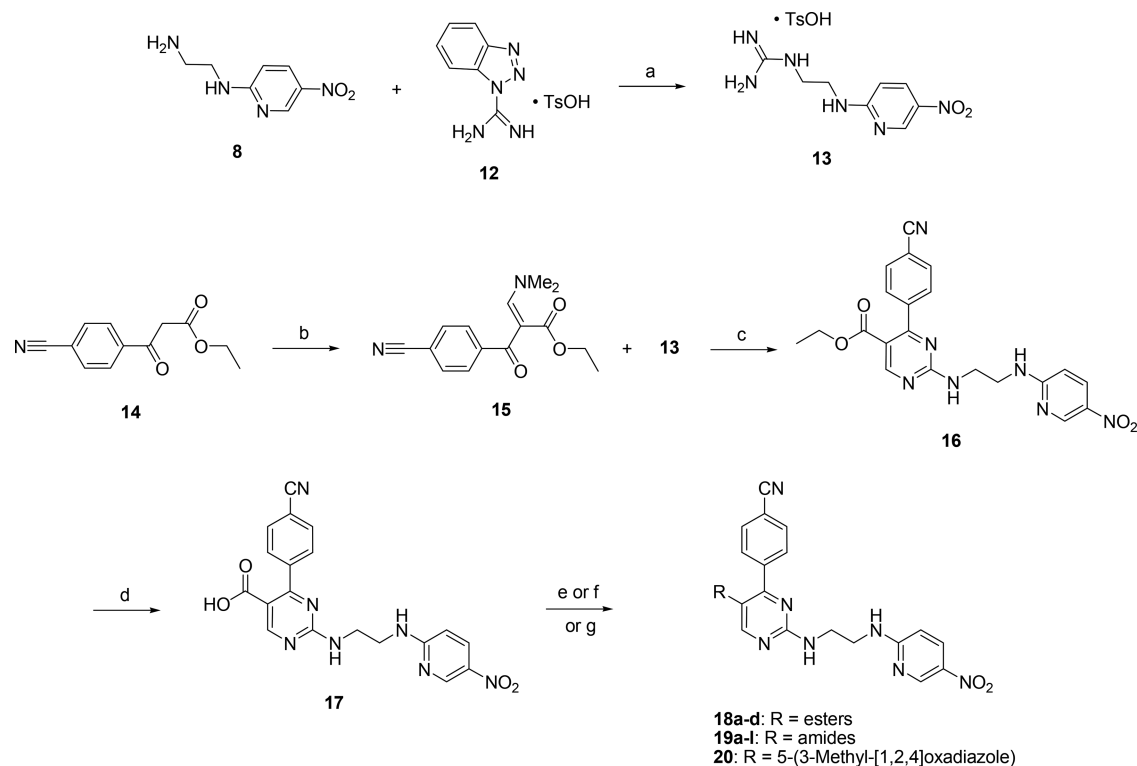
Scheme 1. Synthesis of 9a–c and 11a–d (See Also Table 1)^a

^aReagents and conditions: (a) piperidine, EtOH, dioxane, 25 °C, 20 h; (b) NaHCO₃, NMP, 70 °C, 24 h; (c) (i) AcOH, NMP, 80 °C, (ii) TFA, CH₂Cl₂; (d) DDQ, THF, 25 °C, 30 min.

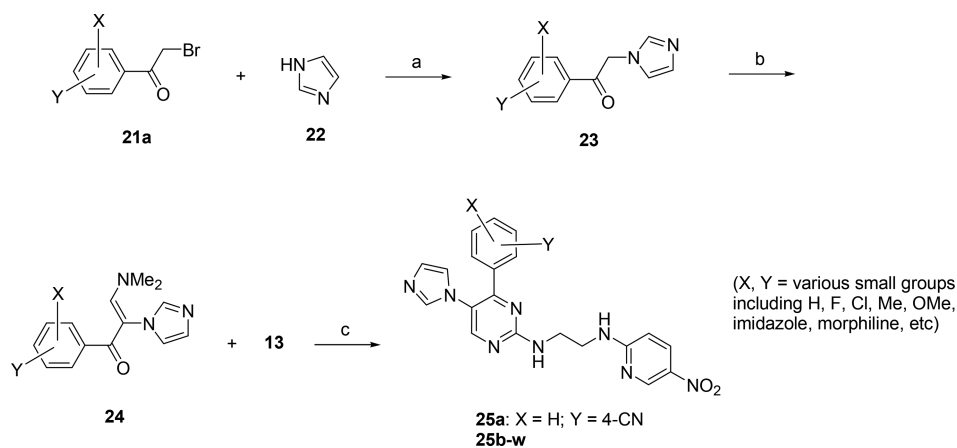
blockers.³⁸ The synthetic scheme incorporated the maximum chemical diversity around the pyrimidine core using simple, easily accessible starting materials as reagents in large excess to drive resin-bound reactions to completion in high purity as described in our previous work.³⁹ Split-and-mix techniques were employed to give focused libraries consisting of 80 pools, with each pool being comprised of a diverse mixture of 18 compounds. Diversity could be introduced into the libraries by varying the substitution of the Rink resin bound aldehyde **3** or the β -ketoester **4** used in the Knoevenagel condensation to yield α -keto substituted cinnamates **5a–c**. Cyclization of the vinyl ketone in **5a–c** with pyrazole carboxamide HCl gave dihydropyrimidines **7a–c** upon neutralization of the HCl salt with solid powdered sodium bicarbonate and dehydration in NMP at 70 °C over 24 h. The pyrazole of **7a–c** could be displaced with a diverse set of primary or secondary amines under mildly acidic conditions at 70 °C over 24–48 h to give a final pool of 18 compounds. Alternately, the resin bound pyrazole of **7a–c** could be substituted with a single amine such as the ethylene diamine **8** to give single dihydropyrimidines **9a–c** after TFA catalyzed cleavage from the solid support. Dihydropyrimidines **7** and **9** slowly aromatize upon exposure to air, leading to some contamination of **9** with the aromatic analogues **11** under normal synthetic conditions. Pure aminopyrimidine library pools or single compounds **11** were easily accessed through DDQ oxidation of dihydropyrimidines **7** which were subsequently elaborated into the final products following the same procedures for amine displacement and

TFA cleavage. Also detected in the final product pools and single compounds made on solid support were the corresponding cyano analogues which presumably formed from the primary amides on the C-4 arene under the anhydrous conditions cleavage conditions catalyzed by TFA and upon standing in dry stock DMSO solutions with residual TFA. Thus, compound **11d**, which was an attractive GSK3 inhibitor hit, was slowly produced from compound **11a** during storage in DMSO (see Table 1 for IC₅₀ activity).

The synthetic scheme had to be modified to produce the desired aminopyrimidines cleanly and with minimal work up using traditional solution phase chemistry. A convergent scheme which brought together the elements of a guanidine and enamineone to give the desired aminopyrimidines gave the quickest access to diversity around the pyrimidine core and was easily scalable to produce gram quantities of material (Scheme 2). Thus, a substituted ethylene diamine **8** was reacted with a guanidylating agent, such as benzotriazole carboxamidinium 4-methylbenzenesulfonate (**12**), to yield a functionalized guanidine salt of interest **13** which could be made in quantity and stored under anhydrous conditions. While many β -ketoesters were available, they could be made on large scale or with a variety of substituted arenes from the appropriate benzoyl chloride and potassium ethyl malonate. The β -ketoester **14** was converted to an enamineone **15** by heating with *N,N*-dimethylformamide dimethyl acetal (DMFDMA). The resulting dimethylamino enamineones, upon evaporation, could be used directly in the subsequent pyrimidine forming

Scheme 2. Synthesis of 16, 17, 18a–d, 19a–l, and 20 (See Also Table 2)^a

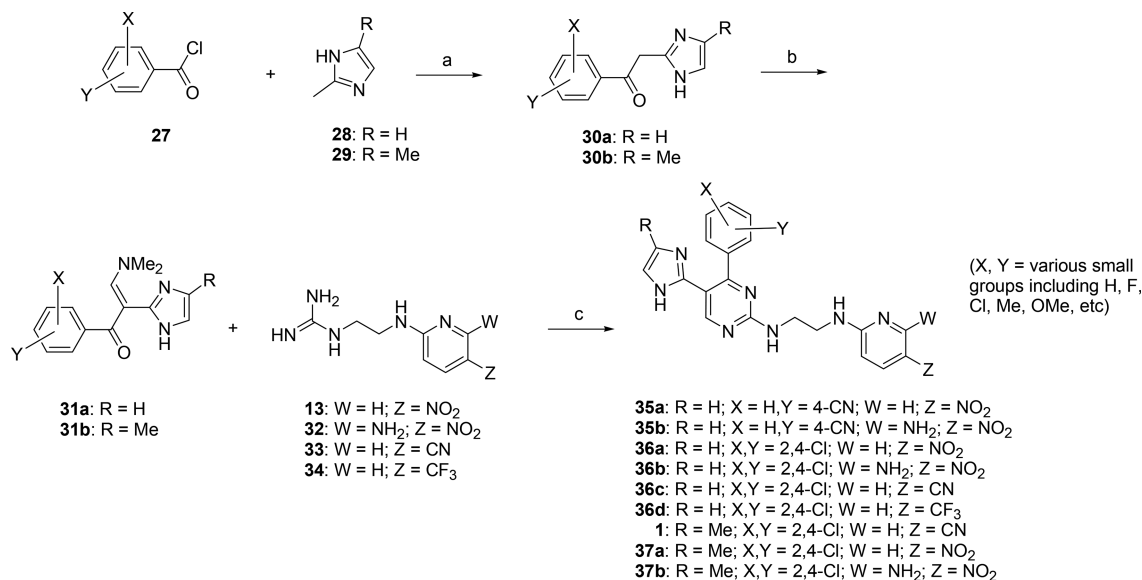
^aReagents and conditions: (a) DIEA, ACN, 25 °C, 12 h; (b) DMFDMA, THF, AcOH, 80 °C, 3 h; (c) EtOH (dry), NaOEt, 80 °C, 12 h; (d) MeOH/H₂O (1:1), NaOH, 65 °C, 45 min; (e) HBTU, various alcohols (ROH), DIEA, DMA, 25 °C; (f) HBTU, various amines (R₂NH), DMA, 25 °C; (g) (i) isobutyl chloroformate, TEA, THF, 25 °C, 12 h, (ii) MeC(NO₂)NH₂, 70 °C, 6 h.

Scheme 3. Synthesis of 25a–w, 26 (See Also Tables 2 and 3)^a

^aReagents and conditions: (a) toluene 75 °C 2.5 h; (b) DMFDMA, reflux, 12 h; (c) Cs₂CO₃, THF or DMF, 80 °C, 8 h.

reactions without further purification. Concentrated solutions of enaminones 15 and guanidine 13 were cyclized into aminopyrimidines, such as 16, with a slight excess of fresh sodium ethoxide and heat. The reactions were sluggish at temperatures below 70 °C, and some reactions would not reach completion after 1–2 h. Upon the basis of speculation that water was retarding the rate of reaction, excess absolute EtOH was added and distilled from the reaction to force it to completion. Reactions typically gave C-5 ester products 16 in high yield and purity. Precipitating the products from organic solvent such as ACN provided 16 in >95% purity. For further elaboration, the ethyl ester of 17 was saponified in a MeOH/

water mixture to solubilize the starting material. Upon heating with NaOH, the reaction was complete as soon as the turbid mixture became clear. From the free acid 17, esters 18a–d and amides 19a–l were produced in high yield using standard peptide coupling conditions with the activating agent *O*-benzotriazole-*N,N,N',N'*-tetramethyluronium-hexafluoro-phosphate (HBTU). The carboxylic acid could also be exploited to make C-5 carbon linked heterocycles. For example, the oxadiazole 20 was fashioned from the acid 17 by coupling acetamidoximine via the mixed anhydride.⁴⁰ The oxadiazole formation did not provide 20 cleanly but was obtained after careful reverse phase preparative HPLC purification.

Scheme 4. Synthesis of 1, 35a,b, 36a–d, and 37a–c (See Also Tables 2,7, and 8)^a

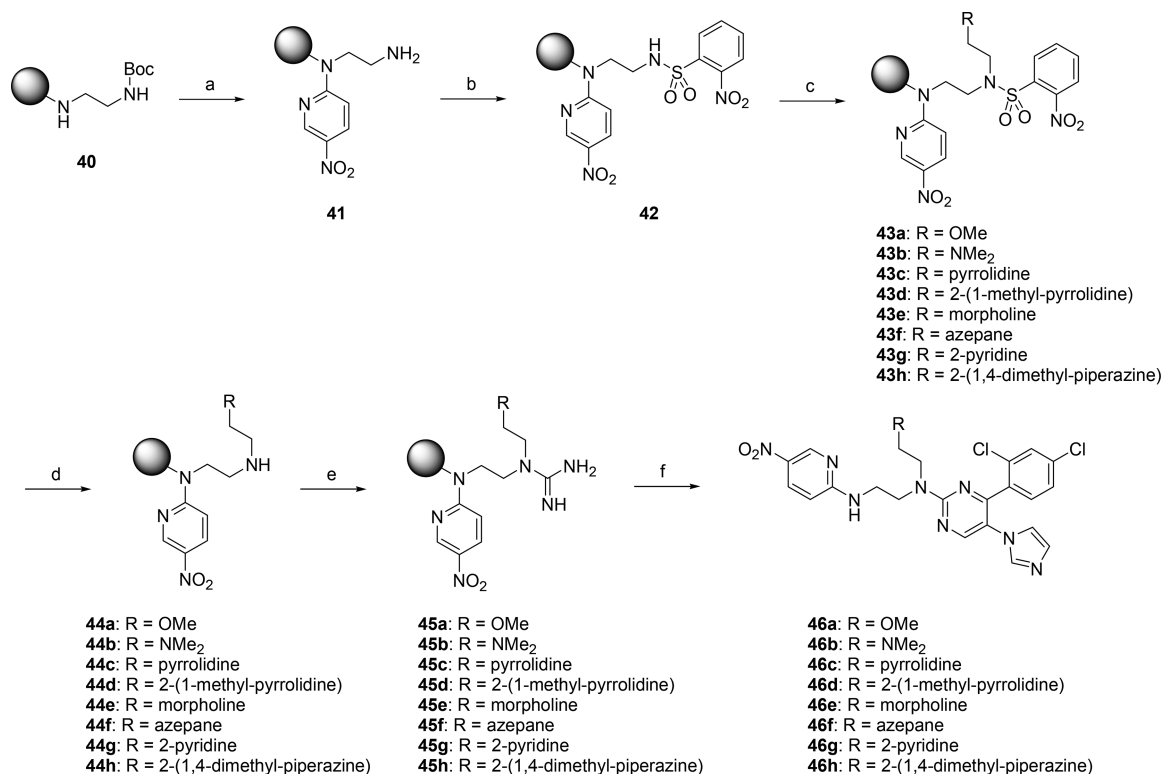
^aReagents and conditions: (a) (i) Hünig's base, CH₂Cl₂, rt to reflux, 3.5 h, (ii) HCl/AcOH; (b) DMFDMA, reflux, 12 h; (c) NaOEt, EtOH, 80 °C, 2.5 h.

Unlike compounds with a carbon at C-5, nitrogen-linked heterocycles at C-5 were typically installed at the acetophenone stage of the synthesis as shown in Scheme 3. A wide array of nucleophilic heterocycles, such as substituted imidazoles, pyrazoles, or triazoles, could be reacted with the appropriate bromo- or chloroacetophenone to eventually provide the products 25a–w and 26 shown in Tables 2 and 3. In a variation of procedures described, a chloro- or bromoacetophenone 21a was added to a toluene solution containing excess nucleophile, such as imidazole (22), followed by heating at 75 °C for 2–3 h to give the substituted acetophenone 23 in high yield and purity.⁴¹ These were typically used without further purification. However, if the acetophenone 23 was obtained as a sticky solid or glass, it could be stirred and manipulated under dry ether or hexanes to produce a free-flowing solid. The powders of acetophenone 23 could be stored for several months under dry conditions at room temperature but did eventually decompose to polymeric side products. After exploring several conditions, we found that the enaminones 24 could be formed cleanly by heating the acetophenones 23 in neat DMFDMA as a solvent for a few hours. After heating for between 3 and 12 h, the excess DMFDMA was stripped away under reduced pressure and the crude enaminones 24 could be used directly in the pyrimidine annulation. The synthesis of aminopyrimidines 25 was optimized by replacing strong bases, such as NaOEt, with cesium carbonate and using THF, DMF, DMA, or NMP as the solvent. If the aminopyrimidines 25 precipitated from the crude mixture upon cooling, the products could be obtained directly from the reactions in high purity. For those compounds requiring purification, silica gel chromatography or recrystallization from EtOAc/hexanes or ethanol/water was carried out.

While attempting to install a carbon-linked imidazole at the C-5 position of the pyrimidine, we met with limited success modifying a C-5 acid or aldehyde into a 2-imidazole. Following the example in Scheme 3, we instead formed the carbon-linked imidazole at the acetophenone step of the synthesis utilizing procedures which react excess benzoyl chloride with a 2-

methylimidazole (Scheme 4).^{42–44} The enaminones 31a,b were formed in neat DMFDMA. It was found that heating at 70–75 °C for 2–3 h was sufficient to convert the acetophenone 30a,b into the products 31a,b. Pyrimidine formation to give 1, 35c, 36b, and 37a using the carbon-linked imidazoles 31a,b was optimized under the earlier conditions of EtOH and NaOEt. The purity and yields of the reactions were greatly enhanced by adding the enaminones 31a,b dissolved in dry EtOH to a preheated mixture of NaOEt and guanidines (13, 32–34) in EtOH at 75–80 °C. The reaction was typically complete within 2–3 h. The rate of reaction could be enhanced further by adding activated powdered 4 Å molecular sieves to the reaction. The reaction was followed by HPLC and worked up as soon as the reaction reached >95% completion based on conversion of 31a,b. Heating longer or using excess base caused side products to form. The products 1, 35a–c, 36a–d, 37a,b, 61a–u, and 62a–g were all made by similar procedures to form the aminopyrimidine core (Tables 2, 7, and 8). The most detailed experimental procedures included are for the synthesis of 1 and 36a–c. For some C-linked imidazole products, such as 62c, the appropriate 2-methylimidazole was synthesized from acetaldehyde, ammonia, and a properly adorned glyoxal or glyoxal equivalent. For example, 2-methyl-4(5)-isopropylimidazole used to make 62c was made from 1-acetoxy-3-methyl-2-butanone and acetaldehyde under conditions of cupric acetate, KOH, and NH₄OH as described.⁴⁵ Other imidazoles were made from 1,2-dicarbonyl compounds reacted with acetaldehyde and ammonia or ammonium hydroxide.⁴⁶

The imidazole (28,29) first reacts with benzoyl chloride on the ring nitrogens, which allows the methyl at C-2 to attack an equivalent of benzoyl chloride. The product of 2-methylimidazole reacting with 3 equiv of benzoyl chloride is an enol benzoate of the desired acetophenone. Thus, as in the synthesis of 30a, the crude intermediate must be hydrolyzed using a mixture of AcOH and concentrated HCl to obtain the carbon-linked acetophenone 30a or 30b. Only the methyl at the 2-position of the imidazole appears to react with the benzoyl chloride. Thus, 2,4-dimethylimidazole 29 used in the synthesis

Scheme 5. Synthesis of 46a–h (Table 4)^a

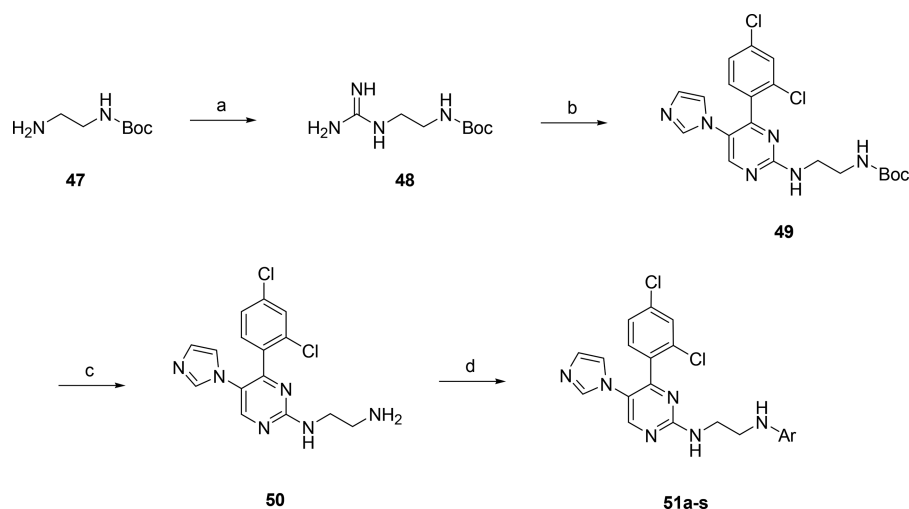
^aReagents and conditions: (a) (i) 2-chloro-5-nitropyridine, DIEA, NMP, 120 °C, 12 h, (ii) TMSOTf, 2,6-lutidine, CH₂Cl₂, 23 °C, 3 h; (b) 2-nitrobenzenesulfonyl chloride, DIEA, CH₂Cl₂, 23 °C, 6 h; (c) RCH₂OH, Ph₃P, DIAD, CH₂Cl₂, 23 °C, 12 h; (d) PhSH, K₂CO₃ (powder), water, DMF, 23 °C, 12 h; (e) 1H-pyrazole-1-carboxamide hydrochloride, DIEA, NMP, 90 °C, 18 h; (f) (i) 1-(2,4-dichlorophenyl)-3-(dimethylamino)-2-imidazolylprop-2-en-1-one (**24**), MTBD, NMP, 120 °C, 20 h, (ii) 80% TFA/CH₂Cl₂, 23 °C, 1.5 h.

of **1** yields only acetophenone **30b**, but none of the product from the methyl at the 4-position, which was confirmed through NMR studies and small-molecule X-ray crystal structures.

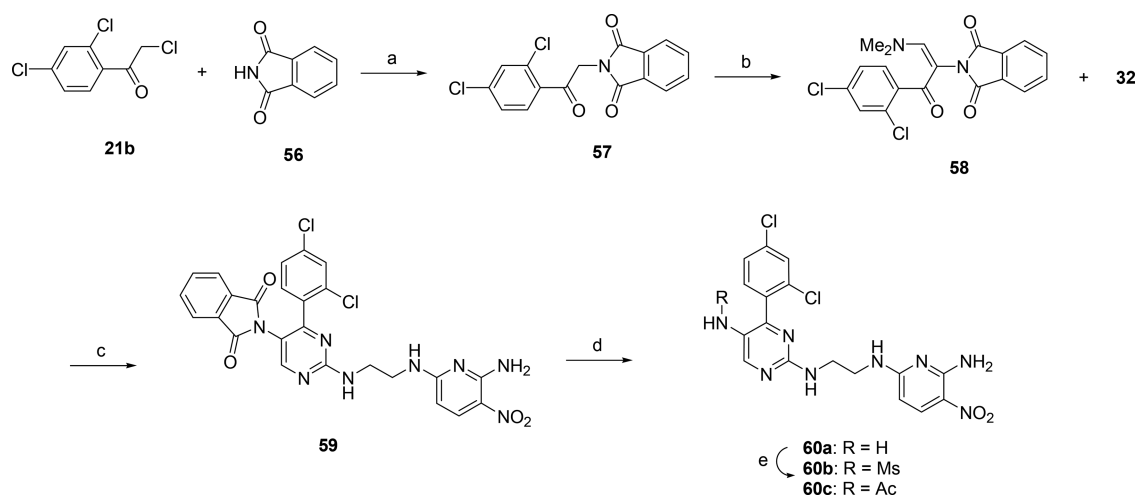
Variations to the linker or ethylene diamine moiety (Table 4) could be carried out by making a suitably modified and protected linker group. However, installing alkyl groups on the linker nitrogen attached to the C-2 position of the pyrimidine core was simply and cleanly accomplished using solid-phase techniques (Scheme 5). A protected ethylene diamine or similar molecule was bound to the resin by reductive amination to give compounds like **40**. The nucleophilic amine was then subject to *SnAr* reaction with an excess of chloropyridine or other active arene to give **41**. After deprotection of the Boc group under mild conditions with TMSOTf and 2,6-lutidine, the exposed primary amine was coupled with 2-nitrobenzenesulfonyl chloride to furnish **42**. The relatively acidic sulfonamide readily undergoes Mitsunobu reaction by first activating with excess Ph₃P and DIAD followed by addition of excess primary alcohol such as 2-(dimethylamino)-ethanol, which leads to the product **43b**. The Mitsunobu reactions were driven to completion through the use of excess reagent and high concentration. The resin-bound 2-nitrobenzenesulfonamides were subject to thiophenol under basic conditions to reveal the secondary amines **44a–h**. To form the pyrimidine products, amines **44a–h** were exposed to excess 1H-pyrazole-1-carboxamide hydrochloride and DIEA (Hünig's base) to produce the guanidines **45a–h**, which were transformed into the desired products through reaction with the proper enaminone, e.g., **24**, and base 7-methyl-1,5,7-

triazabicyclo[4.4.0]dec-5-ene (MTBD) in NMP at 120 °C overnight. The progress of the resin-bound reactions was routinely monitored by HPLC and LCMS by hydrolyzing a small sample (5–10 mg) of washed resin with TFA. The final products **46a–h** were liberated from the acid-sensitive resin in a similar manner using 80% TFA/CH₂Cl₂. A small amount of CH₂Cl₂ used during the cleavage step helps to swell the resin and release most of the product. The resin is filtered after 1 h, washed with CH₂Cl₂, and quickly evaporated under reduced pressure. The products were typically dissolved again in CH₂Cl₂ and evaporated again to drive off residual TFA. The products **46a–h** were dried in vacuo and were usually purified by reverse phase HPLC. For advanced in vitro and in vivo studies, these compounds and others purified by prep HPLC were converted from their TFA salts to free bases by dissolving the products in EtOAc and washing once with satd NaHCO₃. The free bases could be converted to HCl salts by lyophilizing from a solution of 2 equiv of HCl in ACN/water (1:1 v/v) to yield light fluffy powders.

To facilitate the investigation of the distal arene, we envisioned using a linker with a free amine at the distal position. By employing mono-Boc ethylene diamine (**47**), the appropriate guanidine **48** was produced as described for **13** and **32–34** using 1H-pyrazole-1-carboxamide hydrochloride as the guanidylating agent. The mono-Boc ethylene diamine guanidine (**48**) reacted smoothly with enamine **24** using Cs₂CO₃ as the base in NMP. The product pyrimidine was carefully purified at this stage because the Boc protecting group allowed convenient separation on silica gel to give **48** in high purity and ca. 80% yield. The Boc group was removed using

Scheme 6. Synthesis of 51a–s (Table 5)^a

^aReagents and conditions: (a) 1*H*-pyrazole-1-carboxamide hydrochloride, CH₃CN, 80 °C, 24 h; (b) 1-(2,4-dichlorophenyl)-3-(dimethylamino)-2-imidazolylprop-2-en-1-one (**24**), Cs₂CO₃, NMP, 100 °C, 48 h; (c) aq HCl (3 M), CH₃CN, 25 °C, 16 h; (d) chloro-arene, Hünig's base, DMF, 80 °C, 12 h.

Scheme 7. Synthesis of 60a–t (Table 6)^a

^aReagents and conditions: (a) Cs₂CO₃, DMF, 25 °C, 14 h; (b) DMFDMA, 80 °C, 6 h; (c) (i) guanidine **32**, Cs₂CO₃, DMF, 90 °C, 14 h, (ii) gal AcOH, 120 °C, 4 h; (d) hydrazine, ethanol, 75 °C, 2 h; (e) Ms₂O (for **60b**) or Ac₂O (for **60c**), THF, 25 °C, 4 h.

concd HCl in ACN to give the HCl salt cleanly after about 16 h at room temperature. The product **50** was free based by extracting into water and neutralizing the aqueous solution with satd aq NaHCO₃ to precipitate the product. After dissolving the precipitate into organic solvent and drying with Na₂SO₄, **50** could be used directly in subsequent reactions. From the primary amine **50**, a variety of coupling reactions and SnAr reactions gave amides, sulfonamides, ureas, and aminopyridines. Compound **50** was dissolved in DMF or DMA as a stock solution which was added to solutions of chloropyridine, such as 2-methoxy-3-nitro-6-chloro-pyridine, with DIEA to yield a wide array of novel groups at the distal linker position such as **51d**. The products **51a–s** could be purified by column chromatography or directly from the reactions by injection onto a prep HPLC (Scheme 6).

Most groups that were explored at the C-5 position of the pyrimidines were installed at the acetophenone stage as in the synthesis of **1**, **2**, **16**, **26**, **35a**, **36a**, and **50**. Nucleophilic

aromatic or nonaromatic heterocycles such as tetrazoles, morpholine, and piperazine were reacted with 2,4-dichlorophenacyl chloride (**21b**) to give the desired acetophenones which were transformed into the amino pyrimidines **60k,p–r,t** (Table 6) by similar procedures as was described for **25u**. The only exception was 3-trifluoromethyl-1*H*-pyridin-2-one, which gave a mixture of *N*- and *O*-alkylated products when reacted with dichlorophenacyl chloride (**21b**). The *O*-alkylated product was easily hydrolyzed with concd HCl to give pure 1-[2-(2,4-dichloro-phenyl)-2-oxo-ethyl]-3-trifluoromethyl-1*H*-pyridin-2-one, which was used to make **60t**. The 2-pyridine acetophenone needed to produce **60s** was synthesized from dichlorophenacyl chloride (**21b**) and 2-bromopyridine using palladium catalysis.⁴⁷ The tetrazole of **60l** was formed with NaN₃ and ZnCl₂ from the corresponding cyano group at C-5, which was produced in the same manner as **16** but using 3-(2,4-dichloro-phenyl)-3-oxo-propionitrile to obtain the aminopyrimidine.⁴⁸ To synthesize **60i** and **60j**, a C-5 ethyl ester

compound with a C-4 2,4-dichloro-phenyl group, was needed. By utilizing 3-(2,4-dichloro-phenyl)-3-oxo-propionic acid ethyl ester and Boc-protected guanidine **48**, the required C-5 ester was made with the Boc-protected ethylene diamine linker similar to **49**. The ester was reduced with DIBAL to furnish the hydroxy methyl at C-5 which after deprotection and SnAr with 2-chloro-5-nitro-6-aminopyridine gave **60i**. The Boc-protected C-5 hydroxy methyl pyrimidine was oxidized under Swern conditions to the aldehyde and was then reductively aminated with morpholine to eventually give **60j** after installing the distal aminopyridine.

To complete the investigation of the C-5 position of the aminopyrimidine scaffold, we sought to incorporate an aniline at C-5 to produce reverse amides and monoketopiperazines. Attempts to use 1-(2,4-dichloro-phenyl)-2-nitro-ethanone to establish a nitro group at C-5 met with limited success, and reduction of the nitro group at C-5 took strong reducing conditions and led to degradation of starting materials. Alternatively, 2,4-dichlorophenacyl chloride (**21b**) reacted with phthalimide (**56**) using Cs_2CO_3 as the base to provide the substituted acetophenone **57** (Scheme 7). Heating **57** in neat DMFDMA afforded the enaminone **58**, which was reacted with a fully elaborated guanidine such as **32** to give the pyrimidine core. However, during the cyclization of **58** and **32**, a mixture of products was obtained. The C-5 phthalimide suffered partial hydrolysis to the monoamide at C-5. This could not be cleanly deprotected but could be smoothly converted back to the phthalimide by heating the mixture in glacial AcOH at 120 °C for 4 h to yield **59**. The aniline **60a** was easily exposed by treatment of the C-5 phthalimide of **59** with excess hydrazine. Once purified, the aniline **60a** was conveniently coupled with methanesulfonic anhydride or acetic anhydride to afford **60b** and **60c**, respectively. Ureas **60g** and **60h** were fashioned from the aniline **60a** in a two-step process first reacting the aniline with carbonyldiimidazole (CDI) followed by the proper amine. The amides **60d–f** were prepared through standard peptide coupling procedures employing HBTU and the required acid. Coupling aniline **60a** with *N*-Boc valine gave **60f** after deprotection with 20% TFA/ CH_2Cl_2 . The cyclic amides **60m–o** were also made from the aniline **60a**. Initially, attempts to alkylate the aniline with compounds like 4-bromobutyric acid led to multiple alkylation products. The aniline **60a** could be coupled with an appropriately protected acid such as 4-Boc-oxy-butyric acid. After forming the amide bond, the hydroxyl group was deprotected and the amide was cyclized under Mitsunobu conditions to produce **60m**. Attempts to close the cyclic amide by making the terminal mesylate or tosylate did not give the desired products cleanly. Compounds **60n** and **60o** were made by procedures similar to those used for **60m**. The aniline **60a** was coupled with chloro-acetic acid, which was further displaced with the proper ethanolamine. The 2-hydroxy-ethylamino acetyl amide was then cyclized under Mitsunobu conditions to produce the monoketopiperazines **60n** and **60o**. Compounds were typically purified to >95% purity by either silica gel chromatography using a polar eluent system such as 5% methanol/methylene chloride or by reverse-phase preparative HPLC. Most compounds were lyophilized as HCl salts to form free-flowing dry powders which were easily weighed and dissolved for biological evaluation.

In Vitro Activity. From the dihydropyrimidine library hits, specific pools of compounds showing activity were screened again for a GSK3 IC_{50} in an assay that monitored the rate of phosphorylation of a CREB substrate. Only pools containing

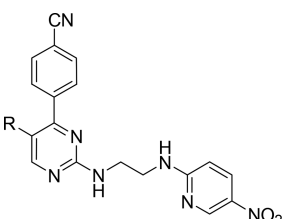
compounds with an ethylene diamine 5-nitropyridine moiety **8** had confirmed IC_{50} activity. Individual dihydropyrimidine analogues **9a–c** were made on solid support and found to have modest micromolar IC_{50} activity (Table 1). Interestingly,

Table 1. Pyrimidines versus Dihydropyrimidines, IC_{50} and EC_{50}

| # | IC_{50} (μM) | EC_{50} (μM) |
|------------|------------------------------------|------------------------------------|
| 9a | 3.40 | |
| 9b | 3.70 | |
| 9c | 2.00 | |
| 11a | 0.12 | 9.6 |
| 11b | 0.14 | |
| 11c | 0.15 | 18.0 |
| 11d | 0.04 | 1.7 |

while optimizing the assay conditions, it was noted that the potency of the DMSO stock solutions of **9a** seemed to steadily increase. Analysis of the DMSO solution showed, along with the expected dihydropyrimidine **9a**, a large contamination of the solution with the fully aromatized pyrimidine **11a** and a small amount of a third compound which was tentatively assigned as the 4-cyano dehydration product of the 4-amide on the C-4 phenyl. Once made, the aromatic amino pyrimidines **11a–c** showed superior potency over the dihydropyrimidines in the range of 100–200 nM IC_{50} . However, when tested in the insulin-receptor expressing CHO cells (CHO-IR), compounds **11a–c** gave little or no change in glycogen deposition in the cells as indicated by the EC_{50} values in the high micromolar range. On the basis of indications that the dehydration product of **11a** might be imparting better cellular potency, the cyano compound **11d** was made, confirming that the 4-cyano group was approximately 3-fold more potent with an IC_{50} = 42 nM and had measurable activity in the CHO-IR whole cell assay (EC_{50} = 1.7 μM). With a potent compound identified, we had an excellent foundation with which to explore the SAR of this novel ATP-competitive GSK3 scaffold.

While many groups were tolerated at the pyrimidine C-6 position, such as the ethyl group in **11a**, these groups did not improve the potency of the series and could be removed to maintain a low molecular weight. For example, removing the C-6 ethyl group from the pyrimidine core of **11a** provided compound **16**, which had nearly identical IC_{50} potency (52 nM) and whole cell activity (EC_{50} = 2.2 μM) (Table 2). With compound **16** representing a lead structure, we next focused on improving the solubility while maintaining the in vitro potency. As the first few esters and amides were made from the acid **17**, it quickly became apparent that a wide variety of groups were tolerated at the C-5 position of the pyrimidine. The C-5 promiscuity proved to be a common theme throughout the series. However, some trends became apparent, for example, within a series steric bulk in the vicinity of the C-4 ester or amide reduced potency. This trend can be seen when comparing the primary amide **19a** and methyl amide **19b** with the bulkier *tert*-butyl amide **19d** and morpholino amide **19k**. Both acidic and basic groups were potent, although primary amines were not as well tolerated as tertiary amines, e.g., **19h** versus **19i**. Exchanging the amide proton **19b** or **19i** for a methyl group **19c** or **19j** was also deleterious. Although the effect could be the result of loss of a hydrogen bond, the magnitude of the difference tends to indicate a steric effect. After an extensive survey of esters and amides, we were unable

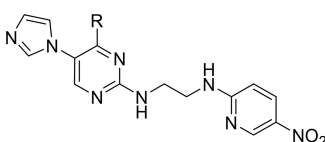
Table 2. Potency of C-5 Groups on C-4 *para*-Cyanophenyl Pyrimidines


| # | R Group | IC ₅₀ (μM) | ED ₅₀ (μM) | # | R Group | IC ₅₀ (μM) | ED ₅₀ (μM) |
|-----|---------|--------------------------|--------------------------|-----|---------|--------------------------|--------------------------|
| 16 | | 0.052 | 2.2 | 19f | | 0.047 | - |
| 18a | | 0.025 | - | 19g | | 0.029 | >10 |
| 18b | | 0.190 | - | 19h | | 0.153 | - |
| 18c | | 0.051 | 8.3 | 19i | | 0.071 | >10 |
| 18d | | 0.050 | 3.4 | 19j | | 0.140 | >10 |
| 17 | | 0.035 | >10 | 19k | | 0.161 | - |
| 19a | | 0.029 | >10 | 19l | | 0.417 | >10 |
| 19b | | 0.033 | >10 | 20 | | 0.033 | 1.5 |
| 19c | | 0.061 | 8.7 | 26 | | 0.019 | 1.0 |
| 19d | | 0.110 | >10 | 25a | | 0.011 | 1.3 |
| 19e | | 0.075 | - | 35a | | 0.019 | 5.0 |

to identify groups which significantly improved the CHO-IR whole cell potency. Postulating that the C-5 esters and amides might not easily penetrate the cell membrane, we thought to explore small five-membered heterocyclic ring systems. This direction quickly proved fruitful when the C-5 oxadiazole **20**, triazole **26**, and *N*-linked 1-imidazole exhibited improved cell-free and whole-cell potency. Interestingly, the more polar C-linked 2-imidazole **35a**, while maintaining the IC₅₀ potency observed with many compact C-5 heteroaromatic rings, lost potency in the CHO-IR cell assay. On the basis of that result, we decided to hold the more potent *N*-linked imidazole constant and optimize the C-4 phenyl and the linker group. The *N*-linked imidazole provided us with our first cellularly active compound which could be employed as a tool to help understand the biology and consequences of inhibiting GSK3 in cells and in rodents as will be discussed in the in vivo efficacy section.

Substitutions around the C-4 phenyl quickly established a well-defined and predictable SAR (Table 3). Unlike the 4-CN-phenyl of **25a**, a bare phenyl (**25b**) had a 10-fold less potent

Table 3. Optimization of C-4 Arene



| # | R Group | IC ₅₀ (μM) | EC ₅₀ (μM) | # | R Group | IC ₅₀ (μM) | EC ₅₀ (μM) |
|-----|---------|--------------------------|--------------------------|-----|---------|--------------------------|--------------------------|
| 25b | | 0.197 | 23.9 | 25m | | 1.117 | - |
| 25c | | 0.200 | - | 25n | | 1.930 | - |
| 25d | | 0.053 | 1.2 | 25o | | 0.024 | 1.24 |
| 25e | | 0.034 | 0.3 | 25p | | 0.884 | - |
| 25f | | 0.040 | 2.5 | 25q | | 0.347 | - |
| 25g | | 0.068 | 2.1 | 25r | | 4.870 | - |
| 25h | | 0.009 | 0.1 | 25s | | 0.646 | - |
| 25i | | 0.124 | - | 25t | | 0.031 | 0.9 |
| 25j | | 0.777 | - | 25u | | 0.006 | 0.3 |
| 25k | | 0.029 | 6.1 | 25v | | 0.038 | 4.2 |
| 25l | | 0.166 | - | 25w | | 0.027 | 1.5 |

IC₅₀. In the *para*-position of the C-4 phenyl, a nonpolar group larger than a fluorine was needed to reestablish the cell-free potency. Small groups in the *para*-position like Cl-, Me-, and CF₃- had about equal IC₅₀s, but the methyl group of **25e** was much more active in cells (EC₅₀ = 0.3 μM). The same trend was seen again when comparing the cellular activity of the 4-MeO (**25g**) to the much more active 4-Et of **25h**. When only a *para*-position group was present, linear alkyl moieties gave the best potencies. Bulkier groups like imidazole **25i** and morpholine **25k** were tolerated but did not give potent cellular activity. A short list of small groups on the *ortho*-position of the C-4 phenyl gave good IC₅₀s, such as Cl (**25o**), Br, Me, and CF₃. Larger groups like methoxy in the *ortho*-position (**25p**) strongly diminished the potency, as did any single group other than fluorine in the *meta*-position, such as **25q** or **25s**. Surprisingly, 2,4-disubstituted phenyls at C-4 were highly active in both IC₅₀ and EC₅₀ assays. Even small groups like fluorine, which imparted little or no enhancement alone, were quite potent when occupying the 2- and 4-positions, e.g., **25t**. The most potent of these arenes was the 2,4-dichlorophenyl of **25u** which gave single-digit nM IC₅₀s and excellent cellular potency. The

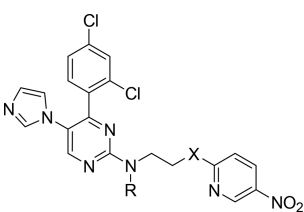
details of the C-4 arene and other interactions between the inhibitors and protein will be discussed in the section covering the X-ray crystal structure of **1** and GSK3 β . Structure-based design and the use of inhibitor/kinase co-crystal structures played a significant role in the course of optimizing the SAR and physical properties of this series, and the structures indicated that the 2,4-dichlorophenyl was making highly productive interactions. While we did continue to explore compounds incorporating the 4-ethyl- and 4-CN-phenyl groups at C-4, we found that the 2,4-dichlorophenyl gave the best activity as we continued to develop the SAR. Therefore, we will focus on the analogues made with the optimized 2,4-dichlorophenyl at C-4 as we discuss the SAR of the linker, distal aminopyridine, and further investigation at the C-5 position.

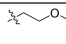
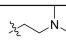
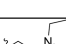
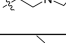
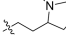
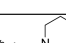
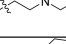
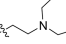
Crystal structures comparing our compounds and ATP in the active site of GSK3 indicated that the distal aminopyridine group overlapped with the ATP purine, making similar H-bond donor and acceptor interactions with the backbone residues in the binding pocket. As we anticipated, modifications to the distal linker amine were detrimental for binding. Replacing the distal linker nitrogen (group X in Table 4) with oxygen resulted

potency, however, we were not able to increase potency at this position. Modeling of this solvent exposed area to identify high value binding contacts proved difficult, and the marginal increases in solubility made by incorporating solubilizing groups were offset by increased molecular weights. Modeling did indicate that the length of the ethylene diamine linker was optimal for correctly arranging the H-bonding aminopyridine and C-4 arene. To validate the model, linkers of varying length, such as propylene diamine, or cyclic linkers, such as piperazine, were tested. All of which were found to give IC₅₀s in the 1 μ M or greater range confirming that the four atom ethylene diamine linker was optimal in this series.

The initially discovered hit compounds had a 2-amino-5-nitropyridine on the linker. Early attempts to replace the aminoarene with other groups capable of making H-bonding donor and acceptor interactions, such as amides and ureas, did not yield compounds with useful GSK3 inhibition. For example, the synthetic intermediate compound **49** with a Boc protecting group in place of the aminopyridine had an IC₅₀ > 10 μ M. Compounds with a nonsubstituted 2-aminopyridine displayed IC₅₀s in the 3 μ M range and a plain 2-aminopyrimidine replacement **51r** showed IC₅₀ > 10 μ M (Table 5). The necessity of a 5-nitro group presented several possibilities: the polar group might be making productive contacts deep in the ATP-binding pocket, the nitro could be adjusting the pK_a of the aminopyridine, or potentially both effects were adding to the potency. To investigate the influence of compact electron withdrawing groups at the 5-position of the aminopyridine, a series of compounds were made with incrementally decreasing calculated pK_as of the 2-aminopyridine group [NO₂ (**25u**; calculated pK_a of 2.83) > CN (**51b**; calculated pK_a of 3.95) > CF₃ (**51h**; calculated pK_a of 4.13) > CO₂Et (**51p**; calculated pK_a of 5.17) > Ac (**51q**; calculated pK_a of 5.64)].^{49,50} The IC₅₀s for this series of aminopyridines show a perfect correlation with the predicted pK_as. In fact, throughout the project, the rank order of binding follows the same trend (NO₂ > CN > CF₃). The position of electron withdrawing groups around the pyridine was also critical. For example, while an isosteric thiazole replacement for pyridine (**51a**) was potent, relocating the cyano group from the pyridine 5- to 4-position led to an approximate 10-fold erosion in potency (**51b** versus **51f**). We hypothesize that the reduction in IC₅₀ for **51f** is due to steric effects and poor alignment of the aminopyridine group in the binding pocket. Steric effects were certainly evident as most large groups at the distal position of the linker were poorly active, e.g. (**51k**), or were more commonly inactive. A few bicyclic aromatic groups, such as (**51e**), exhibited surprisingly good activity. However, these compounds do not easily fit the active site models and may indicate an alternate binding mode. With the intent of installing another H-bond donor in the 6-position of the pyridine, the diamino-nitropyridine group of **2** gave a slight improvement in binding potency but was far more active in the whole cell assay than **25u**. We postulate that the new amino group of **2** makes an H-bond with a main chain amide carbonyl. The boost in potency could be greatly reduced by a single methylation (**51l**) or two methyls (**51m**). Interestingly, adding an amino group to **51b** to give **51c** did not result in the expected increased potency. The nitro-amino interaction must be more subtle than a simple H-bond. Potentially, the pK_a of the amino group or the preorganization by a H-bond between the amino and nitro groups may play a role in the binding interaction with the protein, and presumably the 6-amino/5-nitro combination increases permeability

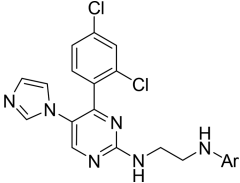
Table 4. Linker Changes

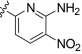
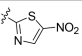
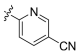
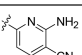
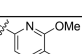
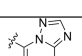
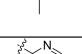
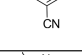
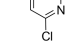
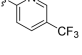


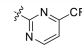
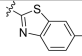
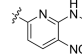
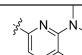
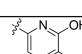
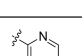
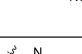
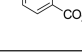
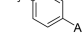
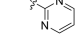
| # | X | R | IC ₅₀ (μ M) | EC ₅₀ (μ M) |
|-----|----|---|-----------------------------|-----------------------------|
| 38 | O | H | 2.829 | - |
| 39 | NH | Me | 0.022 | 0.08 |
| 46a | NH |  | 0.175 | - |
| 46b | NH |  | 0.035 | 0.35 |
| 46c | NH |  | 0.026 | 0.37 |
| 46d | NH |  | 0.027 | 0.11 |
| 46e | NH |  | 0.015 | 0.28 |
| 46f | NH |  | 0.032 | 0.11 |
| 46g | NH |  | 0.113 | - |
| 46h | NH |  | 0.121 | - |

in a nearly inactive compound **38**. Other simple augmentations to X in Table 4 such as methylation were similarly deleterious for potency (data not shown). Modeling suggested that branching out from the C-2 proximal nitrogen might project linear groups toward a solvent exposed area of the active site. Indeed, alkylation on this nitrogen was well tolerated. While most groups appended to the proximal nitrogen were nearly as active as **25u**, no clearly discernible SAR emerged. A wide variety of groups gave acceptable binding and whole cell

Table 5. Optimizing Tails



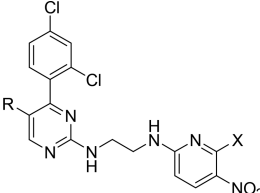
| # | Structure | IC ₅₀ (μM) | EC ₅₀ (μM) |
|-----|---|--------------------------|--------------------------|
| 2 |  | 0.001 | 0.08 |
| 51a |  | 0.024 | >10 |
| 51b |  | 0.025 | 0.79 |
| 51c |  | 0.056 | 1.01 |
| 51d |  | 0.081 | - |
| 51e |  | 0.108 | >10 |
| 51f |  | 0.200 | - |
| 51g |  | 0.201 | 3.90 |
| 51h |  | 0.223 | 3.84 |
| 51i |  | 0.236 | 9.44 |

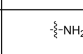
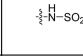
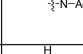
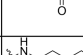
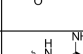
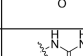
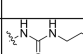
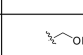
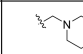

| # | Structure | IC ₅₀ (μM) | EC ₅₀ (μM) |
|-----|---|--------------------------|--------------------------|
| 51j |  | 0.381 | - |
| 51k |  | 0.527 | 12.66 |
| 51l |  | 0.576 | - |
| 51m |  | 1.000 | - |
| 51n |  | 1.000 | - |
| 51o |  | 3.370 | - |
| 51p |  | 3.650 | - |
| 51q |  | 5.950 | - |
| 51r |  | > 10 | - |
| 51s |  | > 10 | - |

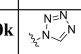
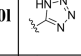
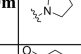
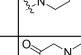
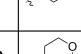
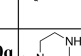
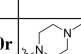
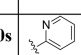
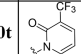
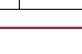
through the CHO cell membrane, resulting in the improved whole cell activity. With the improved CHO-IR potency, we proceeded to fine-tune the SAR holding the linker constant with the 5-nitro, 6-aminopyridine.

Having explored the SAR around the scaffold and optimized each position, we were interested in improving the solubility and physical characteristics of the series to expand our options for a development formulation. The C-5 position was the most pliable and well suited to tolerate a basic charge. By utilizing a new chemical handle by installing an aniline at C-5 (**60a**), we embarked on a campaign of diverse “reverse” amides and ureas (**Table 6**) as compared to the earlier series of esters and amides which lacked whole cell activity (**Table 2**). Small uncharged amides (**60c**) and sulfonamides (**60b**) maintained both IC₅₀ and EC₅₀ potency. A wide variety of basic groups could be appended to the C-5 aniline, however, extended basic groups such as amide **60e** lost CHO-IR cell activity. Amino acid analogues where the positively charged amine was proximal to the amide group and partially shielded by lipophilic groups such as the dimethylamino glycine **60d** and the valine **60f** retained cellular potency. The ureas such as **60g** showed poor EC₅₀s, presumably because of poor penetration of the membrane. A

Table 6. C-5 Groups



| # | R | X | IC ₅₀ (μM) | EC ₅₀ (μM) |
|-----|---|-----------------|--------------------------|--------------------------|
| 60a |  | NH ₂ | 0.010 | 0.29 |
| 60b |  | NH ₂ | 0.009 | 0.39 |
| 60c |  | NH ₂ | 0.006 | 0.19 |
| 60d |  | NH ₂ | 0.025 | 0.67 |
| 60e |  | NH ₂ | 0.024 | 17.70 |
| 60f |  | NH ₂ | 0.014 | 0.86 |
| 60g |  | NH ₂ | 0.027 | 3.00 |
| 60h |  | NH ₂ | 0.016 | 3.00 |
| 60i |  | NH ₂ | 0.007 | 0.15 |
| 60j |  | NH ₂ | 0.017 | 0.84 |

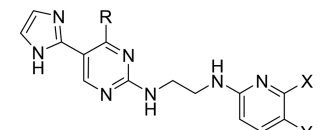
| # | R | X | IC ₅₀ (μM) | EC ₅₀ (μM) |
|-----|---|-----------------|--------------------------|--------------------------|
| 60k |  | H | 0.015 | 0.28 |
| 60l |  | H | 0.031 | 10.00 |
| 60m |  | NH ₂ | 0.006 | 1.58 |
| 60n |  | NH ₂ | 0.015 | 5.41 |
| 60o |  | NH ₂ | 0.004 | 0.03 |
| 60p |  | NH ₂ | 0.007 | 0.07 |
| 60q |  | NH ₂ | 0.018 | 0.51 |
| 60r |  | NH ₂ | 0.006 | 0.05 |
| 60s |  | NH ₂ | 0.007 | 0.01 |
| 60t |  | NH ₂ | 0.004 | 0.04 |

basic group could be introduced close to the C-5 position by reductive amination with lipophilic amines such as the morpholino analogue **60j**. However, the whole cell activity was superior in compounds, such as **60o**, **60p**, and **60r**, where the heterocycle was directly attached to the pyrimidine C-5 position. Mirroring previous results, basic amine groups at C-5 containing an NH may not have penetrated CHO cell membranes as well as the corresponding NMe analogues (**60n** vs **60o** and **60q** vs **60r**). In general, H-bond donors (**60g**, **60h**) tended to exhibit inferior EC₅₀s compared to neutral (**60c**, **60p**) or H-bond acceptor (**60o**, **60r**) groups at C-5. This tendency could be seen in the SAR of the N- versus C-linked imidazoles or in the N- (**60k**) versus C-linked (**60l**) tetrazoles (**Table 6**). Lipophilic aromatic moieties, such as pyridines (**60s**) and pyridones (**60t**), were highly potent in both cell-free and cellular assays but were insufficiently soluble for further advancement. Overall, the C-linked imidazoles at C-5 displayed the best compromise amid all of the characteristics required for a development candidate, including in vitro potency, solubility, formulation, metabolic stability, and PK, which will be discussed in the In vivo efficacy section. Therefore, the C-linked imidazole series was selected for further optimization toward an advanced predevelopment compound. In particular, this entailed replacing the nitro group and addressing PK/metabolism issues.

Throughout the SAR of the series, the order of potency for linker pyridines in both IC₅₀ and EC₅₀ tended to place the nitro

compounds first followed by cyano and then trifluoromethyl. However, with a 2-imidazole at C-5, the CHO-IR cell activity was similar for all of these. Additionally, the IC₅₀s were nearly equipotent, e.g., 36a, 36b, and 36c (Table 7). We attempted to

Table 7. Optimizing the C-4 Arene with C-Linked Imidazole



| # | R | X | Y | IC ₅₀ (μM) | EC ₅₀ (μM) |
|-----|---|-----------------|-----------------|-----------------------|-----------------------|
| 36a | | H | NO ₂ | 0.004 | 0.37 |
| 36b | | NH ₂ | NO ₂ | 0.001 | 0.26 |
| 36c | | H | CN | 0.004 | 0.51 |
| 36d | | H | CF ₃ | 0.035 | 1.24 |
| 61a | | H | H | 2.856 | - |
| 61b | | NH ₂ | NO ₂ | 0.031 | 2.50 |
| 35b | | NH ₂ | NO ₂ | 0.007 | >10 |
| 61c | | NH ₂ | NO ₂ | 0.051 | 5.92 |
| 61d | | NH ₂ | NO ₂ | 0.012 | 0.73 |
| 61e | | NH ₂ | NO ₂ | 0.007 | 0.24 |
| 61f | | NH ₂ | NO ₂ | 0.009 | 5.65 |
| 61g | | NH ₂ | NO ₂ | 0.047 | 3.00 |
| 61h | | NH ₂ | NO ₂ | 0.038 | 6.88 |

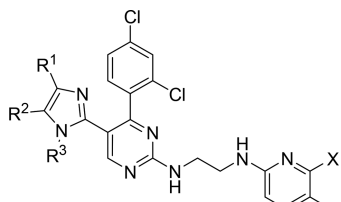
| # | R | X | Y | IC ₅₀ (μM) | EC ₅₀ (μM) |
|-----|---|-----------------|-----------------|-----------------------|-----------------------|
| 61i | | NH ₂ | NO ₂ | 0.032 | - |
| 61j | | NH ₂ | NO ₂ | 0.007 | 0.42 |
| 61k | | NH ₂ | NO ₂ | 0.004 | 0.22 |
| 61l | | NH ₂ | NO ₂ | 0.013 | 3.30 |
| 61m | | NH ₂ | NO ₂ | 0.005 | 1.02 |
| 61n | | NH ₂ | NO ₂ | 0.005 | 0.50 |
| 61o | | NH ₂ | NO ₂ | 0.019 | 2.19 |
| 61p | | NH ₂ | NO ₂ | 0.013 | 2.28 |
| 61q | | NH ₂ | NO ₂ | 0.004 | 0.43 |
| 61r | | NH ₂ | NO ₂ | 0.006 | 0.26 |
| 61s | | NH ₂ | NO ₂ | 0.004 | 0.05 |
| 61t | | NH ₂ | NO ₂ | 0.019 | 0.81 |
| 61u | | NH ₂ | NO ₂ | 0.249 | - |

improve the physical characteristics of the C-linked imidazole series by adjusting the C-4 phenyl substituents. Efforts to improve the PK by replacing the chlorines had the effect of lowering potency in the CHO-IR cell assay. The *ortho*-bromophenyl compound 61e and its analogues 61k, 61r, and 61s were an exception with low EC₅₀ values. However, these compounds did not demonstrate an advantage in solubility, formulation, or eventually efficacy over the 2,4-dichlorophenyl group. Therefore, the 2,4-dichlorophenyl compound 36c with the cyanopyridine moiety looked promising, but we were concerned with the metabolic stability of the imidazole and in vivo half-life.

Subjecting the imidazole compounds to S9 fraction liver microsomes gave acceptable half-lives (>30 min) for rodents and dogs, but some imidazoles were metabolized faster in monkey and human microsomes. Analysis of the metabolic products showed that as expected the primary metabolite was extensive oxidation of the imidazole. To combat the oxidation,

additional methyl groups or other bulky alkyl groups were positioned around the imidazole (Table 8). While most of these

Table 8. Optimizing the C-Linked Imidazole with 2,4-Dichlorophenyl C-4 Arene



| # | R ¹ | R ² | R ³ | X | Y | IC ₅₀ (μM) | EC ₅₀ (μM) |
|-----|-----------------|----------------|----------------|-----------------|-----------------|-----------------------|-----------------------|
| 37a | Me | H | H | H | NO ₂ | 0.008 | 0.29 |
| 37b | Me | H | H | NH ₂ | NO ₂ | 0.002 | 0.12 |
| 1 | Me | H | H | H | CN | 0.005 | 0.77 |
| 62a | H | H | Me | NH ₂ | NO ₂ | 0.001 | 0.25 |
| 62b | CF ₃ | H | H | NH ₂ | NO ₂ | 0.034 | 0.17 |
| 62c | iPr | H | H | NH ₂ | NO ₂ | 0.021 | 0.09 |
| 62d | tBu | H | H | NH ₂ | NO ₂ | 0.027 | 1.07 |
| 62e | Ph | H | H | NH ₂ | NO ₂ | 0.001 | 0.13 |
| 62f | Me | Me | H | NH ₂ | NO ₂ | 0.003 | 0.44 |
| 62g | Me | Me | Me | NH ₂ | NO ₂ | 0.022 | 0.32 |

groups had a positive effect on microsomal stability, the extra molecular weight increased the log *P* and decreased the solubility. The most minimal change which maintained potency while improving microsomal stability was a single additional methyl group at the imidazole 4(5)-position yielding compound 1. This methyl group improved the human microsomal half-life from 33 min for 36c to 109 min for our lead compound 1 in the pyrimidine series.

Binding Mode and Basis of Compound Selectivity. As mentioned in the previous sections, improvements in the series potency and chemical properties were heavily influenced by our in-house structure-based drug design efforts. The series is ATP-competitive and predominately occupies the volume in the active site typically occupied by ATP (Figure 2). The major features of compound 1 which impart the exceptional GSK3-α/β kinase potency are as follows. The hydrogen-bond donor and acceptor of the aminopyrimidine group are perfectly aligned to interact with the main-chain carbonyl and amide of Val135 at the *n* + 2 position. The compound does not make an interaction with the mainchain carbonyl of Asp133 (by definition, position *n*) as does the exocyclic amine of the purine ring of ATP.⁵¹ The 5-cyano moiety extends further into the bottom of the ATP-binding pocket, beyond the region typically occupied by the purine group of ATP. The ethylene diamine linker spans the binding site and positions the C-4 2,4-dichlorophenyl group to form both hydrophobic contacts by positioning the chloro groups both in a hydrophobic dimple within the P-loop, formed by residues Ile62, Gly63, and Val70, and in a hydrophobic pocket at formed by residues Val70, Lys85, and Asp200, in the bottom of the ATP-binding pocket, respectively. An additional π–π interaction is putatively formed between Phe67, at the tip of the P-loop, and the 2,4-dichlorophenyl group, which in turn forms a putative π–π interaction with the aminopyrimidine group.^{52–54} The formation of the π–π interaction with Phe67 and the compound requires the phenylalanine to move approximately 7 Å from its native, extended position when binding ATP and to rotate at a 90°

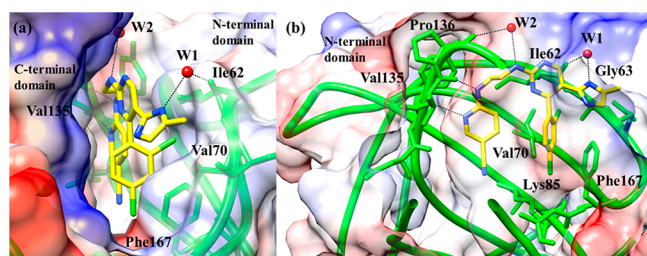


Figure 2. Co-crystal structure of compound **1** in the ATP-binding site of human GSK3- β . The electrostatic potential is superimposed on the solvent-accessible surface of human GSK3- β . The calculations and visualizations were performed using the CHIMERA program.⁵⁸ The ranges of red (negative) and blue (positive) represent electrostatic potentials of < -7 to $> +7$ k_bT , where k_b is the Boltzmann constant and T is temperature. White surface represents nonpolar amino acid residues. In the figures, the N-terminal and C-terminal domains of the kinase are positioned as indicated. (a) Overall view into the ATP-binding pocket with the compound bound; key hydrogen bonds are shown as dashed lines and key residues are labeled; key waters are shown as red spheres. Note the position of Phe167, which forms the edge of the binding pocket. (b) Orthogonal view of the pocket at a 90° rotation to view (a). The co-crystal structure was refined against diffraction data collected to 2.6 Å.

angle (using the costructure of human GSK3- β :AMPPNP, RSCB accession code 1J1B as a reference⁵¹). This arrangement provides significant stabilization of the compound as the series of π - π interactions spans the length of the active site. The 2,4-dichlorophenyl group occupies the area typically occupied by the ribose ring of ATP.⁵¹ Both the linker length and flexibility was critical in positioning the hydrogen-bonding groups of the aminopyridine and the 2,4-dichlorophenyl group. The imidazole group forms a hydrogen bond with an adjacent structural water, which in turns forms a hydrogen bond with the main chain carbonyl of Ile62. Finally, there is a hydrogen bond formed between the ethylene diamine linker and a structural water, which subsequently hydrogen-bonds to the main chain

carbonyl of Pro136. The kinase maintains an active, DFG-in conformation.

Three interactions form the basis of the exquisite selectivity of compound **1** (Table 9). The first is the interaction of the compound with the mainchain carbonyl of Val135. The presence of Pro136 at the $n + 3$ position ensures that the main chain carbonyl faces inward to allow this interaction. Only a small number of human kinases contain a proline at the $n + 3$ position of the hinge region and allow such interactions.⁵⁵ The interaction of the compound linker with Pro136 via a structural water also likely provides some selectivity for the same reasons. The second is the positioning of the 2,4-dichlorophenyl group to insert a chloro-group into the hydrophobic dimple within the P-loop. The third is the interaction between the 2,4-dichlorophenyl group and Phe67 to form a face-to-face π - π interaction. In both isoforms of GSK3, these two interactions can be formed with the compound without compromising the donor-acceptor interactions of the compound with the main chain of Val135. In the other kinases, even closely related kinases like CDC2, sequence differences within the P-loop that comprise the area of the hydrophobic dimple or the residue equivalent to Phe67 ablate the possibility for the formation of the hydrophobic dimple and/or the π - π interaction at the tip of the P-loop. In both CDC2 and ERK2 kinases, where the sequence within the P-loop is highly homologous, there is a tyrosine (Tyr15 in CDC2 and Tyr36 in ERK2) at the position equivalent to Phe67 at the tip of the P-loop. However, an equivalent conformation of the aromatic side chain which allows an similar π - π interaction to form with the 2,4-dichlorophenyl group cannot be attained as the exocyclic hydroxyl group of the tyrosine group would collide with the main chain of the P-loop itself, thereby sterically excluding the necessary conformation and abrogating this interaction. These so-called folded P-loop conformations have been seen with other selective kinase inhibitors and are associated with a high degree of selectivity.^{56,57} The C-5 substituent also likely plays a role in selectivity because its removal, while reducing potency

Table 9. Kinase Selectivity of GSK3-Specific ATP Competitive Inhibitors

| kinase | species | kinase group | identity (%) | IC ₅₀ (μM) 1 | IC ₅₀ (μM) 2 | IC ₅₀ (μM) 36b |
|-----------------|---------|--------------|--------------|--------------------------------|--------------------------------|----------------------------------|
| GSK3- β | human | CMGC3 | 100 | 0.0049 | 0.0006 | 0.0006 |
| GSK3- α | human | CMGC3 | 91 | 0.0078 | 0.0070 | 0.0271 |
| CDC2 | human | CMGC1 | 30 | 8.8 | 4.0 | >10 |
| ERK2 | human | CMGC2 | 31 | >10 | >10 | >10 |
| PKC- α | human | AGC2 | 22 | >10 | >10 | >10 |
| PKC- ζ | human | AGC2 | 19 | >10 | na | >10 |
| AKT1/PKB | human | AGC3 | 21 | >10 | >5 | >10 |
| p70S6K | rat | AGC6 | 22 | >10 | >1 | >10 |
| p90RSK2 | rabbit | C6, CAMK6% | 22 | >10 | >10 | na |
| TIE2 | human | PTK13 | 18 | >5 | >5 | >25 |
| FLT1 | human | PTK14 | 17 | >5 | >5 | >5 |
| KDR | human | PTK14 | 18 | >5 | >2 | >5 |
| bFGFR TK | human | PTK15 | 20 | >5 | >1 | >5 |
| IGF1RTK | human | PTK16 | 16 | >10 | >2 | >10 |
| insulin RTK | human | PTK16 | 16 | >10 | >2 | na |
| AMP kinase | rat | OPK | 22 | >10 | na | >10 |
| PDK1 | human | OPK | 23 | >10 | na | >10 |
| CHK1 | human | OPK | 21 | >10 | >10 | >10 |
| CK1- ϵ | human | OPK | 17 | >5 | >5 | >10 |
| DNA protein | human | PI3K | low | >10 | >10 | >10 |
| PI3 kinase | human | PI3K | low | >10 | >5 | >5 |

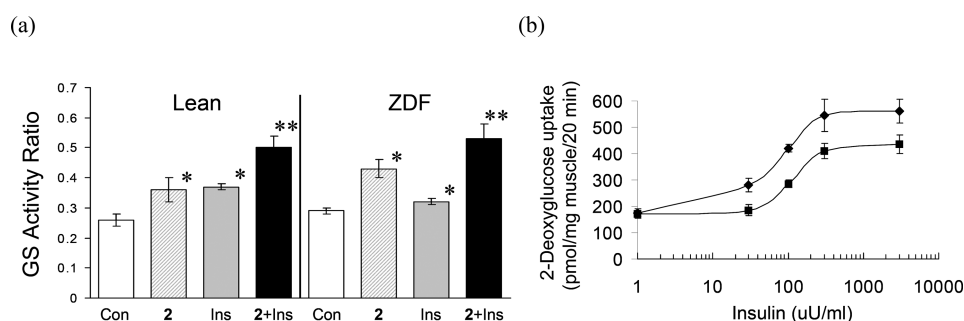


Figure 3. (a) Activation of GS in isolated rat soleus muscle with insulin or compound **2**. Isolated rat soleus muscle was incubated with vehicle as a control (Con), compound **2**, insulin (Ins), or both **2** and insulin (**2** + Ins) for 15 min. The effects of GSK3 inhibitor and insulin were tested in muscle from lean normal rats (left) or muscle from diabetic ZDF rats (right). Inhibitor was used at 0.5 μ M and insulin at 2 mU/mL. Data represent means \pm SE for five muscles per group. * P < 0.05 vs vehicle; ** P < 0.05 vs all other groups. (b) Effect of compound **2** on insulin stimulated glucose transport in isolated soleus muscle from diabetic ZDF rats. Muscles were incubated with increasing concentrations of insulin and intracellular 2-deoxyglucose accumulation was measured. The EC_{50} values for insulin stimulated glucose transport were 115 nM for insulin alone bottom line (■) and 66 nM for insulin plus 0.5 μ M compound **2** top line (◆). Values are means \pm SE for five muscles per group.

for GSK3, increased the affinity for closely related kinases, such as CDC2 and erk1. However, the SAR was promiscuous and most likely the C-5 group acts as an additional anchor for holding the pyrimidine core in position.

DISCUSSION AND CONCLUSIONS

In Vitro Efficacy. With compounds that inhibit GSK3 at least 1000-fold better than any other kinase in our assay panel, our compounds can be used as highly specific probes to modulate GSK3 activity. Our GSK3 inhibitors were also very selective against a wide variety of pharmacologically relevant receptors and nonkinase enzymes.¹ The most potent activity we found for **1** was for phosphodiesterase III (K_i = 8.3 μ M) with no significant activity for nonkinase enzymes at 20 μ M.⁵⁹ The excellent kinase and nonkinase selectivity gave us confidence that biological activity would be the result of pharmacological modulation of GSK3 and not off-target effects. In CHO-IR cells which express the insulin receptor, our compounds can activate glycogen synthase, many with EC_{50} s below 500 nM. The maximal effect of insulin on CHO-IR cells yields an increase in GS activation ratio of ~50% at 10 nM. Compound **2** can also achieve a 50% increase in GS activation in CHO-IR cells at 500 nM (EC_{50} = 80 nM). Thus, by direct inhibition of GSK3, GS inhibition in CHO cells can be relieved to the same extent as with the signal cascade initiator, insulin. Presumably, GS activation occurs through dephosphorylation of the GSK3 phosphorylation sites by endogenous phosphatases.⁶⁰ While CHO-IR cells were a convenient functional assay, we wanted to investigate the utility of our GSK3 inhibitors in more biologically relevant cells and tissues. Activation of GS in liver should improve disposal of excess circulating blood glucose. Thus, in primary rat hepatocytes, compound **2** reached a maximal GS activation at the same concentration as in CHO cells and exhibited an EC_{50} of 100 nM, which suggested that the compounds would activate GS in normal mammalian liver cells.

Other than liver, muscle is a major tissue involved in glucose disposal. GSK3 inhibition should activate GS in muscle cells but additionally could increase insulin-dependent glucose transport. To investigate the effect of a GSK3 inhibitor in muscle tissue, isolated rat soleus muscle was incubated with insulin, compound **2**, or both and compared to a vehicle treated group (Figure 3a). Using a maximally effective concentration of GSK3 inhibitor **2** (0.5 μ M), the GS activity increased to the

same level as that elicited by insulin (~40%) in type I skeletal muscle from lean rats as compared to the nonstimulated control group. Soleus muscle from diabetic ZDF rats was, as expected, markedly resistant to insulin-stimulated GS activation, but the GS activity responded to compound **2** to approximately the same level as normoglycemic muscle. Notably, the effect of insulin plus a GSK3 inhibitor was additive in muscle from both lean and diabetic rats. The increase in insulin-stimulated GS activity with compound **2** in diabetic muscle was 3-fold better than insulin stimulation alone, reaching a similar level as that in lean rat muscle. As predicted from the mechanism of action, the total GS activity was not altered by the GSK3 inhibitor in muscle from either lean or ZDF rat. The improvement in glucose deposition into glycogen in both liver and muscle cells was very encouraging. However, a defect in GLUT4 and glucose transport into the cells of diabetics might attenuate the effect of a GSK3 inhibitor by restricting the passage of glucose from blood into the cell.

To explore the effects of GSK3 inhibition on glucose transport, we again used soleus muscles from lean and diabetic ZDF rats (Figure 3b). Treatment of muscle from the ZDF rat with compound **2** at a maximally effective concentration (0.5 μ M) improved glucose transport and insulin sensitivity. GSK3 inhibition increased the maximal rate of glucose disposal approximately 30% over that of insulin stimulation alone (bottom line in Figure 3b). However, in response to compound **2**, glucose uptake was only increased to about 70% of the rate achieved in lean muscle.⁵⁹ While glucose transport rates were not returned to nondiabetic levels, GSK3 inhibition did improve the ZDF muscle sensitivity to insulin signaling, as shown by the shift in insulin EC_{50} from 115 nM in untreated muscle to 66 nM in the muscle incubated with compound **2**. The insulin EC_{50} in lean rat muscle was 59 nM. Thus, GSK3 inhibitor treatment of diabetic ZDF muscle resulted in a reestablishment of glucose transport insulin sensitivity to near normal levels. Compound **2** also increased the GS activation, glucose uptake, and insulin sensitivity in type IIb epitrochlearis muscle from diabetic ZDF rats.⁶¹ Further, GSK3 inhibition was shown to improve glucose transport in response to insulin but did not increase the basal glucose uptake without insulin. The improvement in glucose transport was associated with an increase of cell surface GLUT4 in both skeletal muscle groups but only in response to insulin. This indicates that GSK3 inhibition relieves a diabetic defect in insulin-stimulated

Table 10. Efficacy of GSK3 Inhibitors in Oral Glucose Tolerance Test (oGTT) in Diabetic *db/db* Mice and ZDF (*fa/fa*) Rats

| # | IC ₅₀ (nM) | EC ₅₀ (μM) | mouse efficacy reduction in plasma glucose (AUC %) ^a | mouse plasma conc (μg/mL) ^b | ZDF efficacy reduction in plasma glucose (AUC %) ^c | ZDF % F ^d | ZDF T _{1/2} (min) ^d | formulation ^e |
|-----|-----------------------|-----------------------|---|--|---|----------------------|---|--------------------------|
| 25a | 11 | 1.3 | 12 | 5 | | | | A |
| 35a | 19 | 5.0 | 12 | 1 | | | | A |
| 2 | 0.6 | 0.08 | 25 | 7 | | | | A |
| 51b | 25 | 0.79 | 15 | 13 | | | | A |
| 60a | 10 | 0.29 | 3 | 1 | | | | B |
| 60i | 7 | 0.15 | 9 | 12 | | | | A |
| 60o | 4 | 0.03 | 13 | 4 | | | | A |
| 60p | 7 | 0.07 | 3 | 1 | | | | A |
| 60r | 6 | 0.05 | 0 | 3 | | | | C |
| 36a | 4 | 0.37 | 35 | 97 | 29 | 33 | 143 | A |
| 36b | 1 | 0.26 | 30 | 19 | 29 | 6 | 46 | C |
| 36c | 4 | 0.51 | 23 | 29 | 18 | 21 | 52 | A |
| 61r | 6 | 0.26 | 34 | 13 | | | | C |
| 37a | 8 | 0.29 | 2 | 19 | | | | C |
| 37b | 2 | 0.12 | 23 | 10 | 24 | 7 | 58 | C |
| 1 | 5 | 0.77 | 29 | 15 | 38 | 36 | 92 | B |

^aDiabetic *db/db* mice were used except where noted. Compound was dosed orally (30 mg/kg) at −4.5 and −0.5 h relative to *t* = 0 oral glucose challenge. Groups of 6–8 mice per treatment fasted for ~6 h prior to oGTT. Efficacy is measured as the percent reduction in circulating plasma glucose AUC post inhibitor treatment compared to untreated following an oral glucose challenge. ^bConcentration of compound (μg/mL) in mouse plasma at 20 min after second dose, *t* = −0.16 h relative to *t* = 0 oral glucose challenge. ^cObese 10 week-old ZDF (*fa/fa*) rats (*n* = 8/group) fasted overnight and treated orally with compound (8 mg/kg) at 4.5 and 0.5 h prior to oGTT. Efficacy is measured as the percent reduction in circulating plasma glucose AUC post inhibitor treatment compared to untreated following an oral glucose challenge. ^dObese 10 week-old ZDF (*fa/fa*) rats (*n* = 8/group) fasted overnight and treated orally with compound (8 mg/kg). ^eA = 15% captisol, B = 1% CMC, C = water (pH was adjusted as needed).

GLUT4 translocation in ZDF muscle. Unfortunately, compound **2** did not increase glucose transport in soleus or epitrochlearis muscle from lean rats.⁶¹ GSK3 inhibition may not improve glucose uptake in normal lean muscle because the insulin stimulatory effects may already be maximal. The impairment in ZDF rats might be due to GSK3 dysregulation. In studies of **2** and **36a** in human skeletal muscle, stimulation of glucose transport required more prolonged exposure to the inhibitors.¹⁰ Increased insulin-stimulated glucose uptake was detected at 6 h of treatment with a GSK3 inhibitor, and the effect increased with continuous exposure up to 24 h. With increased cell surface GLUT4 but not total cellular GLUT4, the mechanism of GSK3 inhibition seems to be associated with insulin-stimulated translocation signals. Along with the increase of glucose transport in human muscle, IRS-1 protein abundance was decreased while maximal insulin-stimulated AKT phosphorylation was not altered.¹⁰ GSK3 phosphorylation of IRS-1 can impair insulin signaling,⁶² and hyperphosphorylation of IRS-1 induces its degradation by proteasomes.^{10,63} Thus, a GSK3 inhibitor may enhance glucose transport by reducing IRS-1 phosphorylation and/or augmenting its translation through eIF2B activity, also a substrate for GSK3.⁶⁴ GSK3 inhibition clearly mimics some of the downstream effects of insulin by activating GS while the insulin-sensitizing effects on glucose uptake could be additive or different from those of the insulin pathway.

In Vivo Efficacy. The investigation of the pharmacology of our GSK3 inhibitors began with the assumption that dysregulation of GSK3 might play a role in NIDDM or type II diabetes. Insulin resistance, which is also observed in obesity and metabolic syndrome (syndrome X), results in impaired glucose uptake and/or metabolism by the key regulatory peripheral tissues (muscle, adipose, and liver).^{65,66} A major pathway for glucose metabolism in the body is muscle glycogen synthesis, which is defective in type II diabetics.⁶⁷ While it has been hypothesized that the reduced GS activity might be

related to downregulation by kinase-mediated phosphorylation, only recently has the link with GSK3 been established. In type II diabetics and other insulin-resistant individuals, GS activity was reduced, but not protein level. The reduced GS activity was correlated with an increase in total GSK3 activity and protein level.⁹ Additionally, because suboptimal glycogenesis in type II diabetics may be linked to impaired glucose transport,⁶⁸ it is apparent that the rates of both glucose uptake and glycogen synthase (GS) can be limiting for glycogen accumulation.⁶⁹ With the knowledge that our GSK3 inhibitors could improve the activity of GS in muscle and liver cells and improved the rate of insulin-activated glucose transport in muscle, the *in vitro* studies supported the potential use of our inhibitors for the improvement of glucose metabolism in type 2 diabetes.

Because GSK3 was a novel target for intervention in diabetes, we decided to characterize our compounds in a broad range of animal models and study designs. We expected that this approach would help us establish a detailed pharmacological profile which would help direct chemical optimization and guide clinical development. Compounds which passed our initial potency criteria (IC₅₀ < 25 nM and EC₅₀ < 1 μM) were first assessed in *db/db* and/or *ob/ob* diabetic mice. These mice, which have a genetic leptin or leptin receptor deficiency respectively, are well validated for their predictive value with other diabetes therapeutics and share similar dysregulation as that reported in humans.⁷⁰ Compounds which gave significant oral efficacy in these models in an oral glucose tolerance test (oGTT) and which had acceptable bioavailability and formulation properties were further examined in Zucker diabetic fatty (ZDF) (*fa/fa*) GMI rats which are insulin-resistant and perhaps the most well-established animal model for type II diabetes.^{70–74} A potential link to GSK3 stems from a report that the obese ZDF rats exhibit downregulated IRS-1 and IRS-2 in liver and muscle.⁷⁵ Additionally, obese, but not lean, ZDF (*fa/fa*) rats showed an increase in basal GSK3 activity in skeletal muscle.⁷⁶ These models would provide the

(a) Improved glucose tolerance with insulin conservation. (b) Plasma exposure profile of compound 1.

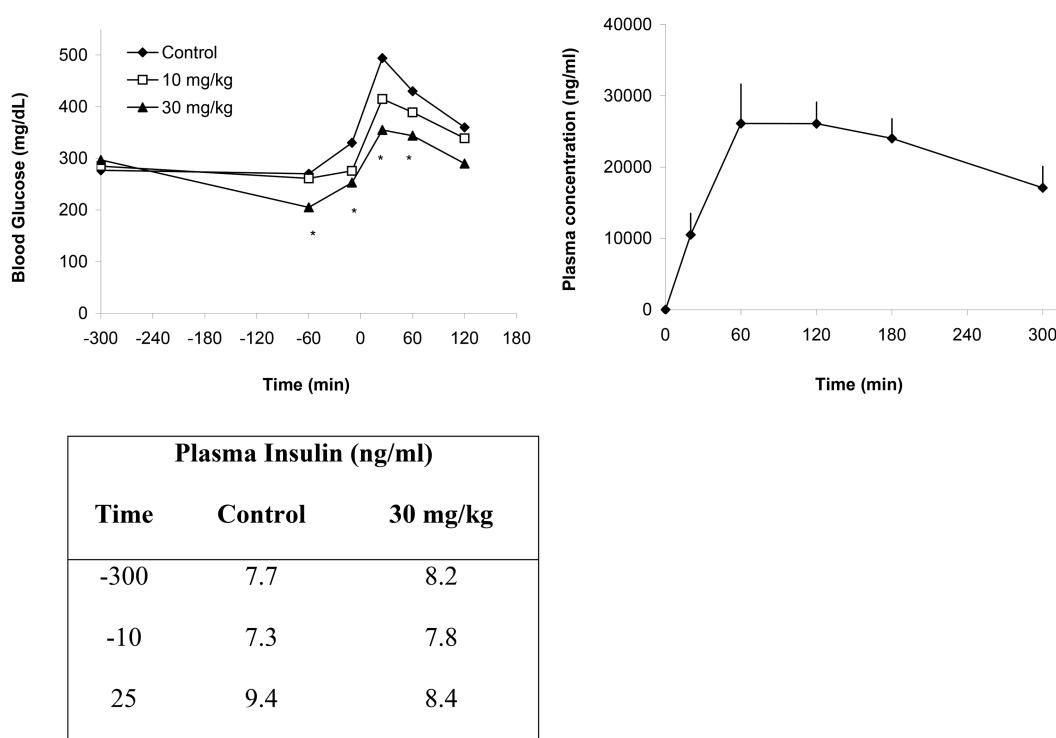


Figure 4. Oral exposure and efficacy of compound 1 administered to diabetic *db/db* mice. (a) Improved glucose tolerance with insulin conservation. Treatment with vehicle control (10% captisol) or indicated doses of compound 1 at -4.5 and -0.5 h relative to $t = 0$ oral glucose. Groups of 6–8 mice per treatment fasted for ~ 6 h prior to a oGTT, SEM $\leq 15\%$. (b) Plasma concentration vs time profile: 50 mg/kg compound 1 formulated in 15% captisol administered once orally to 8–9 week old female *db/db* mice. Quantitation by LC/MS/MS. Results are mean \pm SE from six animals.

foundation for evaluating PD/PK relationships and insight for further in vivo optimization as our program advanced.

Our first probes for in vivo activity, **25a** and **35a**, gave modest reductions in percent plasma glucose AUC following an oral glucose challenge (Table 10). However, as the plasma half-life of these and other similar molecules being screened often ranged 1–2 h in rodents, we chose to dose twice prior to the oGTT (at 4.5 and 0.5 h prior to glucose administration) to improve the sensitivity of the assay as well as to allow responsiveness to compounds of varying pharmacokinetics. The concentration of compound in circulation was monitored following the dosing and during the oGTT at intervals to help assess and compare the efficacy between compounds. While encouraging, the potency of **25a** and **35a** was hampered by poor solubility and bioavailability. With a great boost in in vitro potency, compound **2** gave our first significant ($>20\%$) improvement in glucose disposal in the oGTT. While **2** suffered from the same obstacles for formulation and absorption, the improved potency of the compound seemed to partially compensate for its low bioavailability. Bioavailability improved with **51b**, the cyanopyridine analogue of **2**, but the efficacy fell in relation to the in vitro potency. Thus, we sought to improve the bioavailability and solubility of the compounds while maintaining the excellent potency of the series. However, this proved to be difficult. With a wide array of polar groups at C-5 (Table 6) showing in vitro potency, few were yielding improvements in oral absorption or efficacy in the *db/db* mouse oGTT. Strong basic charges at C-5 like the monoketopiperazine **60o** did not seem to have good bioavailability. Alternately, the noncharged hydroxymethyl compound **60i**

was well absorbed but might not be reaching the important tissues for glucose metabolism, such as muscle, which might account for the low oGTT activity. We turned our attention back to the C-linked imidazoles at C-5 of the pyrimidine. This group appeared to boost bioavailability and increase solubility. Compound **36a** proved to be a turning point for the optimization of the series.

In captisol formulation, **36a** was well absorbed and gave excellent potency in the mouse oGTT (Table 10). When advanced to the ZDF rat model, **36a** was remarkably efficacious at 8 mg/kg, showing a 29% reduction in glucose AUC following the oGTT. Additionally, the compound was acceptably bioavailable (33%) with a half-life of more than 2 h in rat. With the C-linked imidazole, the compounds were more bioavailable and more easily formulated. However, when formulated in slightly acidic water, the absorption fell, as seen in **36b**. However, despite the 6% bioavailability and 43 min half-life, **36b** was still as highly efficacious as **36a**. The in vivo potency of **36b** seems to indicate enhanced tissue distribution to important compartments for efficacy. Compound **36c**, while possessing better bioavailability than **36b**, was less active in mice and ZDF rats. A detailed analysis of the tissue distribution demonstrated that efficacy in the oGTT studies was correlated with good bioavailability and with compounds which partitioned well into muscle and liver tissue. Efficacy did not correlate with plasma protein binding, but lower protein binding was associated with broader tissue distribution. Many of the similar C-5 imidazole analogues, such as **61r**, were potent in vivo but did not show improvements in bioavailability or half-life. Caco-2 experiments indicated that these compounds

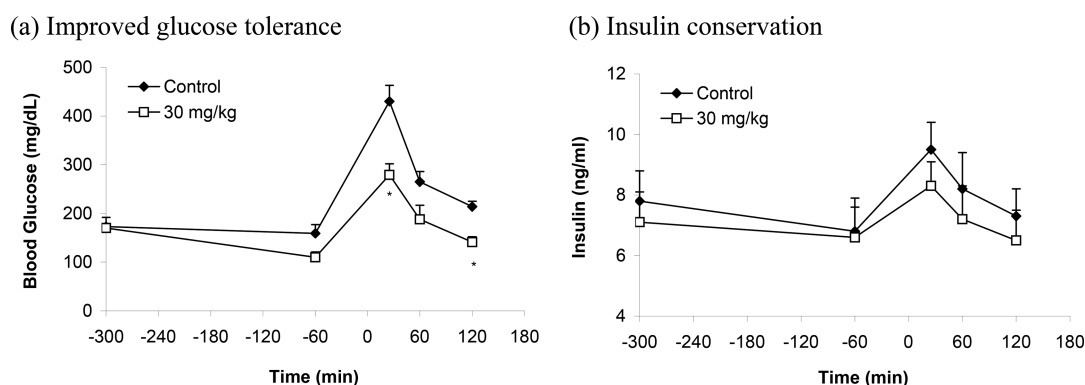
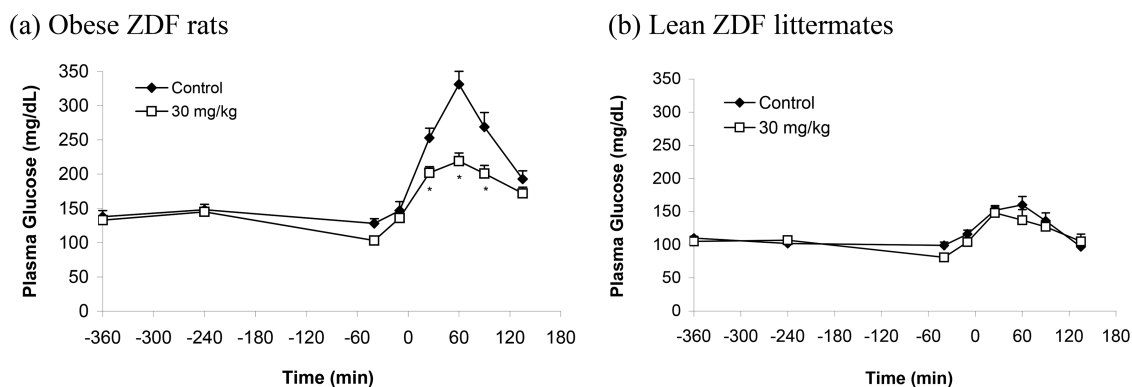


Figure 5. Improved glucose tolerance with insulin sparing in diabetic *ob/ob* mice treated orally with compound 1. (a) Improved glucose tolerance. oGTT as described in Figure 4 with 9–10 week old *ob/ob* mice. $n = 6–8$ animals/group, mean \pm SEM. (b) Insulin conservation. Plasma insulin levels ($n = 6–8$ animals/group, mean \pm SEM).



| Plasma Insulin (ng/ml \pm SEM) | | |
|----------------------------------|---------------|---------------|
| Time (min) | Control | Compound 1 |
| -250 | 7.2 \pm 0.6 | 6.3 \pm 0.3 |
| -45 | 6.9 \pm 0.3 | 5.3 \pm 0.3 |
| 25 | 8.5 \pm 0.7 | 4.8 \pm 0.2 |
| 60 | 7.8 \pm 0.8 | 5.2 \pm 0.5 |

| Plasma Insulin (ng/ml \pm SEM) | | |
|----------------------------------|---------------|---------------|
| Time (min) | Control | Compound 1 |
| -250 | 0.2 \pm 0.1 | 0.3 \pm 0.1 |
| -45 | 0.2 \pm 0.1 | 0.3 \pm 0.1 |
| 25 | 0.4 \pm 0.1 | 0.6 \pm 0.1 |
| 60 | 0.3 \pm 0.1 | 0.4 \pm 0.1 |

Figure 6. Differential responsiveness of obese vs lean ZDF rats to oral treatment with compound 1. (a) Obese ZDF rats. Ten-week-old ZDF (*fa/fa*) rats fasted overnight and treated with vehicle control (captisol solution) or 30 mg/kg compound 1 4.5 and 0.5 h prior to oGTT. Methods as described above, $n = 8$ /group, results are mean \pm SEM. (b) Lean littermates. Same as in (a) except age-matched lean littermates.

were not PGP pump substrates. In general, the compounds tended to be permeable but poorly soluble. Bioavailability could be enhanced with formulations such as captisol. As noted earlier, another factor in efficacy and PK was metabolism. The C-imidazole underwent first pass metabolism which could be addressed by installing a methyl group. Also noted during the rodent studies was the increased absorption of the cyanopyridine group. Bringing these enhancements together in compound 1 yielded a compromise between potency, efficacy, and bioavailability. While compound 1 was not easily formulated in water as a solution, it was readily absorbed as a microcrystalline CMC suspension as the free base. Possessing superior efficacy in the ZDF model (38% reduction in oGTT)

and a 90 min half-life, compound 1 became our first lead compound and advanced into more sophisticated pharmacological evaluation.

Oral administration of 1 to *db/db* mice prior to an oral glucose challenge yielded a dose-related improvement in glucose disposal (Figure 4a). The PD/PK relationship closely matched the time course of the PK studies at doses relevant for efficacy in the *db/db* mouse oGTT (Figure 4b). At the higher dose of 30 mg/kg, there was a trend for reduced hyperglycemia prior to the glucose administration. In treated animals, plasma insulin levels were similar, or possibly conserved, relative to vehicle controls. During oGTT studies, glucose levels in the urine were not elevated in compound- or vehicle-treated

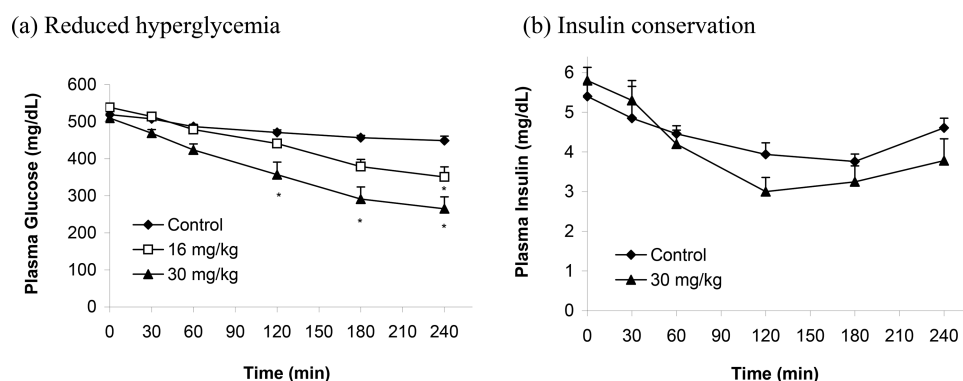


Figure 7. Given orally, compound **1** reduces hyperglycemia with insulin conservation in ZDF (*fa/fa*) rats. (a) Reduced hyperglycemia. Twelve week old male ZDF (*fa/fa*) rats with food removal 3–4 h prior to single oral administration of vehicle control (15% captisol) or indicated doses of compound **1**. Serial tail-snip bleeds from $n = 8$ /group. (b) Insulin conservation. Plasma insulin levels in same animals. Results are mean \pm SEM.

rodents (data not shown); therefore, it was concluded that there was a dose-dependent improvement in whole body glucose disposal. By employing the oGTT, efficacy could be quantified as the percent reduction in glucose AUC for comparison between GSK3 inhibitors and reference therapeutics, such as troglitazone, rosiglitazone, and metformin. The magnitude of improved glucose disposal observed with compound **1** at 30 mg/kg was comparable to that following treatment with metformin or troglitazone. Notably, however, efficacy can be seen 30 min after dosing with compound **1** while observable improvement in oGTT typically requires several days to 2 weeks of dosing with metformin or troglitazone.

Similar results were observed with compound **1** when tested in an oGTT in *ob/ob* mice. Glucose disposal was improved in an insulin-sparing manner (Figure 5). Within the age ranges tested, the *ob/ob* mice are less hyperglycemic and insulin resistant than the *db/db* mice and generally exhibited slightly greater efficacy upon comparison. Further, monitoring of blood glucose levels for an extended period up to 20 h following GSK3 inhibitor treatment indicated that there was no compensatory rebound hyperglycemia in the treated animals. To further demonstrate the utility of our GSK3 inhibitors beyond genetic defects in leptin or leptin receptor (*ob/ob* or *db/db* mice respectively), we made use of an alternative mouse model based on a high fat diet and intermittent streptozotocin treatment wherein animals progress to glucose intolerance and then overt diabetes as is observed in man.⁷⁷ Employing the same test compound **1** and regimen, these mice were likewise tested in an oGTT and showed improved glucose tolerance (53% reduction in postchallenge glucose AUC) in an insulin-conserving manner (data not shown). Thus, in three different mouse models of hyperglycemia, compound **1** consistently improved glucose disposal without an increase in peripheral insulin levels, increasing our confidence in GSK3 as a target for therapeutic intervention in type II diabetes.

To further validate the concept for GSK3 inhibition, we wanted to demonstrate that inhibitor treatment, while lowering hyperglycemia, would not induce hypoglycemia which can be caused by other treatments such as insulin. To investigate the potential for hypoglycemia at an efficacious dose, compound **1** was evaluated in 12-week-old ZDF (*fa/fa*) obese, diabetic rats for alteration of glucose disposal in a oGTT model as described above. Oral administration of **1** led to significant improvement of glucose disposal accompanied by insulin sparing relative to controls at dose levels of 30–48 mg/kg (Figure 6a). To

determine if the glucose response to GSK3 inhibition was limited to insulin-resistant, glucose-intolerant animals rather than animals with normal metabolic control, we treated lean littermates of 10-week-old obese, mildly diabetic animals with compound **1** at 30 mg/kg dose. Confirming our expectation that GSK3 inhibition would only have a significant effect in diabetic animals, the metabolically impaired animals showed normalization of their oral glucose tolerance following treatment with **1** (Figure 6a), whereas the lean littermates showed little or no change in plasma glucose or insulin response (Figure 6b). This indicates that GSK3 inhibition should only correct hyperglycemia in diabetic animals to normoglycemic levels and underscores an important safety profile for an antidiabetic therapy. As in the nongenetic mouse model, a recently derived rat model of obesity and glucose-intolerance uses SHHF rats which also exhibit congestive heart failure (SHHF rats were purchased from Charles River). Because the metabolic abnormality in SHHF rats is not linked to a leptin defect as in ZDF rats, the impressive reduction in hyperglycemia and improved glucose tolerance observed with treatment of SHHF rats represented an additional element of concept validation for GSK3 inhibition (data not shown).

To better understand the pharmacodynamics of GSK3 inhibition in a setting more closely aligned with diabetic treatment in humans, we investigated the regulation of glucose metabolism by compound **1** independent of glucose challenges. Acute studies were performed to monitor the effect of GSK3 inhibition on plasma hyperglycemia and insulin levels. The GSK3 inhibitor was orally administered once to moderately diabetic ZDF (*fa/fa*) rats with a fasted basal hyperglycemia at 500–550 mg/dL. A dose-related and significant (at 30 mg/kg) reduction in hyperglycemia was observed which initiated within 60 min of administration and yielded a maximum reduction of ≥ 150 mg/dL (Figure 7a). However, there was only a trend toward insulin lowering relative to the vehicle controls (Figure 7b). The pharmacodynamics correlated well with the pharmacokinetics as the onset of glucose lowering coincided with compound plasma levels approaching maximal concentrations (C_{max}) and later with diminishing response coinciding with compound elimination. In ZDF rat, compound **1** had an oral half-life of 92–98 min, %F of 36–43%, oral C_{max} of 0.4 μ g/mL, oral AUC of 85 μ g-min/mL, iv CL of 43 (mL/min)/kg, and iv V_{ss} of 3.6 L/kg. In the longer-term studies, compound **1** was continuously infused intravenously over a 4-day period at a total dose of ~ 92 mg/kg/d in order to ascertain the impact of high, sustained GSK3 inhibitor exposure on circulating glucose

and insulin levels. Interestingly, a significant reduction in fasting hyperglycemia to nearly normoglycemia was observed without a significant change in plasma insulin (Table 11). Further

Table 11. Effect of Sustained Compound 1 Exposure^a on ZDF (*fa/fa*) Rat Glycemia and Insulinemia

| parameter | time | control ^a | compd 1 ^a |
|------------------------------|--------------|----------------------|----------------------|
| glucose (mg/dL) ^b | pretreatment | 188 ± 18 | 223 ± 18 |
| | day 4 | 181 ± 20 | 116 ± 6 |
| Insulin (ng/mL) ^b | pretreatment | 3.5 ± 0.4 | 3.9 ± 0.6 |
| | day 4 | 4.0 ± 0.4 | 3.1 ± 0.4 |

^aIntravenous prime (5 mg/kg) with continuous infusion at 64 μ g/kg/min for 4 days to 12–13 week old ZDF (*fa/fa*) rats. ^bPlasma samples from overnight-fasted animals.

studies using compound 1 suggest that glucose disposal occurs primarily in the liver due to a 2–3-fold increase in liver glycogen formation with a concomitant ~40% reduction in basal endogenous glucose output.⁷⁸ However, on the basis of our previous findings that compound 1 activates GS and improves insulin-initiated glucose uptake in muscle cells, chronic treatment may lead to increased glucose disposal in muscle. Both acute and chronic studies indicate that compound 1, and GSK3 inhibitors of this class in general, have the potential to significantly reduce circulating plasma hyperglycemia with an onset of action just 1–2 h after dosing without an immediate hyperglycemic rebound. Together, these results indicate that GSK3 inhibitors, like compound 1, can correct glucose metabolism in insulin-resistant nonfasted hyperglycemic animals which would be comparable to the disease state in man.

Because of GSK3's role in the wnt pathway, there is concern that inhibition of GSK3 might lead to increased risk of cancer or tumorigenicity.⁷⁹ The wnt pathway is important in early embryonic development in mammals, but overexpressed or mutated components of wnt signaling, such as mutated β -catenin or APC, have been identified in cancer.^{80–82} GSK3 phosphorylation of β -catenin leads to the degradation of the protein. Many colon cancers are associated with mutated β -catenin which, like GSK3 inhibition, renders the protein resistant to degradation. Mice which express β -catenin lacking the GSK3 phosphorylation sites quickly develop intestinal polyps.⁸³ On the basis of these and other observations, there is concern that long-term GSK3 inhibition may increase carcinogenic risk as a result of raised β -catenin levels and β -catenin-regulated transcription. Further, lithium ions, a non-specific GSK3 inhibitor, have been shown to increase the concentration of β -catenin in transformed cells.⁸⁴ However, lithium treatment, which has been used for over 50 years at therapeutic concentrations which should inhibit GSK3, does not lead to increased incidence of cancer.^{85,86} In fact, use of lithium seems to correlate with increased survival rates in some cancers.⁸⁷ Chronic lithium inhibition was tested in the APC multiple intestinal neoplasia mouse model, which resulted in no increase in tumorigenesis.⁸⁸ This indicates that GSK3 inhibitors may not exacerbate intestinal polyp formation. Studies with our GSK3 inhibitors indicate that β -catenin is not stabilized in primary cells following inhibitor treatment.⁵⁹ In contrast, we and others have observed elevation of β -catenin in partially transformed cells with GSK3 inhibitors.^{84,89} Unlike transformed cells with an activated ras oncogene, our GSK3 inhibitors were unable to induce cell growth in NIH3T3 cells or rat 1 fibroblasts

in soft agar. Furthermore, a 20 h infusion of compound 1 in ZDF rats (equivalent to 130 mg/kg/day), which is 3-fold above the efficacious dose, does not elevate β -catenin levels or cyclin D1 mRNA in brain, liver, lung, colon, or adipose tissue.⁵⁹ These results may indicate that GSK3 inhibition alone is not enough to increase β -catenin levels in normal cells but might require that additional transforming signals already exist. For example, in contrast to intestinal polyposis, stabilization of β -catenin and activation of the Wnt pathway is not sufficient for hepatocarcinogenesis.⁹⁰ In standard preclinical 5 day toxicity studies in rodents, the compounds were well tolerated at many-fold above their efficacious doses. Active compounds, such as 1, and structurally related inactive compounds ($IC_{50} > 1 \mu$ M, no CHO cell activity) showed similar mild adverse effects at high doses, which mostly included liver chemistry changes. Because superior in vitro potency and in vivo efficacy did not correlate with toxicity, these studies suggest that our observed adverse side effects were not target related. While these studies are very encouraging, long-term animal studies will certainly be needed to assess the carcinogenic risk and effects of chronic dosing of GSK3 inhibitors.

In addition to demonstrated efficacy in the treatment of NIDDM, 1 has been evaluated for treatment of several other indications. These include the treatment type I diabetes-related cardiac parasympathetic dysfunction⁹¹ as well as the treatment of hyperglycemia and dyslipidemia for reducing atherogenesis.⁹² It has shown potential outside of the metabolic disease area in the treatment of human pancreatic cancer.⁹³ Compound 1 has also been used to investigate the role of GSK3- β in multiple pathways using chemogenomics. It has also shown value in keeping embryonic stem cells in a pluripotent state, thus allowing more efficient culturing.^{94,95}

In conclusion, we have developed highly selective, potent, low-molecular-weight GSK3 inhibitors. The series was found to be ATP-competitive and X-ray crystallography confirmed that the compounds bound in the ATP-binding site. Selectivity arose from lipophilic interactions in areas unique to GSK3. We have demonstrated that our inhibitor series activates GS in liver and muscles cells and has the ability to improve glucose transport in treated muscle cells. The ability of compound 1 to enhance insulin action in insulin-resistant rodent models was shown in studies of acute glucose tolerance (oGTT) and in reduction of fasting basal hyperglycemia. Enhanced glucose disposal was associated with a trend toward insulin sparing. The onset of improved glucose disposal was observed within 1–2 h of acute dosing with a tight PD/PK relationship. In comparison to other diabetes treatments, GSK3 inhibition does not lead to hypoglycemia when lean nondiabetic rodents are given efficacious doses of compound 1. Our research indicates that GSK3 inhibitors hold promise as novel insulin sensitizers and potentially a new treatment for diabetes. Characterization of our compounds in conjunction with metformin and thiazolidinediones may show that combination therapy will yield enhanced benefits over monotherapy.

EXPERIMENTAL SECTION

General. Unless otherwise noted, all starting materials and dry solvents were obtained from commercial suppliers and were used without further purification. Solvents were stored with 3 Å molecular sieves under dry argon. Reactions involving air and/or moisture sensitive reagents were executed under an atmosphere of dry argon, and the glassware was flame-dried under vacuum. All compounds which were synthesized on resin were first cleaved under acidic (TFA)

conditions, filtered to remove most polymer residue, and dried to remove solvents before undergoing physical characterization by NMR, HPLC, LCMS (HPLC/MS), and elemental analysis. While the same number is used for both the resin-bound and the related cleaved material, only resin free material was characterized, only yields of cleaved material was reported, and every attempt was made to clearly indicate which material was being described in the text and through footnotes. Nuclear magnetic resonance (NMR) analysis was performed with a Varian 300 MHz NMR (Palo Alto, California). Proton (^1H , 300 MHz) and carbon (^{13}C , 75 MHz) nuclear magnetic resonance (NMR) spectra were obtained as solutions in deuteriochloroform (CDCl_3) unless otherwise indicated. ^1H and ^{13}C chemical shifts are reported in parts per million (ppm, δ) downfield relative to tetramethylsilane (TMS), which was referenced to the solvent. Coupling constants are reported in hertz (Hz). Spectral splitting patterns are designated as s, singlet; d, doublet; t, triplet; q, quartet; m, multiplet; and br, broad.

Analytical HPLC samples were run on a Waters Millennium chromatography system with a 2690 separation module (Milford, Massachusetts) using reverse phase analytical columns (Alltima 5 μ C-18, 4.6 mm \times 250 mm from Alltech (Deerfield, Illinois)). A gradient elution was used, typically starting with 5% acetonitrile/95% water and progressing to 100% acetonitrile over a period of 40 min. All solvents contained 0.1% trifluoroacetic acid (TFA). Compounds were detected by ultraviolet light (UV) absorption at 220 and 254 nm. Liquid chromatography/mass spectrometric analysis (LCMS) was performed on either a Waters Micromass Platform LCZ or a Hewlett-Packard (HP) 1100 series LC/MSD electrospray mass spectrometer with an LC module. High resolution mass spectrometry (HRMS) was performed at UC Berkeley's mass spectrometry facility or on a Fisons VG electrospray mass spectrometer. All masses are reported as those of the protonated parent ions. Elemental analysis of compounds was determined by Desert Analytics (Tucson, Arizona). Melting points were determined on a Laboratory Devices Mel-Temp apparatus (Holliston, Massachusetts).

Flash chromatography was performed according to the established protocol with Merck silica gel 60 Å (230–400 ASTM). Purity was assessed by thin layer chromatography (TLC) using glass or plastic backed silica gel plates, such as, for example, Baker-Flex Silica Gel 1B2-F flexible sheets. TLC results were readily detected visually under ultraviolet light or by employing well-known iodine vapor and other various staining techniques. Preparative separations were carried out using either a Flash 40 chromatography system and a KP-Sil, 60 Å (Biotage, Charlottesville, Virginia), a Chromatotron radial chromatography device (Harrison Research, Palo Alto, California), or by HPLC using a C-18 reversed phase HPLC column. Typical solvents employed were dichloromethane, methanol, ethyl acetate, hexane, acetonitrile water, TFA, and triethyl amine.

Syntheses. All compounds were examined for purity by HPLC, HPLC/MS, and/or ^1H NMR, as specified below. Unless explicitly stated, all compounds have a purity of at least 95%.

6-[2-[4-(2,4-Dichloro-phenyl)-5-(4-methyl-1H-imidazol-2-yl)-pyrimidin-2-ylamino]-ethylamino]-nicotinonitrile (1). A solution of sodium ethoxide (0.62 g, 8.66 mmol) dissolved in abs ethanol (15 mL) was added to a stirred mixture of 1-(2,4-dichloro-phenyl)-3-dimethylamino-2-(4-methyl-1H-imidazol-2-yl)-propenone (**31b**) (2.67 g, 8.25 mmol), *N*-[2-(5-cyano-pyridin-2-ylamino)-ethyl]-guanidine (**33**) (2.08 g, 8.65 mmol), and abs ethanol (20 mL). The reaction was then heated to 75–80 °C for 2.5 h. On cooling, the reaction was diluted with ethyl acetate (400 mL) washed with satd aq NaHCO_3 (100 mL), distilled water (2 \times 100 mL), and brine (100 mL), dried (Na_2SO_4), filtered, and concentrated. The crude product (~50% purity) was purified by flash chromatography over silica gel. The column was run starting with ethyl acetate/hexane (50:50 v/v), then ethyl acetate which was used until all of the fast moving impurities had been removed. The product was eluted with 1.5% methanol/ethyl acetate (1.5:98.5 v/v). The column was monitored by TLC using methanol/ethyl acetate (5:95 v/v) as the solvent system. The product had UV activity in the long wavelength region. The proper fractions were condensed. The off-white solid was dried overnight in vacuo,

giving 1.04 g (28%) of final product 6-[2-[4-(2,4-dichloro-phenyl)-5-(4-methyl-1H-imidazol-2-yl)-pyrimidin-2-ylamino]-ethylamino]-nicotinonitrile (**1**) (HPLC, 99% at 482 nm; HPLC/MS, m/z 324 [MH^+]). ^1H NMR ($\text{DMSO}-d_6$) δ 8.65 (d, J = 20 Hz, 1H), 8.40–8.17 (m, 2H), 7.81 (br s, 1 H), 7.73–7.43 (m, 4H), 7.30 (s, 1 H), 6.55 (dd, J = 22, 9 Hz, 1H), 4.12–3.05 (br m, 4H), 2.23 (s, 3H). ^{13}C NMR (pyridine- d_5 , 70 °C) δ 11.96 (br s, 3H), 9.29 (s, 1H), 8.57 (br s, 1H), 8.46 (d, J = 2 Hz, 1H), 8.37 (br s, 1H), 7.70 (d, J = 8 Hz, 1H), 7.47 (dd, J = 9, 2 Hz, 1H), 7.37 (d, J = 2 Hz, 1H), 7.25 (dd, J = 8, 2 Hz, 1H), 7.21 (s, 2H), 6.73 (d, J = 9 Hz, 1H), 4.02–3.86 (br m, 4H), 2.29 (s, 3H). ^{13}C NMR ($\text{DMSO}-d_6$) δ 163.1, 161.1, 160.3, 153.4, 141.5, 138.8, 136.0, 133.8, 133.6, 131.6, 129.8, 127.8, 119.4, 118.2, 110.8, 96.3, 41.7, 10.9. ^{13}C NMR (pyridine- d_5) δ 163.2, 162.1, 160.5, 156.8, 142.7, 136.5, 134.0, 133.8, 129.9, 128.1, 121.9, 119.7, 111.5, 42.1, 41.9. HRMS (FAB+): m/z calcd for $\text{C}_{22}\text{H}_{19}\text{Cl}_2\text{N}_8$ [MH^+] 465.1104, found 465.1099. Anal. ($\text{C}_{22}\text{H}_{18}\text{Cl}_2\text{N}_8$ + HCl) Calcd: C, 52.66; H, 3.82; N, 22.33; Cl, 21.20, Found: C, 52.36; H, 3.86; N, 22.04; Cl, 21.17.

***N*°-[2-[4-(2,4-Dichloro-phenyl)-5-imidazol-1-yl-pyrimidin-2-ylamino]-ethyl]-3-nitro-pyridine-2,6-diamine (2).** Compound **2** was made by similar procedures as compound **25u** except that the pyrimidine formation was carried out in DMF with (2-(6-amino-5-nitro(2-pyridyl)amino)ethyl)carboxamidinium 4-methylbenzenesulfonate (**32**) and the mixture was stirred for 8 h at 100 °C. The mixture was cooled, filtered, and the filtrate diluted with ethyl acetate and washed with saturated aqueous sodium bicarbonate. Concentration of the organic layers yielded to give 143 mg (76%) of **2** as a yellow solid (HPLC, 99% at 220 nm; HPLC/MS, m/z 486 [MH^+]). ^1H NMR ($\text{AcOD}-d_4$) δ 8.76 (br s, 1H), 8.59 (br s, 1H), 8.28 (br s, 1H), 8.02 (d, J = 15 Hz, 1H), 7.56–7.34 (m, 3H), 7.21 (s, 1H), 6.21 (s, 1H), 3.86–3.62 (br m, 4H). Anal. ($\text{C}_{20}\text{H}_{17}\text{Cl}_2\text{N}_9\text{O}_2$) Calcd: C, 49.39; H, 3.52; N, 25.92; Cl, 14.58, Found: C, 49.11; H, 3.42; N, 24.15; Cl, 14.94.

2-(4-Carbamoyl-benzylidene)-3-oxo-pentanoic Acid Ethyl Ester (5a). A suspension of 4-formyl-benzamide-bound Rink resin **3** (1g, 0.52 mmol) in 8 mL of 1:1 ethanol:dioxane was treated with 3-oxo-pentanoic acid ethyl ester (**4a**) (317 mg, 2.2 mmol) and piperidine (111 mg, 1.3 mmol). The reaction mixture was shaken for 20 h at room temperature. The resin was then filtered, washed with dichloromethane (4 \times 10 mL), dried in vacuo, and used in its subsequent reaction without further purification (after TFA cleavage, crude yield: ~100%. HPLC: 95% at 220 nm. HPLC/MS: m/z 276 [MH^+]).

3-(4-Carbamoyl-phenyl)-2-(pyridine-4-carbonyl)-acrylic Acid Ethyl Ester (5b). Starting from **3** and **4b**, intermediate **5b** was prepared in a similar manner as **5a** (after TFA cleavage, crude yield: ~100%. HPLC: 97% at 220 nm. HPLC/MS: m/z 325 [MH^+]).

3-(4-Carbamoyl-phenyl)-2-(4-nitro-benzoyl)-acrylic Acid Ethyl Ester (5c). Starting from **3** and **4c**, intermediate **5c** was prepared in a similar manner as **5a** (after TFA cleavage, crude yield, ~100%; HPLC, 98% at 220 nm; HPLC/MS, m/z 369 [MH^+]).

6-(4-Carbamoyl-phenyl)-4-ethyl-2-pyrazol-1-yl-1,6-dihydro-pyrimidine-5-carboxylic Acid Ethyl Ester (7a). Resin-bound 2-(4-carbamoyl-benzylidene)-3-oxo-pentanoic acid ethyl ester (**5a**) (100 mg, 0.052 mmol) was treated with pyrazole carboxamide hydrochloride (**6**) (38 mg, 0.26 mmol), powdered NaHCO_3 (11 mg, 0.13 mmol), and *N*-methylpyrrolidinone (1 mL). The reaction mixture was shaken at 70 °C for 24 h. Following cooling, the resin was filtered and washed successively with water (10 mL), methanol (10 mL), DMF (10 mL), methylene chloride (10 mL), and ether (10 mL), then dried in vacuo and used in its subsequent reaction without further purification (after TFA cleavage, crude yield, ~100%; HPLC, 96% at 220 nm; HPLC/MS, m/z 368 [MH^+]).

6-(4-Carbamoyl-phenyl)-2-pyrazol-1-yl-4-pyridin-4-yl-1,6-dihydro-pyrimidine-5-carboxylic Acid Ethyl Ester (7b). Starting from **5b** and **6**, intermediate **7b** was prepared in a similar manner as **7a** (after TFA cleavage, crude yield, ~100%; HPLC, 94% at 220 nm; HPLC/MS, m/z 417 [MH^+]).

6-(4-Carbamoyl-phenyl)-4-(4-nitro-phenyl)-2-pyrazol-1-yl-1,6-dihydro-pyrimidine-5-carboxylic Acid Ethyl Ester (7c). Starting from **5c** and **6**, intermediate **7c** was prepared in a similar manner as **7a** (after

TFA cleavage, crude yield, ~100%; HPLC, 95% at 220 nm; HPLC/MS, m/z 461 $[MH^+]$.

(2-Aminoethyl)(5-nitro(2-pyridyl))amine (8). 2-Chloro-5-nitropyridine (2.0 g, 12.6 mmol) in acetonitrile (10 mL) was added dropwise to ethylenediamine (2.5 mL) in acetonitrile (10 mL). The mixture was stirred overnight at room temperature. Caution is needed at this stage, as when the diamine is added, this reaction can become exothermic. The solvent was removed by rotary evaporation, and the residue was partitioned between dichloromethane (100 mL) and 2.5 M aqueous sodium hydroxide (25 mL). The aqueous layer was further extracted with dichloromethane (4×10 mL). The combined organic layers were washed with a saturated sodium chloride solution (20 mL), dried (Na_2SO_4), and concentrated in vacuo to give (2-aminoethyl)(5-nitro(2-pyridyl))amine as an orange solid 1.74 g (76%), which was used without further purification (HPLC, 99% at 220 nm; HPLC/MS, m/z 183 $[MH^+]$). 1H NMR ($DMSO-d_6$) δ 7.99 (d, J = 9 Hz, 2H), 5.93 (d, J = 9 Hz, 1H), 3.48 (t, J = 6 Hz, 2H), 2.82 (t, J = 6 Hz, 2H). ^{13}C NMR ($DMSO-d_6$) δ 162.6, 157.4, 135.5, 119.1, 103.5, 44.6, 42.0.

6-(4-Carbamoyl-phenyl)-4-ethyl-2-[2-(5-nitro-pyridin-2-ylamino)-ethylamino]-1,6-dihydro-pyrimidine-5-carboxylic Acid Ethyl Ester (9a). A suspension of dihydropyrimidine 7a (50 mg, 0.026 mmol) in NMP (0.75 mL) was treated with N^1 -(5-nitro-pyridin-2-yl)-ethane-1,2-diamine (8) (182 mg, 1 mmol) and acetic acid (16 mg, 0.26 mmol). The reaction mixture was shaken at 80 °C for 24–48 h. After cooling, the resin was filtered and washed with methanol (4×10 mL), DMF (4×10 mL), and methylene chloride (4×10 mL). The resin was then dried in vacuo, and a solution of 5% trifluoroacetic acid in methylene chloride was added. The resin was shaken for 2 h, then filtered and washed with methylene chloride (3×2 mL). The combined filtrates were concentrated, taken up in 1:1 water/acetonitrile and lyophilized to dryness (crude yield, 79%; HPLC, 92% at 220 nm; HPLC/MS, m/z 482 $[MH^+]$).

6-(4-Carbamoyl-phenyl)-2-[2-(5-nitro-pyridin-2-ylamino)-ethylamino]-4-pyridin-4-yl-1,6-dihydro-pyrimidine-5-carboxylic Acid Ethyl Ester (9b). Starting from 7b and amine 8, intermediate 9b was prepared in a similar manner as 9a (crude yield, 75%; HPLC, 88% at 220 nm; HPLC/MS, m/z 531 $[MH^+]$).

6-(4-Carbamoyl-phenyl)-4-(4-nitro-phenyl)-2-[2-(5-nitro-pyridin-2-ylamino)-ethylamino]-1,6-dihydro-pyrimidine-5-carboxylic Acid Ethyl Ester (9c). Starting from 7c and amine 8, intermediate 9c was prepared in a similar manner as 9a (crude yield, 83%; HPLC, 90% at 220 nm; HPLC/MS, m/z 575 $[MH^+]$).

4-(4-Carbamoyl-phenyl)-6-ethyl-2-pyrazol-1-yl-pyrimidine-5-carboxylic Acid Ethyl Ester (10a). The dihydropyrimidine-bound resin 7a (50 mg, 0.026 mmol) was then suspended in THF followed by addition of dicyanodichloroquinone (DDQ) (7 mg, 0.029 mmol). The resulting slurry was stirred for 30 min, at which time the resin was filtered, washed with DMF (2×10 mL), 10% Na_2HCO_3 (2×10 mL), H_2O (2×10 mL), DMF (2×10 mL), methanol (2×10 mL), methylene chloride (2×10 mL), and ether (2×10 mL), dried in vacuo, and used in its subsequent reaction without further purification (after TFA cleavage, crude yield, ~100%; HPLC, 98% at 220 nm; HPLC/MS, m/z 366 $[MH^+]$).

4-(4-Carbamoyl-phenyl)-2-pyrazol-1-yl-6-pyridin-4-yl-pyrimidine-5-carboxylic Acid Ethyl Ester (10b). Starting from dihydropyrimidine 7b and treating with DDQ, intermediate 10b was prepared in a similar manner as 10a (after TFA cleavage, crude yield, ~100%; HPLC, 95% at 220 nm; HPLC/MS, m/z 415 $[MH^+]$).

4-(4-Carbamoyl-phenyl)-6-(4-nitro-phenyl)-2-pyrazol-1-yl-pyrimidine-5-carboxylic Acid Ethyl Ester (10c). Starting from dihydropyrimidine 7c and treating with DDQ, intermediate 10c was prepared in a similar manner as 10a (after TFA cleavage, crude yield, ~100%; HPLC, 97% at 220 nm; HPLC/MS, m/z 459 $[MH^+]$).

4-(4-Carbamoyl-phenyl)-6-ethyl-2-[2-(5-nitro-pyridin-2-ylamino)-ethylamino]-pyrimidine-5-carboxylic Acid Ethyl Ester (11a). A suspension of pyrimidine 10a (50 mg, 0.026 mmol) in NMP (0.75 mL) was treated with N^1 -(5-nitro-pyridin-2-yl)-ethane-1,2-diamine (8) (182 mg, 1 mmol) and acetic acid (16 mg, 0.26 mmol). The reaction mixture was shaken at 80 °C for 24–48 h. After cooling, the resin was filtered and washed with methanol (4×10 mL), DMF (4×10 mL), and methylene chloride (4×10 mL). The resin was then dried in

vacuo, and a solution of 5% trifluoroacetic acid in methylene chloride was added. The resin was shaken for 2 h, then filtered and washed with methylene chloride (3×2 mL). The combined filtrates were concentrated, taken up in 1:1 water/acetonitrile and lyophilized to dryness (crude yield, 81%; HPLC, 96% at 220 nm; HPLC/MS, m/z 480 $[MH^+]$).

4-(4-Carbamoyl-phenyl)-2-[2-(5-nitro-pyridin-2-ylamino)-ethylamino]-6-pyridin-4-yl-pyrimidine-5-carboxylic Acid Ethyl Ester (11b). Starting from pyrimidine 10b and amine 8, intermediate 11b was prepared in a similar manner as 11a (crude yield, 72%; HPLC, 95% at 220 nm; HPLC/MS, m/z 529 $[MH^+]$).

4-(4-Carbamoyl-phenyl)-6-(4-nitro-phenyl)-2-[2-(5-nitro-pyridin-2-ylamino)-ethylamino]-pyrimidine-5-carboxylic Acid Ethyl Ester (11c). Starting from pyrimidine 10c and amine 8, intermediate 11c was prepared in a similar manner as 11a (crude yield, 83%; HPLC, 97% at 220 nm; HPLC/MS, m/z 531 $[MH^+]$).

N-[2-(5-Nitro-pyridin-2-ylamino)-ethyl]-guanidine (13). A mixture of 2-(2-aminoethylamino)-5-nitropyridine (8) (43 g, 236 mmol), 1H-pyrazole-1-carboxamide hydrochloride (35 g, 236 mmol), and acetonitrile (500 mL) were stirred overnight (ca. 20 h) at 70–80 °C. Upon cooling, a yellow precipitate was collected by filtration. The yellow solid was washed thoroughly with acetonitrile (3×100 mL), ethyl ether (3×100 mL), and dried overnight in vacuo, resulting in 53.5 g (87%) of hygroscopic N-[2-(5-nitro-pyridin-2-ylamino)-ethyl]-guanidine (13) (HPLC, 99% at 482 nm; HPLC/MS, m/z 225 $[MH^+]$).

4-(4-Cyano-phenyl)-2-[2-(5-nitro-pyridin-2-ylamino)-ethylamino]-pyrimidine-5-carboxylic Acid Ethyl Ester (16). Benzotriazole carboxamidinium 4-methylbenzenesulfonate (12) (2.0 g, 6.6 mmol) was added to a mixture of amine (8) (1.2 g, 6.6 mmol) and DIEA (1.16 mL, 6.6 mmol) in dry acetonitrile (10 mL) stirred at room temperature overnight. Addition of ether resulted in the precipitation of amino[2-[(5-nitro(2-pyridyl))amino]ethyl]carboxamidinium 4-methylbenzenesulfonate (13) as a yellow solid. The solid was quickly filtered and dried in vacuo and used without further purification in its subsequent step (crude yield, ~100%; HPLC, 98% at 220 nm; HPLC/MS, m/z 397 $[MH^+]$).

N,N -Dimethylformamide dimethyl acetal (DMFDMA) (53 μ L, 0.4 mmol) was added to a stirred solution of ethyl 3-(4-cyanophenyl)-3-oxopropionate (14) (65 mg, 0.3 mmol) in THF (1 mL). After the addition, the solution was heated at 70 °C for 3 h. The reaction solution of 15 was then added to a mixture of amino[2-[(5-nitro(2-pyridyl))amino]ethyl]carboxamidinium 4-methylbenzenesulfonate (13) (120 mg, 0.3 mmol), ethanol (dry) (1 mL), and 1.0 M sodium ethoxide (0.35 mL). The mixture was heated at 80 °C and stirred overnight. Upon cooling, the mixture was diluted with dichloromethane (60 mL) and washed with saturated aqueous sodium bicarbonate (10 mL). The organic layer was concentrated in vacuo and then dissolved in acetonitrile (~10 mL). The solid product 16 was precipitated by addition of water (~10 mL), filtered, and dried in vacuo to give 120 mg (92%) of the product as a yellow solid (HPLC, 97% at 220 nm; HPLC/MS, m/z 434 $[MH^+]$). 1H NMR ($DMSO-d_6$) δ 8.86 (s, 1H), 8.78 (s, 1H), 8.21 (d, J = 12 Hz, 1H), 7.85 (d, J = 11 Hz, 2H), 7.78–7.63 (m, 3H), 6.67 (br s, 1H), 6.56 (br s, 1H), 4.14 (qt, J = 10 Hz, 2H), 2.83 (d, J = 21 Hz, 4H), 1.02 (t, J = 10 Hz, 3H).

4-(4-Cyano-phenyl)-2-[2-(5-nitro-pyridin-2-ylamino)-ethylamino]-pyrimidine-5-carboxylic Acid (17). Powdered sodium hydroxide (60 mg, 1.5 mmol) was added to a suspension of ethyl 4-(4-cyanophenyl)-2-[(2-[(5-nitro(2-pyridyl))amino]ethyl]amino)-pyrimidine-5-carboxylate (16) (1.0 g, 2.3 mmol) in 1:1 methanol/water (25 mL). The mixture was warmed to 60 °C for 45 min with stirring, during which time the reaction became clear. After cooling, the reaction was adjusted to approximately pH 5, which caused the product to precipitate from solution. This yellow solid was collected and dried in vacuo to give 890 mg (98% yield) of 2-[(2-[(5-nitro(2-pyridyl))amino]ethyl)amino]-4-(4-cyanophenyl)-pyrimidine-5-carboxylate (16) as a light-yellow powder (crude yield, ~100%; HPLC, 96% at 220 nm; HPLC/MS, m/z 406 $[MH^+]$).

4-(4-Cyano-phenyl)-2-[2-(5-nitro-pyridin-2-ylamino)-ethylamino]-pyrimidine-5-carboxylic Acid 2-Dimethylamino-ethyl Ester

(18d). O-Benzotriazole-*N,N,N',N'*-tetramethyluronium-hexafluorophosphate (HBTU) was added to a mixture of 2-((2-((5-nitro(2-pyridyl)amino)ethyl)amino)-4-(4-cyanophenyl)-pyrimidine-5-carboxylate (17) (300 mg, 0.74 mmol) and 2-(dimethylamino)ethanol (2 mL) in DMA (2 mL) at room temperature. After 18 h, the solution was partitioned between water (25 mL) and EtOAc (60 mL). The aqueous layer was extracted with ethyl acetate (2 × 10 mL). The combined organic layers were washed with brine (10 mL), dried with sodium sulfate, filtered, and concentrated in vacuo to give 348 mg (99%) of the product **18d** as a yellow solid (HPLC, 99% at 220 nm; HPLC/MS, *m/z* 477 [MH⁺]). ¹H NMR (acetone-*d*₆) δ 9.37 (s, 1H), 9.19 (s, 1H), 8.64 (d, *J* = 9 Hz, 1H), 7.74–7.99 (m, 5H), 6.87 (br s, 4H), 6.77 (t, *J* = 6 Hz, 2H), 6.65 (t, *J* = 9 Hz, 2H), 6.65 (t, *J* = 9 Hz, 2H), 3.72 (t, *J* = 6 Hz, 2H), 8.30 (s, 6H).

4-[5-(3-Methyl-[1,2,4]oxadiazol-5-yl)-2-[2-(5-nitro-pyridin-2-ylamino)-ethylamino]-pyrimidin-4-yl]-benzonitrile (20). To a mixture of ethyl 4-(4-cyanophenyl)-2-((2-((5-nitro(2-pyridyl)amino)ethyl)amino)pyrimidine-5-carboxylate (17) (28 mg, 0.069 mmol) and triethylamine (19.3 μL, 0.14 mmol) in THF (1 mL) was added isobutyl chloroformate (13.4 μL, 0.14 mmol). After stirring at room temperature overnight, acetamidoximine⁴⁰ (10 mg, 0.14 mmol) was added and the mixture was stirred at 70 °C for 6 h until complete as determined by LCMS. The reaction was allowed to cool to room temperature. After stirring an additional 72 h, a light-yellow precipitate was filtered. The solid filter cake was washed successively with methanol (2 × 5 mL) and water (2 × 5 mL) and dried under vacuum. The crude product was purified by preparative C18 reverse phase HPLC to give 3 mg (10%) of the desired oxadiazole (**20**). (HPLC, 97% at 220 nm; HPLC/MS, *m/z* 444 [MH⁺]).

4-[5-Imidazol-1-yl-2-[2-(5-nitro-pyridin-2-ylamino)-ethylamino]-pyrimidin-4-yl]-benzonitrile (25a). 4-(2-Imidazol-1-yl-acetyl)-benzonitrile (**23**) was prepared following a variation of the method described in by Sakurai et al.⁴¹ A solution of 4-cyanophenacyl bromide (**21a**) (0.72 g, 3.2 mmol) and imidazole (**22**) (0.55 g, 8.0 mmol) in toluene (20 mL) was heated at 75 °C for 2.5 h. The mixture was concentrated to dryness in vacuo. The residue was dissolved in dichloromethane (60 mL), washed with a 5% aqueous potassium carbonate solution (10 mL) and water (10 mL), dried (Na₂SO₄), filtered, and concentrated in vacuo to give 0.35 g (53%) of 4-(2-imidazol-1-yl-acetyl)-benzonitrile (**23**) as a pink solid which was used in its subsequent reaction without further purification (HPLC, 97% at 220 nm; HPLC/MS, *m/z* 212 [MH⁺]).

4-(2-Imidazol-1-yl-acetyl)-benzonitrile (**23**) (63 mg, 0.3 mmol) was heated with DMFDMA (2 mL) at 105 °C for 9 h. The solvent was removed in vacuo, and the residue of **24** was dissolved in dry THF (2 mL). The resulting solution of **24** was added to a mixture of amino[2-((5-nitro(2-pyridyl)amino)ethyl)carboxamidinium 4-methylbenzenesulfonate (**13**) (105 mg, 0.3 mmol) and cesium carbonate (326 mg, 1.0 mmol) in THF (15 mL). The mixture was heated overnight at 80 °C, then concentrated in vacuo, redissolved in dichloromethane (60 mL), washed with a saturated sodium bicarbonate solution (10 mL) and brine (10 mL), dried (Na₂SO₄), filtered, and concentrated in vacuo to give the crude product as a yellow solid. The residue was crystallized from ethanol/water to give 83 mg (65%) of **25a** as yellow needles (HPLC, 99% at 220 nm; HPLC/MS, *m/z* 428 [MH⁺]). ¹H NMR (DMSO-*d*₆) δ 8.89 (br s, 1H), 8.41 (br s, 1H), 8.45 (br s, 1H), 8.25 (br s, 1H), 7.78 (br s, 2H), 7.62 (s, 1H), 7.38 (d, *J* = 9 Hz, 2H), 7.19 (s, 1H), 7.03 (s, 1H), 6.58 (br s, 1H), 3.73–3.51 (br m, 4H). Anal. (C₂₁H₁₇N₉O₂/2CH₃CH₂OH) Calcd: C, 57.79; H, 5.63; N, 24.26; O, 12.32, Found: C, 57.92; H, 4.91; N, 24.86; O, 12.07. HRMS (FAB+): *m/z* calcd for C₂₁H₁₈N₉O₂ [MH⁺] 428.1577, found 428.1560.

N-[4-(2-Dichloro-phenyl)-5-imidazol-1-yl-pyrimidin-2-yl]-N'-(5-nitro-pyridin-2-yl)-ethane-1,2-diamine (25u). 1-(2,4-Dichloro-phenyl)-2-imidazol-1-yl-ethanone (**23**) was prepared following a variation of the method described by Sakurai et al.⁴¹ A solution of 2,4-dichlorophenacyl chloride (**21b**) (1.42 g, 6.4 mmol) and imidazole (**22**) (1.18 g, 16.0 mmol) in toluene (40 mL) were heated at 75 °C with stirring for 2.25 h. The mixture was concentrated to dryness in vacuo. The residue was dissolved in dichloromethane (100 mL),

washed with 5% aqueous potassium carbonate solution (10 mL), water (10 mL), and brine (10 mL), dried (Na₂SO₄), filtered, and concentrated in vacuo. The crude product was purified by passage over a pad of silica gel (50 g), eluting with 5% methanol in dichloromethane to give 1.04 g (64%) of 1-(2,4-dichloro-phenyl)-2-imidazol-1-yl-ethanone (**23**) as an orange solid after drying in vacuo (HPLC, 95% at 220 nm; HPLC/MS, *m/z* 255 [MH⁺]).

A solution of 1-(2,4-dichloro-phenyl)-2-imidazol-1-yl-ethanone (**23**) (95 mg, 0.37 mmol) and DMFDMA (2 mL) was heated with stirring at 105 °C for 9 h. The solvent was removed in vacuo, and the residue (**24**) was dissolved in dry THF (2 mL) and added to a mixture of amino[2-((5-nitro(2-pyridyl)amino)ethyl)carboxamidinium 4-methylbenzenesulfonate (**13**) (147 mg, 0.37 mmol) and cesium carbonate (200 mg, 0.6 mmol). The mixture was heated overnight at 80 °C then concentrated in vacuo. The residue was taken up in dichloromethane (50 mL), washed with saturated aqueous sodium bicarbonate (5 mL), water (5 mL), and brine (5 mL), dried (Na₂SO₄), filtered, and concentrated in vacuo to give the crude product. The crude product was purified by radial chromatography on silica gel eluting with MeOH in dichloromethane to give 134 mg (77%) of *N*-[4-(2,4-dichloro-phenyl)-5-imidazol-1-yl-pyrimidin-2-yl]-N'-(5-nitro-pyridin-2-yl)-ethane-1,2-diamine (**25u**) as a yellow solid (HPLC, 96% at 220 nm; HPLC/MS, *m/z* 471 [MH⁺]). ¹H NMR (DMSO-*d*₆) δ 8.86 (br s, 1H), 8.47 (br s, 1H), 8.22 (br s, 1H), 8.19 (br s, 1H), 7.91 (br s, 1H), 7.57 (d, *J* = 42 Hz, 2H), 7.48 (s, 1H), 6.93 (d, *J* = 42 Hz, 2H), 6.58 (br s, 1H), 3.75–3.21 (br m, 4H). Anal. (C₂₀H₁₆Cl₂N₈O₂) Calcd: C, 50.97; H, 3.42; N, 23.78; O, 6.79; Cl, 15.04, Found: C, 50.41; H, 3.39; N, 22.83; O, 10.24; Cl, 13.85.

Compounds **25b–25w** were prepared by similar procedures as **25u**. Identity and purity were minimally assessed by HPLC and HPLC/MS.

4-[2-[2-(5-Nitro-pyridin-2-ylamino)-ethylamino]-5-[1,2,4]triazol-1-yl-pyrimidin-4-yl]-benzonitrile (26). Following a variation of the method described in by Sakurai et al.,⁴¹ a solution of 4-cyanophenacyl bromide (0.72 g, 3.2 mmol) and 1*H*-[1,2,4]triazole (0.55 g, 8 mmol) in toluene (20 mL) was heated at 75 °C for 2.5 h. The mixture was concentrated to dryness in vacuo. The residue was dissolved in dichloromethane (60 mL) and washed with a 5% aqueous potassium carbonate solution (2 × 10 mL) and water (10 mL), dried (Na₂SO₄), filtered, and concentrated in vacuo to give 0.35 g (74%) of 4-(2-[1,2,4]triazol-1-yl-acetyl)-benzonitrile as an off-white solid which was used in its subsequent reaction without further purification (HPLC, 98% at 220 nm; HPLC/MS, *m/z* 213 [MH⁺]).

A solution of 4-(2-[1,2,4]triazol-1-yl-acetyl)-benzonitrile (64 mg, 0.3 mmol) in DMFDMA (1 mL) was heated at 105 °C with stirring for 8 h. The solvent was removed in vacuo, and the residue was dissolved in dry THF (2 mL). The resulting solution was added to a mixture of amino[2-((5-nitro(2-pyridyl)amino)ethyl)carboxamidinium 4-methylbenzenesulfonate (**13**) (120 mg, 0.3 mmol), cesium carbonate (326 mg, 1.0 mmol), and THF (15 mL). The reaction was heated overnight at 80 °C, then concentrated in vacuo, redissolved in dichloromethane (60 mL), washed with a saturated sodium bicarbonate solution (10 mL) and brine (10 mL), dried (Na₂SO₄), filtered, and concentrated in vacuo to give the crude yellow product. The organic layer was concentrated in vacuo. The residue was purified by crystallization ethanol/water to give 47 mg (35%) of **26** as a yellow solid (HPLC, 98% at 220 nm; HPLC/MS, *m/z* 429 [MH⁺]). ¹H NMR (DMSO-*d*₆) δ 8.90 (s, 1H), 8.64 (s, 1H), 8.45 (s, 1H), 8.38 (d, *J* = 10 Hz, 1H), 8.30 (s, 1H), 8.22 (d, *J* = 12 Hz, 2H), 7.75 (d, *J* = 10 Hz, 2H), 6.65 (d, *J* = 10 Hz, 1H), 3.62–3.44 (m, 4H).

1-(2,4-Dichloro-phenyl)-2-(1*H*-imidazol-2-yl)-ethanone (30a). Using procedures similar to those described by Macco et al.,^{42–44} a solution of 2,4-dichlorobenzoyl chloride (**27**) (153 g, 731 mmol) in dichloromethane (75 mL) was added dropwise over 30 min to a stirred solution of 2-methylimidazole (**28**) (20 g, 244 mmol) in dichloromethane (500 mL) (The imidazole was heated to dissolve it in CH₂Cl₂) and *N,N*-diisopropylethylamine (Hünig's base) (101 g, 780 mmol). The reaction mixture was cooled during the addition using an ice–water bath. The ice bath was used to keep the reaction from refluxing. Precooling caused the imidazole to precipitate. The reaction mixture was then heated to reflux for 3.5 h. A thick reddish-black

mixture formed. To dilute the thick heterogeneous reaction, additional dichloromethane (100–200 mL) was added as needed to maintain stirring. On cooling, dichloromethane (500 mL) was added, and the solution was transferred to a separatory funnel. The organic layer was washed with distilled water (3 × 200 mL). An emulsion formed that broke apart on sitting for 15 min or by filtering. The wet organic layer was directly concentrated under reduced pressure without drying. The solid product was then dried in vacuo for several hours. To the resulting dry solid was added a solution of glacial acetic acid and aq concd HCl (2:1 v/v, 500–600 mL). The mixture was then stirred at reflux for ca. 75 min. The acetic acid was removed via rotary evaporator under reduced pressure at 60–80 °C. Distilled water (800 mL) and benzene (400 mL) were added to the solid residue, which was vigorously stirred for 15 min. The solids were filtered off, and the filtrate was transferred to a separatory funnel. After the organic layer was discarded, the aqueous layer was washed with benzene (4 × 150 mL). The aqueous layer was transferred to a large beaker (4 L) and diluted with isopropyl ether (100 mL), which was chosen as a solvent due to its high boiling point. The stirred mixture was basified (pH 7–8) by careful addition of sodium bicarbonate, which leads to the formation of a white solid. Do not use NaOH or any strong bases; this causes the formation of side products. After 2 h of additional stirring, the desired solid was filtered, washed with distilled water (3 × 60 mL) and isopropyl ether (2 × 60 mL), and dried in vacuo overnight, giving 35.0 g (56%) of 1-(2,4-dichloro-phenyl)-2-(1H-imidazol-2-yl)-ethanone (**30a**) (HPLC, 99% at 482 nm; HPLC/MS, m/z 255 [MH^+]). 1H NMR (DMSO- d_6) δ 7.61 (d, J = 6 Hz, 2H), 7.43 (d, J = 6 Hz, 1H), 7.06 (s, 2 H), 5.74 (s, 1H). ^{13}C NMR (DMSO- d_6) δ 160.4, 147.3, 135.8, 133.1, 131.3, 130.9, 129.3, 127.1, 118.3, 87.3.

1-(2,4-Dichloro-phenyl)-2-(4-methyl-1H-imidazol-2-yl)-ethanone (30b). Prepared by a method similar to that of Macco,^{42–44} a solution of 2,4-dichlorobenzoyl chloride (**27**) (37.9 g, 181.0 mmol) in dichloromethane (25 mL) was added dropwise over 20 min to an overhead stirred solution of 2,4-dimethylimidazole (**29**) (5.8 g, 60.3 mmol) (the 2,4-dimethylimidazole (**29**) was heated to dissolve it in CH_2Cl_2) and *N,N*-diisopropylethylamine (Hünig's base) (24.9 g, 193 mmol) in dichloromethane (75 mL). The reaction mixture was cooled during the addition using a water bath. The water bath was only used to keep the reaction from excessive refluxing. Precooling or excessive cooling may cause the imidazole to precipitate. The reaction mixture was then heated to reflux for 5 h. The reaction can turn a darker color. The product was stripped of solvent under reduced pressure, and the resulting solid was dried in vacuo for 1 h. To the resulting dry solid was added a solution (2:1 v/v, 120 mL) of glacial acetic acid and aq concd HCl. The mixture was then stirred at reflux for ca. 90 min. It is important to reflux the mixture at approximately 110–125 °C for 90 min or more as needed to completely break up the benzoyl intermediates. The acetic acid was removed via rotary evaporator. Upon cooling, distilled water (200 mL) and toluene (100 mL) were added to the solid residue, which was vigorously stirred for 30 min. The solids were filtered, rinsed with 50 mL of distilled water, and discarded. The filtrate was transferred to a separatory funnel. After the organic layer was discarded, the aqueous layer was washed with toluene (2 × 100 mL). The aqueous layer was transferred to a large beaker (2 L) and diluted with isopropyl ether (50 mL), which was used due to its higher boiling point. The stirred mixture was basified (pH 7–8) by careful addition of sodium bicarbonate, which led to the formation of a sticky white solid (do not use NaOH or any strong bases; this causes the formation of side products). Dichloromethane (200 mL) was added and stirring continued for 10 min. The organic layer was separated, and the aqueous layer was again extracted with dichloromethane (100 mL). The organic layers were combined and washed with satd aq $NaHCO_3$ (100 mL), distilled water (100 mL), and brine (100 mL), dried (Na_2SO_4), filtered, concentrated, and dried in vacuo, giving 7.4 g (46%) of 1-(2,4-dichloro-phenyl)-2-(4-methyl-1H-imidazol-2-yl)-ethanone (**30b**) (HPLC, 99% at 482 nm; HPLC/MS, m/z 269 [MH^+]). 1H NMR (DMSO- d_6 , 70 °C) δ 7.60 (d, J = 8 Hz, 1H), 7.55 (s, 1H), 7.41 (d, J = 8 Hz, 1H), 6.71 (s, 1H), 5.68 (s, 1H), 3.21 (s, 1H), 2.18 (s, 3H). ^{13}C NMR (DMSO- d_6 , 70 °C) δ 160.3, 146.7, 135.9, 135.9, 132.7, 131.0, 130.5, 129.0, 126.7, 113.8, 86.7, 10.7.

1-(2,4-Dichloro-phenyl)-3-dimethylamino-2-(1H-imidazol-2-yl)-propanone (31a). A mixture of 1-(2,4-dichloro-phenyl)-2-(1H-imidazol-2-yl)-ethanone (**30a**) (15 g, 59 mmol) and *N,N*-dimethylformamide dimethyl acetal (DMFDMA) (150 mL) was stirred for 2.5 h at 70–75 °C. The DMFDMA was then removed under reduced pressure and dried under high vacuum for several hours, giving an orange-yellow solid **31a** in quantitative yield. The enaminone product **31a** was typically used without further purification. The product can be redissolved in solvent and evaporated several times to give a better solid. This can be done if the product is not free flowing (HPLC, 99% at 482 nm; HPLC/MS, m/z 310 [MH^+]).

1-(2,4-Dichloro-phenyl)-3-dimethylamino-2-(4-methyl-1H-imidazol-2-yl)-propanone (31b). A mixture of 1-(2,4-dichloro-phenyl)-2-(4-methyl-1H-imidazol-2-yl)-ethanone (**30b**) (2.22 g, 8.25 mmol) and *N,N*-dimethylformamide dimethyl acetal (DMFDMA, **9**) (25 mL) was stirred for 2.5 h at 70–75 °C. The DMFDMA was then removed under reduced pressure and dried under high vacuum for several hours, giving a light-orange solid **31b** in quantitative yield. The enaminone product **31b** was typically used without further purification. The product can be redissolved in solvent and evaporated several times to give a better solid. This can be done if the product is not free flowing (HPLC, 99% at 482 nm; HPLC/MS, m/z 324 [MH^+]).

***N*-[2-(6-Amino-5-nitro-pyridin-2-ylamino)-ethyl]-guanidine (32).** A mixture of 2-(2-aminoethyl)amino-6-amino-5-nitropyridine (prepared by similar procedures as **8**) (6.50 g, 33.0 mmol), 1H-pyrazole-1-carboxamide hydrochloride (**6**) (4.84 g, 33.0 mmol), and acetonitrile (75 mL) were stirred overnight (ca. 24 h) at 75–80 °C. Upon cooling, a yellow precipitate was collected by filtration. The yellow solid was washed thoroughly with acetonitrile (3 × 50 mL) and ethyl ether (3 × 50 mL) and dried overnight in vacuo, giving 7.49 g (82%) of *N*-[2-(6-amino-5-nitro-pyridin-2-ylamino)-ethyl]-guanidine (**32**) as the HCl salt (HPLC, 92% at 482 nm; HPLC/MS, m/z 240 [MH^+]). 1H NMR (DMSO- d_6) δ 7.93 (d, J = 9 Hz, 1H), 5.97 (d, J = 9 Hz, 1H), 3.48–3.39 (br m, 2H), 3.36–3.26 (br m, 2H).

***N*-[2-(5-Cyano-pyridin-2-ylamino)-ethyl]-guanidine (33).** A mixture of 6-(2-amino-ethylamino)-nicotinonitrile (see procedure below) (9.14 g, 56.4 mmol), 1H-pyrazole-1-carboxamide hydrochloride (**6**) (8.26 g, 56.4 mmol), and acetonitrile (120 mL) were stirred ca. 24 h at 75–80 °C. Upon cooling, a precipitate was collected by filtration. The white solid was washed thoroughly with acetonitrile (2 × 100 mL) and ethyl ether (3 × 100 mL) and dried overnight in vacuo, giving 11.0 g (82%) of *N*-[2-(5-cyano-pyridin-2-ylamino)-ethyl]-guanidine (**33**) as the HCl salt (HPLC, 99% at 482 nm; HPLC/MS, m/z 205 [MH^+]). 1H NMR (DMSO- d_6 , 70 °C) δ 8.36 (d, J = 2 Hz, 1H), 7.90 (br s, 1H), 7.63 (dd, J = 9, 2 Hz, 1H), 7.34 (br s, 3H), 6.65 (d, J = 9 Hz, 1H), 3.45 (t, J = 5 Hz, 2H), 3.36 (t, J = 5 Hz, 2H). ^{13}C NMR (DMSO- d_6 , 70 °C) δ 159.6, 157.1, 152.4, 138.2, 118.3, 108.5, 94.8, 40.0, 39.6.

6-(2-Amino-ethylamino)-nicotinonitrile. A mixture of 2-chloro-5-cyanopyridine (10.0 g, 72.2 mmol), acetonitrile (120 mL), and ethylene diamine (85 mL) were stirred overnight (ca. 16 h) at 75–80 °C under argon. Caution must be taken as the chloropyridine might need to be heated to completely dissolve. *When the diamine is added, this reaction can become exothermic!* The ethylene diamine was removed under reduced pressure and then dried in vacuo for 2–3 h. The residual solution was basified with 1 M sodium hydroxide solution (~100 mL). The aqueous solution was saturated with sodium chloride and extracted with a solution of ethyl acetate/methanol (95:5 v/v) (3 × 150 mL) and with a solution of 95% acetonitrile/methanol (95:5 v/v) (3 × 150 mL). The organic extracts were combined and extracted with a saturated sodium chloride solution (2 × 70 mL). The organic layer was dried with sodium sulfate, filtered, and concentrated under reduced pressure. The crude white to tan solid was triturated with ether (2 × 50 mL) and dried overnight in vacuo, resulting in 9.14 g (78%) of 6-(2-amino-ethylamino)-nicotinonitrile (HPLC, 98% at 482 nm; HPLC/MS, m/z 163 [MH^+]). 1H NMR (DMSO- d_6 , 70 °C) δ 8.33 (d, J = 2 Hz, 1H), 7.60 (dd, J = 9, 2 Hz, 1H), 7.42 (br s, 1H), 6.56 (d, J = 9 Hz, 1H), 3.38–3.26 (m, 2H), 2.73 (t, J = 6 Hz, 2H), 1.98 (br s, 2H). ^{13}C NMR (DMSO- d_6 , 70 °C) δ 159.8, 152.4, 137.9, 118.5, 107.7, 94.0, 44.0, 40.7.

4-[5-(1*H*-imidazol-2-yl)-2-[2-(5-nitro-pyridin-2-ylamino)-ethylamino]-pyrimidin-4-yl]-benzonitrile (**35a**). A solution of 4-(2-imidazol-2-ylacetyl)benzenecarbonitrile (**30a**) (0.32 g, 1.5 mmol) (prepared from 4-cyano-benzoyl chloride (**27**) and 2-methylimidazole (**28**) according to the procedure described by Macco et al.^{42–44}) and DMFDMA (15 mL) was stirred at reflux for 12 h. After concentration of this solution in vacuo, the residual solid was dissolved in DMF (15 mL). To the resulting solution was added Cs₂CO₃ (0.98 g, 3.0 mmol) and (2-(5-nitro(2-pyridyl)amino)ethyl)carboxamidinium 4-methylbenzenesulfonate (**13**) (0.59 g, 1.5 mmol), and the mixture stirred for 8 h at 100 °C. The mixture was cooled, filtered and the filtrate diluted with ethyl acetate (100 mL), and washed with saturated aqueous sodium bicarbonate (2 × 10 mL), water (4 × 10 mL), and brine (10 mL), dried (Na₂SO₄), filtered, and concentrated in vacuo to give 513 mg (80%) of the product as a yellow solid (HPLC, 94% at 220 nm; HPLC/MS, *m/z* 428 [MH⁺]).

Compounds **35b** and **36a–d** were synthesized by procedures similar to those used to produce **36a** with the exception that the correct 1-(substituted phenyl)-2-(1*H*-imidazol-2-yl)-ethanone (**30a**) was used to form the pyrimidine products. Identity and purity were minimally assessed by HPLC and HPLC/MS.

N-[4-(2,4-Dichloro-phenyl)-5-(1*H*-imidazol-2-yl)-pyrimidin-2-yl]-*N'*-(5-nitro-pyridin-2-yl)-ethane-1,2-diamine (**36a**). A solution of sodium ethoxide (4.0 g, 58.8 mmol) dissolved in abs ethanol (100 mL) was added to a stirred mixture of enaminone **31a** (18.2 g, 58.8 mmol), guanidine **13** (15.6 g, 60.0 mmol), and abs ethanol (260 mL). The reaction was stirred at room temperature for 15 min and then at 75–80 °C for 2.5 h. On cooling, a yellow precipitate was collected by filtration. The filtrate was stored for possible further isolation and purification of **36a**. The solid product was washed with abs ethanol (3 × 50 mL), distilled water (3 × 50 mL), and ethyl ether (3 × 50 mL). The yellow solid was dried overnight in vacuo, giving 14.6 g (53%) of final product *N*-[4-(2,4-dichloro-phenyl)-5-(1*H*-imidazol-2-yl)-pyrimidin-2-yl]-*N'*-(5-nitro-pyridin-2-yl)-ethane-1,2-diamine (**36a**) (HPLC, 99% at 482 nm; HPLC/MS, *m/z* 471 [MH⁺]). ¹H NMR (DMSO-*d*₆) δ 8.84 (s, 1H), 8.62 (s, 1H), 8.21 (br s, 1H), 8.01 (br s, 1H), 7.65 (s, 1H), 7.47 (s, 1H), 7.35 (d, *J* = 11 Hz, 2H), 6.90 (s, 2H), 6.51 (br s, 1H), 4.12–3.05 (br m, 4H). ¹³C NMR (DMSO-*d*₆) δ 161.6, 161.3, 158.5, 158.0, 146.9, 141.9, 137.2, 134.4, 133.7, 132.6, 132.2, 131.7, 128.6, 127.2, 114.3, 108.8. HRMS (FAB+): *m/z* calcd for C₂₀H₁₇Cl₂N₈O₂ [MH⁺] 471.0846, found 471.0859.

*N*⁶-[2-[4-(2,4-Dichloro-phenyl)-5-(1*H*-imidazol-2-yl)-pyrimidin-2-ylamino]-ethyl]-3-nitro-pyridine-2,6-diamine (**36b**). A solution of sodium ethoxide (0.27 g, 4.00 mmol) dissolved in abs ethanol (8 mL) was added to a stirred mixture of 1-(2,4-dichloro-phenyl)-3-dimethylamino-2-(1*H*-imidazol-2-yl)-propanone (**31a**) (1.24 g, 4.00 mmol), *N*-[2-(6-amino-5-nitro-pyridin-2-ylamino)-ethyl]-guanidine **32** (1.13 g, 4.08 mmol), and abs ethanol (7 mL). The reaction was then heated to 75–80 °C for 2.5 h (Note: use of excess base or heat can cause side products). On cooling, a yellow precipitate was collected by filtration. The filtrate was stored for possible further isolation and purification of **36b**. The solid product was washed with abs ethanol (3 × 10 mL), distilled water (3 × 10 mL), and ethyl ether (3 × 10 mL). The yellow solid was dried overnight in vacuo, giving 1.36 g (70%) of final product *N*⁶-[2-[4-(2,4-dichloro-phenyl)-5-(1*H*-imidazol-2-yl)-pyrimidin-2-ylamino]-ethyl]-3-nitro-pyridine-2,6-diamine (**36b**) (HPLC, 98% at 482 nm; HPLC/MS, *m/z* 486 [MH⁺]). ¹H NMR (DMSO-*d*₆) δ 8.68 (d, *J* = 22 Hz, 1H), 8.41 (br s, 1H), 8.28 (br s, 1H), 7.91 (dd, *J* = 26, 9 Hz, 2H), 7.68–7.42 (m, 5H), 5.95 (dd, *J* = 26, 9 Hz, 2H), 4.12–3.05 (br m, 4H). ¹H NMR (CDCl₃) δ 9.40 (br s, 4H), 9.29 (s, 1H), 8.70 (s, 1H), 8.13 (d, *J* = 9 Hz, 1H), 7.70 (d, *J* = 9 Hz, 1H), 7.61 (s, 1H), 7.44 (s, 2H), 7.34 (d, *J* = 3 Hz, 1H), 7.28 (dd, *J* = 9, 3 Hz, 1H), 6.27 (d, *J* = 9 Hz, 1H), 4.04–3.83 (br m, 4H). ¹³C NMR (pyridine-*d*₅) δ 163.2, 162.1, 160.5, 156.8, 142.7, 136.5, 134.0, 133.8, 129.9, 128.1, 121.9, 119.7, 111.5, 42.1, 41.9. HRMS (FAB+): *m/z* calcd for C₂₀H₁₈Cl₂N₉O₂ [MH⁺] 486.0955, found 486.0937.

6-[2-[4-(2,4-Dichloro-phenyl)-5-(1*H*-imidazol-2-yl)-pyrimidin-2-ylamino]-ethylamino]-nicotinonitrile (**36c**). A solution of 1-(2,4-dichloro-phenyl)-3-dimethylamino-2-(1*H*-imidazol-2-yl)-propanone (**31a**) (2.67 g, 8.25 mmol) in abs EtOH (10 mL) was added to a

stirring and preheated solution of sodium ethoxide [(0.62 g, 8.66 mmol) (dissolved in abs ethanol (15 mL))], *N*-[2-(5-cyano-pyridin-2-ylamino)-ethyl]-guanidine (**33**) (2.18 g, 9.08 mmol), and abs ethanol (10 mL) at 75–80 °C. The reaction was then heated to 75–80 °C for 2.5 h. The reaction can be monitored by HPLC or by TLC by using 5% methanol in ethyl acetate as the solvent system. The product has UV activity in the long wavelength region. On cooling, the reaction was diluted with ethyl acetate (400 mL) washed with satd aq NaHCO₃ (100 mL), distilled water (2 × 100 mL), and brine (100 mL), dried (Na₂SO₄), filtered, and concentrated under reduced pressure. Please note: Dry over Na₂SO₄ for only 10–20 min. Longer times may cause the product to precipitate over the drying agent! The crude product ca. 2 g (~50–70% purity) was dried in vacuo, resulting in a hard tacky white glass. To the dry glass was added a solution of MeOH/Et₂O (15:85 v/v) (10 mL). The glass was manipulated and stirred to break up any lumps of material until a fine suspension forms. The suspension was allowed to stand for 10–15 min and then filtered. The off-white solid was washed with a solution of MeOH/Et₂O (10:90 v/v) (2 × 5 mL) and then with Et₂O (2 × 5 mL). This procedure gave material in a purity range of 90–99% and ca. 50% yield. The compound can be purified further using a prep HPLC. Impure **36c** (1 g) was loaded onto a large prep HPLC in DMSO (4 mL) containing TFA (100 μL). Using a C18 reverse phase column, the gradient was started at 90:10 H₂O/CH₃CN with a 1 mL/min gradient. After 45 min, the gradient reached 45:50 H₂O/CH₃CN. The compound typically eluted at about 20–25 min. 6-[2-[4-(2,4-Dichloro-phenyl)-5-(1*H*-imidazol-2-yl)-pyrimidin-2-ylamino]-ethylamino]-nicotinonitrile (**36c**) was obtained in high purity (99% pure) with yields between 25 and 45% (HPLC, 99% at 482 nm; HPLC/MS, *m/z* 451 [MH⁺]). ¹H NMR (DMSO-*d*₆) δ 8.67 (d, *J* = 20 Hz, 1H), 7.75–7.43 (m, 6H), 6.62 (dd, *J* = 23, 9 Hz, 1H), 4.12–3.05 (br m, 4H). ¹³C NMR (DMSO-*d*₆) δ 163.3, 162.7, 162.5, 160.1, 159.3, 159.1, 151.9, 151.4, 140.6, 140.5, 139.0, 135.5, 134.0, 132.0, 131.8, 129.1, 128.9, 128.0, 120.2, 118.7, 118.5, 107.1, 106.9, 94.8. HRMS (FAB+): *m/z* calcd for C₂₁H₁₇Cl₂N₈ [MH⁺] 451.0947, found 451.0937.

Compounds **37a** were synthesized by procedures similar to those used to produce **1** with the exception that the correct 1-(2,4-dichloro-phenyl)-2-(4-methyl-1*H*-imidazol-2-yl)-ethanone (**30b**) was used to form the pyrimidine products. Identity and purity were minimally assessed by HPLC and HPLC/MS.

*N*²-(2-(4-(2,4-Dichlorophenyl)-5-(4-methyl-1*H*-imidazol-2-yl)-pyrimidin-2-ylamino)ethyl)-5-nitropyridine-2,6-diamine (**37b**). Compound **37b** was synthesized by procedures similar to those used to produce **1**, with the exception that 2-(2-aminoethyl)amino-6-amino-5-nitropyridine was used to form the pyrimidine (HPLC, 99% at 482 nm; HPLC/MS, *m/z* 500 [MH⁺]). ¹H NMR (DMSO-*d*₆) δ 8.67 (d, *J* = 21 Hz, 1H), 8.53 (br s, 1H), 8.25 (br s, 2H), 7.90 (dd, *J* = 29, 9 Hz, 1H), 7.62–7.43 (m, 3H), 7.29 (s, 1H), 5.97 (dd, *J* = 29, 9 Hz, 1H), 3.82–3.22 (br m, 4H), 2.23 (s, 3H). ¹³C NMR (DMSO-*d*₆) δ 163.6, 163.0, 160.5, 159.9, 158.9, 155.6, 154.9, 140.2, 135.9, 135.9, 135.5, 134.4, 132.6, 132.4, 130.4, 129.6, 128.4, 117.3, 107.7, 103.1, 41.3, 40.3, 10.9. HRMS (FAB+): *m/z* calcd for C₂₁H₂₀Cl₂N₉O₂ [MH⁺] 500.1111, found 500.1106.

Preparation of Polymer-Bound N-BOC-ethylenediamine (40). To a suspension of Merrifield resin (30 g, 21 mmol) and NMP (200 mL) was added 4-hydroxy-2-methoxybenzaldehyde (6.4 g, 42 mmol) and K₂CO₃ (8.7 g, 63 mmol). The resulting mixture was heated at 120 °C with shaking for 16 h. The resulting light-brown mixture was filtered, and the resin was washed with H₂O, NMP, and CH₂Cl₂. The resin was dried under vacuum at 40 °C for 12 h. To a suspension of the resin-bound aldehyde (30 g, 21 mmol) and (MeO)₃CH (200 mL) was added *N*-BOC-ethylenediamine (6.7 mL, 42 mmol). The resulting mixture was shaken at 23 °C for 12 h, filtered, and washed with CH₂Cl₂. The resin-bound imine was used immediately, slightly moist, with CH₂Cl₂. To a suspension of the resin-bound imine (30 g, 21 mmol) and MeOH/CH₂Cl₂/HOAc (200 mL, 2:2:1) was added borane–pyridine complex (6.8 mL, 67 mmol). The resulting mixture was shaken at 23 °C for 12 h, filtered, and washed with NMP and CH₂Cl₂. The resin was dried under vacuum at 30 °C for 12 h to yield polymer-bound *N*-BOC-ethylenediamine.

Polymer-Bound (2-Aminoethyl)(5-nitro(2-pyridyl))amine (41). To a suspension of polymer-bound *N*-BOC-ethylenediamine (**40**) (30 g, 21 mmol), NMP (200 mL), and *i*-Pr₃NEt (18.3 mL, 105 mmol) at 23 °C was added 2-chloro-5-nitropyridine (16.6 g, 105 mmol). The resulting mixture was heated at 120 °C with shaking for 12 h, filtered, and washed with NMP, H₂O, and CH₂Cl₂. To the resin-bound, *N*-BOC-protected amine was added a solution of 2,6-lutidine and CH₂Cl₂ (100 mL, 150 mmol), followed by a solution of TMSOTf and CH₂Cl₂ (100 mL, 100 mmol). The resulting mixture was shaken at 23 °C for 3 h, filtered, and washed with MeOH, TEA, and CH₂Cl₂. The resin was air-dried to yield polymer-bound (2-aminoethyl)(5-nitro(2-pyridyl))amine. A sample of the reaction was checked for purity. The air-dried resin (10 mg) was suspended in 80% TFA/CH₂Cl₂ (1 mL) for 1 h, filtered, washed with CH₂Cl₂ (1 mL), and concentrated under a stream of air to yield a light-yellow residue (HPLC, 99% at 220 nm; HPLC/MS, *m/z* 183 [MH⁺]).

Polymer-Bound {2-[(5-Nitro(2-pyridyl))amino]ethyl}[(2-nitrophenyl)sulfonyl]amine (42). To a suspension of resin-bound (2-aminoethyl)(5-nitro(2-pyridyl))amine (**41**) (30 g, 21 mmol), CH₂Cl₂ (250 mL), and *i*-Pr₃NEt (18.3 mL, 105 mmol) at 23 °C was added 2-nitrobenzenesulfonyl chloride (23.3 g, 105 mmol). The resulting mixture was shaken at 23 °C for 6 h, filtered, washed with NMP, H₂O, and CH₂Cl₂ and air-dried to yield polymer-bound {2-[(5-nitro(2-pyridyl))amino]ethyl}[(2-nitrophenyl)sulfonyl]amine (**42**). A sample of the reaction was checked for purity. The air-dried resin (10 mg) was suspended in 80% TFA/CH₂Cl₂ (1 mL) for 1 h, filtered, washed with CH₂Cl₂ (1 mL), and concentrated under a stream of air to yield a light-yellow residue (HPLC, 98% at 220 nm; HPLC/MS, *m/z* 368 [MH⁺]).

Polymer-Bound [2-(Dimethylamino)ethyl]{2-[(5-nitro(2-pyridyl))-amino]ethyl}[(2-nitrophenyl)sulfonyl]amine (43b). To a solution of Ph₃P (11 g, 42 mmol) and CH₂Cl₂ (20 mL) at 23 °C was added DIAD (6.6 mL, 42 mmol), and the resulting yellow solution was maintained at 23 °C for 30 min. To this solution was added 2-(dimethylamino)-ethanol (4.2 mL, 42 mmol), and the resulting solution was maintained at 23 °C for 5 min then added to a suspension of resin-bound {2-[(5-nitro(2-pyridyl))amino]ethyl}[(2-nitrophenyl)sulfonyl]amine (**42**) (3.0 g, 2.1 mmol) and CH₂Cl₂ (30 mL). The resulting mixture was shaken at 23 °C for 12 h, filtered, washed with NMP, H₂O, and CH₂Cl₂, and air-dried to yield polymer-bound [2-(dimethylamino)ethyl]{2-[(5-nitro(2-pyridyl))amino]ethyl}[(2-nitrophenyl)sulfonyl]amine (**43b**). A sample of the reaction was checked for purity. The air-dried resin (10 mg) was suspended in 80% TFA/CH₂Cl₂ (1 mL) for 1 h, filtered, washed with CH₂Cl₂ (1 mL), and concentrated under a stream of air to yield a light-yellow residue (HPLC, 98% at 220 nm; HPLC/MS, *m/z* 439 [MH⁺]).

Polymer-Bound Dimethyl[2-({2-[(5-nitro(2-pyridyl))amino]ethyl}-amino)ethyl]amine (44b). To a suspension of resin-bound [2-(dimethylamino)ethyl]{2-[(5-nitro(2-pyridyl))-amino]ethyl}[(2-nitrophenyl)sulfonyl]amine (**43b**) (3.0 g, 2.1 mmol) and DMF (30 mL) at 23 °C was added H₂O (2 drops), K₂CO₃ (2.9 g, 21 mmol), and PhSH (2.2 mL, 21 mmol). The resulting mixture was shaken at 23 °C for 12 h, filtered, washed with NMP, H₂O, and CH₂Cl₂, and air-dried to yield polymer-bound dimethyl[2-({2-[(5-nitro(2-pyridyl))amino]ethyl}amino)ethyl]amine (**44b**). A sample of the reaction was checked for purity. The air-dried resin (10 mg) was suspended in 80% TFA/CH₂Cl₂ (1 mL) for 1 h, filtered, washed with CH₂Cl₂ (1 mL), and concentrated under a stream of air to yield a light-yellow residue (HPLC, 98% at 220 nm; HPLC/MS, *m/z* 254 [MH⁺]).

Polymer-Bound Amino[2-(dimethylamino)ethyl]{2-[(5-nitro(2-pyridyl))amino]ethyl}carboxamide Hydrochloride (45b). To a suspension of polymer-bound dimethyl[2-({2-[(5-nitro(2-pyridyl))-amino]ethyl}amino)ethyl]amine (**44b**) (3.0 g, 2.1 mmol), NMP (30 mL), and *i*-Pr₃NEt (3.7 mL, 21 mmol) at 23 °C was added 1*H*-pyrazole-1-carboxamide hydrochloride (3.1 g, 21 mmol). The resulting mixture was heated at 90 °C for 18 h, filtered, washed with NMP, H₂O, and CH₂Cl₂, and air-dried to yield polymer-bound amino[2-(dimethylamino)ethyl]{2-[(5-nitro(2-pyridyl))amino]ethyl}-carboxamide hydrochloride (**45b**). A sample of the reaction was checked for purity. The air-dried resin (10 mg) was suspended in 80%

TFA/CH₂Cl₂ (1 mL) for 1 h, filtered, washed with CH₂Cl₂ (1 mL), and concentrated under a stream of air to yield a light-yellow residue (HPLC, 96% at 220 nm; HPLC/MS, *m/z* 296 [MH⁺]).

***N*-[4-(2,4-Dichloro-phenyl)-5-imidazol-1-yl-pyrimidin-2-yl]-*N*-(2-dimethylamino-ethyl)-*N'*-(5-nitro-pyridin-2-yl)-ethane-1,2-diamine (46b).** To a suspension of resin-bound amino[2-(dimethylamino)-ethyl]{2-[(5-nitro(2-pyridyl))amino]ethyl}-carboxamide hydrochloride (**45b**) (3.0 g, 2.1 mmol), and NMP (30 mL) at 23 °C was added 7-methyl-1,5,7-triazabicyclo[4.4.0]dec-5-ene (MTBD) (1.5 mL, 10.5 mmol) and 1-(2,4-dichlorophenyl)-3-(dimethylamino)-2-imidazolylprop-2-en-1-one (**24**) (1.3 g, 4.2 mmol). The resulting mixture was heated at 120 °C for 20 h, filtered, washed with NMP, H₂O, and CH₂Cl₂, and air-dried to yield resin-bound [4-(2,4-dichlorophenyl)-5-imidazolylpyrimidin-2-yl][2-(dimethylamino)-ethyl]{2-[(5-nitro(2-pyridyl))amino]ethyl}amine (**46b**). The resin was suspended in 80% TFA/CH₂Cl₂ (30 mL) and shaken at 23 °C for 1.5 h, filtered, and concentrated in vacuo. The resulting crude material was purified by reversed-phase HPLC (gradient of 95:5 H₂O:MeCN to 5:95 H₂O:MeCN), and the recovered material was dissolved in MeCN/0.5 M HCl (3 mL, 1:1), frozen, and lyophilized to yield 182 mg (16%) of **46b** as a yellow solid HCl salt (HPLC, 99% at 220 nm; HPLC/MS, *m/z* 542 [MH⁺]).

Compounds **46a,c–h** were prepared by similar procedures as **46b**. Identity and purity were minimally assessed by HPLC and HPLC/MS.

Preparation of *N*-[4-(2,4-Dichloro-phenyl)-5-imidazol-1-yl-pyrimidin-2-yl]-*N'*-(5-nitro-pyridin-2-yl)-*N*-(2-pyrrolidin-1-yl-ethyl)-ethane-1,2-diamine (46c). Compound **46c** was made using the same procedures as for **46b** except that 2-pyrrolidin-1-yl-ethanol was used to give 2 mg of the product as a yellow solid HCl salt in 10% yield (HPLC, 99% at 220 nm; HPLC/MS, *m/z* 568 [MH⁺]).

***N*-[4-(2,4-Dichloro-phenyl)-5-imidazol-1-yl-pyrimidin-2-yl]-*N*-(2-morpholin-4-yl-ethyl)-*N'*-(5-nitro-pyridin-2-yl)-ethane-1,2-diamine (46e).** Compound **46e** was made using the same procedures as for **46b** except that 4-(2-hydroxyethyl)morpholine was used to give the product as a yellow solid HCl salt (HPLC, 99% at 220 nm; HPLC/MS, *m/z* 584 [MH⁺]).

***N*-(2-Aminoethyl)(*tert*-butoxy)carboxamide (47).** A solution of *tert*-butyl [(*tert*-butyl)oxycarbonyloxy]formate (Boc₂O) (181.1 g, 0.83 mol) in dichloromethane (1 L) was added slowly (3 h) to a mechanically stirred solution of ethylene diamine (250 g, 4.16 mol) in dichloromethane (2.5 L) at room temperature. After 24 h, the reaction solution was washed with water (3 × 500 mL) and brine (500 mL), dried with Na₂SO₄, filtered, and concentrated under reduced pressure. The pure *N*-(2-aminoethyl)(*tert*-butoxy)carboxamide (**47**) (66.5 g, 50%) was obtained as a thick clear syrup and was used in its subsequent reactions without further purification (HPLC, 99% at 220 nm; HPLC/MS, *m/z* 161 [MH⁺]). Note: Upon standing, a white precipitate forms which is a disproportionated product, diBoc ethylene diamine. The diBoc ethylene diamine can be removed by adding ACN to make a free-flowing suspension which was then filtered. Excess ACN and ethylene diamine can be removed in vacuo.

***N*-[2-(Amidinoamino)ethyl](*tert*-butoxy)carboxamide, Hydrochloride (48).** Portions of solid 1*H*-pyrazole-1-carboxamide hydrochloride (91.10 g, 0.62 mol) are added to a stirred solution of *N*-(2-aminoethyl)(*tert*-butoxy)carboxamide (**47**) (99.3 g, 0.62 mol) in CH₃CN (1 L) at 80 °C. After 24 h, the reaction was stripped of solvent under reduced pressure. The residue was triturated with ether (3 × 100 mL) and dried in vacuo. The *N*-[2-(amidinoamino)ethyl](*tert*-butoxy)carboxamide hydrochloride (**48**) was obtained in approximately 100% yield containing a small amount of pyrazole. The *N*-[2-(amidinoamino)ethyl](*tert*-butoxy)carboxamide (**48**) hydrochloride was used without further purification (HPLC, 99% at 220 nm; HPLC/MS, *m/z* 203 [MH⁺]).

{2-[4-(2,4-Dichloro-phenyl)-5-imidazol-1-yl-pyrimidin-2-ylamino]ethyl}-carbamic Acid *tert*-Butyl Ester (49). 1-(2,4-Dichlorophenyl)-3-dimethylamino-2-imidazol-1-yl-propenone (**24**) (9.3 g, 30.0 mmol) in NMP (5 mL) was added to a stirred mixture of *N*-[2-(amidinoamino)ethyl](*tert*-butoxy)carboxamide hydrochloride (**48**) (13.8 g, 45 mmol) and Cs₂CO₃ (11.72, 36.0 mmol) in NMP (15 mL). The reaction was heated to 100 °C for 48 h. The reaction was followed by HPLC. Upon completion, the reaction was

partitioned with water (50 mL) and dichloromethane (250 mL). The organic layer was separated and washed with water (2 × 50 mL) and brine (50 mL), dried Na₂SO₄, filtered, and concentrated under reduced pressure. The product was purified by flash chromatography eluting with 10% methanol in dichloromethane. After stripping off the solvents and drying in vacuo, 11.2 g (83%) of **49** was obtained as a dark-red glass (HPLC, 99% at 220 nm; HPLC/MS, *m/z* 449 [MH⁺]). ¹H NMR (CDCl₃) δ 8.33 (s, 1H), 7.37 (d, *J* = 15 Hz, 1H), 7.29–7.23 (m, 2H), 7.17 (d, *J* = 9 Hz, 1H), 7.03 (s, 1H), 6.77 (s, 1H), 5.82 (br s, 1H), 4.89 (br s, 1H), 3.68–3.52 (br m, 2H), 3.44–3.35 (br m, 2H), 1.43 (s, 9H).

N¹-[4-(2,4-Dichloro-phenyl)-5-imidazol-1-yl-pyrimidin-2-yl]-ethane-1,2-diamine (50). Aqueous 3 M HCl (15–30 mL) was added to a stirred solution of [2-[4-(2,4-dichloro-phenyl)-5-imidazol-1-yl-pyrimidin-2-ylamino]-ethyl]-carbamate *tert*-butyl ester (**49**) (3.3 g, 7.4 mmol) in CH₃CN (50 mL) at room temperature until the reaction became slightly turbid. After 16 h, the reaction was partitioned between dichloromethane (200 mL) and 1 M HCl (200 mL). The layers were separated, and the aqueous layer was extracted with dichloromethane (3 × 200 mL). The aqueous layer was basified carefully with solid NaHCO₃ to pH 7–8. A solid forms which can be filtered and dissolved in CH₃CN (100 mL). The organic solution is washed with satd aq NaHCO₃ (50 mL) and brine (50 mL), dried with Na₂SO₄, filtered, and concentrated. The crude product was purified by flash chromatography over silica gel. The column was eluted first with a 1:1 mixture of dichloromethane/methanol followed by a mixture of 5% TEA/10% water/85% methanol to elute the product. The proper fractions were condensed. The dark-yellow glass was dried overnight in vacuo, giving 2 g (77%) of final product **50** (HPLC, 99% at 220 nm; HPLC/MS, *m/z* 349 [MH⁺]).

Compounds **51a,c,e–s** were synthesized by procedures similar to those used to produce **51d**. Identity and purity were minimally assessed by HPLC and HPLC/MS.

6-[2-(4-(2,4-Dichlorophenyl)-5-(1H-imidazol-1-yl)pyrimidin-2-ylamino)ethylamino]pyridine-3-carbonitrile (51b). Compound **51b** was synthesized by procedures similar to those used to produce **51d**. (HPLC, 99% at 220 nm; HPLC/MS, *m/z* 451 [MH⁺]). ¹H NMR (DMSO-*d*₆) δ 8.48 (br s, 1H), 8.37 (br s, 1H), 7.88 (br s, 1H), 7.69 (br s, 1H), 7.62 (s, 1H), 7.51 (d, *J* = 42 Hz, 2H), 6.93 (d, *J* = 42 Hz, 2H), 6.57 (br s, 1H), 3.62–3.21 (br m, 4H). Anal. (C₂₁H₁₆Cl₂N₈) Calcd: C, 55.89; H, 3.57; N, 24.83; Cl, 15.71. Found: C, 54.08; H, 3.54; N, 23.97; Cl, 15.55.

N-[4-(2,4-Dichloro-phenyl)-5-imidazol-1-yl-pyrimidin-2-yl]-N'-(6-methoxy-5-nitro-pyridin-2-yl)-ethane-1,2-diamine (51d). To a solution of N¹-[4-(2,4-dichloro-phenyl)-5-imidazol-1-yl-pyrimidin-2-yl]-ethane-1,2-diamine (**50**) (20 mg, 0.06 mmol) in DMF (1 mL), 2-methoxy-3-nitro-6-chloro-pyridine (see procedure below) (8.3 mg, 0.04 mmol), and diisopropylethyl amine (31 μL, 0.18 mmol) were added. The reaction mixture was stirred for 12 h at 80 °C. The crude mixture was concentrated in vacuo and subjected to column chromatography (10% methanol in methylene chloride) to afford 10 mg (50%) N-[4-(2,4-dichloro-phenyl)-5-imidazol-1-yl-pyrimidin-2-yl]-N'-(6-methoxy-5-nitro-pyridin-2-yl)-ethane-1,2-diamine (**51d**) as bright-yellow solid (HPLC, 96% at 220 nm; HPLC/MS, *m/z* 501 [MH⁺]).

6-Chloro-2-methoxy-3-nitro-pyridine. To a suspension of sodium hydride (684 mg, 28.49 mmol) in xylene (100 mL), methanol (0.98 mL, 25.9 mmol) in xylene (30 mL) was added under nitrogen. The mixture was stirred for 20 min. A solution of 2,6-dichloro-3-nitropyridine (5.0 g, 25.9 mmol) in xylene (100 mL) was added to the reaction mixture and stirred at room temperature overnight. Water (50 mL) was added and the organic layer was separated. The organics was washed with water (1 × 50 mL) and brine (2 × 50 mL), dried, and concentrated in vacuo. The crude product was purified by flash chromatography (10:1 methylene chloride and acetone) to provide 4.4 g (90%) of the desired compound, 6-chloro-2-methoxy-3-nitro-pyridine, as the only isomer as light-yellow solid (HPLC, 99% at 220 nm; HPLC/MS, *m/z* 189 [MH⁺]).

2-[2-(2,4-Dichlorophenyl)-2-oxoethyl]isoindoline-1,3-dione (57). A solution of 2,4-dichlorophenacyl chloride (**21b**) (223 mg, 1

mmol) in DMF (5 mL) was added dropwise to a mixture of phthalimide (**56**) (294 mg, 2 mmol) and Cs₂CO₃ (652 mg, 2 mmol) in DMF (10 mL) at room temperature. After 14 h, the reaction was concentrated in vacuo and then purified by trituration with diethyl ether to obtain 0.317 g (95%) 2-[2-(2,4-dichlorophenyl)-2-oxoethyl]-isoindoline-1,3-dione (**57**) (HPLC, 99% at 220 nm; HPLC/MS, *m/z* 334 [MH⁺]).

2-[2-(2,4-Dichlorophenyl)-1-[(dimethylamino)methylene]-2-oxoethyl]isoindoline-1,3-dione (58). A solution of 2-[2-(2,4-dichlorophenyl)-2-oxoethyl]isoindoline-1,3-dione (**57**) (334 mg, 1 mmol) was heated to 80 °C in neat *N,N*-dimethylformamidedimethyl (DMFDMA) acetal (10 mL) for 6 h. The reaction mixture was concentrated in vacuo and purified by trituration with diethyl ether to obtain 0.378 g (97%) of 2-[2-(2,4-dichlorophenyl)-1-[(dimethylamino)methylene]-2-oxoethyl]-isoindoline-1,3-dione (HPLC, 99% at 220 nm; HPLC/MS, *m/z* 389 [MH⁺]).

2-[2-[(2-[(6-Amino-5-nitro(2-pyridyl))amino]ethylamino)-4-(2,4-dichlorophenyl)pyrimidin-5-yl]isoindoline-1,3-dione (59). A mixture of 2-[2-(2,4-dichlorophenyl)-1-[(dimethylamino)methylene]-2-oxoethyl]isoindoline-1,3-dione (**58**) (334 mg, 1 mmol), amino[2-[(6-amino-5-nitro(2-pyridyl))amino]ethyl]carboxamide (**32**) (240 mg, 1 mmol), and Cs₂CO₃ (978 mg, 3 mmol) in DMF (10 mL) were stirred at 90 °C for 14 h. The reaction mixture was concentrated in vacuo, diluted with water (20 mL), and extracted with ethyl acetate (50 mL). The solution was extracted with ethyl acetate (3 × 25 mL), dried over sodium sulfate, filtered, and concentrated under reduced pressure to obtain a mixture of the desired product (**59**) and half-hydrolyzed open phthalimide that was cyclized to the desired compound by refluxing the mixture in glacial acetic acid for 4 h and then concentrated in vacuo to obtain 0.367 g (65%) of 2-[2-[(2-[(6-amino-5-nitro(2-pyridyl))amino]ethylamino)-4-(2,4-dichlorophenyl)pyrimidin-5-yl]isoindoline-1,3-dione (**59**) (HPLC, 99% at 220 nm; HPLC/MS, *m/z* 565 [MH⁺]).

N²-[2-(6-Amino-5-nitro-pyridin-2-ylamino)-ethyl]-4-(2,4-dichloro-phenyl)-pyrimidine-2,5-diamine (60a). A solution of 2-[2-[(2-[(6-amino-5-nitro(2-pyridyl))amino]ethylamino)-4-(2,4-dichlorophenyl)pyrimidin-5-yl]isoindoline-1,3-dione (**59**) (565 mg, 1 mmol) and hydrazine (641 mg, 20 mmol) in ethanol (10 mL) were stirred at 75 °C for 2 h. The resulting mixture of crude product and 2-amino-isoindole-1,3-dione was purified by column chromatography eluting with 5% methanol/methylene chloride gave 0.39 g (90%) N²-[2-(6-amino-5-nitro-pyridin-2-ylamino)-ethyl]-4-(2,4-dichloro-phenyl)-pyrimidine-2,5-diamine (**60a**) (HPLC, 99% at 220 nm; HPLC/MS, *m/z* 435 [MH⁺]).

N-[2-[2-(6-Amino-5-nitro-pyridin-2-ylamino)-ethylamino]-4-(2,4-dichloro-phenyl)-pyrimidin-5-yl]-methanesulfonamide (60b). A solution of N²-[2-(6-amino-5-nitro-pyridin-2-ylamino)-ethyl]-4-(2,4-dichloro-phenyl)-pyrimidine-2,5-diamine (**60a**) (435 mg, 1 mmol) and methanesulfonic anhydride (174 mg, 1 mmol) in THF (10 mL) were stirred at 25 °C for 4 h. The reaction mixture was concentrated in vacuo, diluted with water (10 mL), and extracted with ethyl acetate (30 mL). The solution was extracted with ethyl acetate (3 × 10 mL), dried over sodium sulfate, filtered, concentrated under reduced pressure, and purified by column chromatography eluting with 5% methanol/methylene chloride to obtain 0.33 g (65%) of N-[2-[2-(6-amino-5-nitro-pyridin-2-ylamino)-ethylamino]-4-(2,4-dichloro-phenyl)-pyrimidin-5-yl]-methanesulfonamide (**60b**) (HPLC, 99% at 220 nm; HPLC/MS, *m/z* 513 [MH⁺]).

N-[2-[2-(6-Amino-5-nitro-pyridin-2-ylamino)-ethylamino]-4-(2,4-dichloro-phenyl)-pyrimidin-5-yl]-acetamide (60c). A solution of N²-[2-(6-amino-5-nitro-pyridin-2-ylamino)-ethyl]-4-(2,4-dichloro-phenyl)-pyrimidine-2,5-diamine (**60a**) (435 mg, 1 mmol) and acetic anhydride (102 mg, 1 mmol) in THF (10 mL) was stirred at 25 °C for 4 h. The reaction mixture was concentrated in vacuo, diluted with water (10 mL), and extracted with ethyl acetate (30 mL). The solution was extracted with ethyl acetate (3 × 10 mL), dried over sodium sulfate, filtered, concentrated under reduced pressure, and purified by column chromatography eluting with 5% methanol/methylene chloride to obtain 0.405 g (85%) N-[2-[2-(6-amino-5-nitro-pyridin-

2-ylamino)-ethylamino]-4-(2,4-dichloro-phenyl)-pyrimidin-5-yl]-acetamide (**60c**) (HPLC, 99% at 220 nm; HPLC/MS, m/z 477 [MH⁺]).

Compounds **60d–f** were synthesized by procedures similar to those used to produce **60b**, with the exception that the acids were coupled with HBTU and **60f** was deprotected from the Boc-valine to final product with TFA in CH₂Cl₂. Identity and purity were minimally assessed by HPLC and HPLC/MS.

Compounds **60g,h** were synthesized by procedures similar to those used to produce **60b**, with the exception that the aniline **60a** was first reacted with carbonyldiimidazole and then the appropriate amine. Identity and purity were minimally assessed by HPLC and HPLC/MS.

[2-[2-(6-Amino-5-nitro-pyridin-2-ylamino)-ethylamino]-4-(2,4-dichloro-phenyl)-pyrimidin-5-yl]-methanol (60i). 2-Chloro-5-nitro-6-aminopyridine (143 mg, 0.9 mmol) was added to a stirred suspension of [2-(2-amino-ethylamino)-4-(2,4-dichloro-phenyl)-pyrimidin-5-yl]-methanol tri-TFA salt (see procedure below) (540 mg, 0.9 mmol) and cesium carbonate (1.47 g, 4.50 mmol) in anhydrous THF (3 mL) at 25 °C. To the resulting mixture was heated at 70 °C for 18 h. The reaction mixture was filtered, concentrated under reduced pressure, and the residue purified by column chromatography (silica gel, 5% methanol/methylene chloride) to give 216 mg (53%) of [2-[2-(6-amino-5-nitro-pyridin-2-ylamino)-ethylamino]-4-(2,4-dichloro-phenyl)-pyrimidin-5-yl]-methanol (**60i**) as a yellow solid (HPLC, 99% at 220 nm; HPLC/MS, m/z 450 [MH⁺]).

[2-[4-(2,4-Dichloro-phenyl)-5-hydroxymethyl-pyrimidin-2-ylamino]-ethyl]-carbamic Acid tert-Butyl Ester. A solution of DIBAL-H (1 M in THF) (25 mL, 25.0 mmol) was added dropwise to a stirred suspension of ethyl 4-(2,4-dichlorophenyl)-2-({2-[(*tert*-butoxy)-carbonylamino]ethyl}amino)pyrimidine-5-carboxylate (2.2 g, 4.7 mmol) (made from **48** and 3-(2,4-dichloro-phenyl)-3-oxo-propionic acid ethyl ester by procedures similar to those used to make compound **16** and **17**) in THF (10 mL) at room temperature under nitrogen. During the DIBAL-H addition, the suspension gradually turned into a homogeneous yellow solution. After 1 h, the resulting solution was heated to 70 °C for an additional 7 h. The reaction was then cooled, and the reaction was quenched by the addition of Rochelle's salt. The resulting suspension was partitioned between CH₂Cl₂ (150 mL) and water (30 mL). The aqueous layer was extracted twice with CH₂Cl₂ (2 × 10 mL) and the combined organic layers washed with brine (30 mL), dried with sodium sulfate, and concentrated under reduced pressure to give 2.05 g of crude product as a yellow foam. Column chromatography on silica gel (110 g) using 5% methanol/ether as eluent gave 430 mg (22%) of {2-[4-(2,4-dichloro-phenyl)-5-hydroxymethyl-pyrimidin-2-ylamino]-ethyl}-carbamic acid *tert*-butyl ester as a colorless foam (HPLC, 99% at 220 nm; HPLC/MS, m/z 413 [MH⁺]).

[2-(2-Amino-ethylamino)-4-(2,4-dichloro-phenyl)-pyrimidin-5-yl]-methanol. {2-[4-(2,4-Dichloro-phenyl)-5-hydroxymethyl-pyrimidin-2-ylamino]-ethyl}-carbamic acid *tert*-butyl ester (372 mg, 0.90 mmol) was dissolved in anhydrous trifluoroacetic acid (2 mL) and stirred at room temperature for 2 h. Evaporation of the solvent afforded 540 mg of [2-(2-amino-ethylamino)-4-(2,4-dichloro-phenyl)-pyrimidin-5-yl]-methanol, as its trifluoroacetate salt, in approximately quantitative yield (HPLC, 99% at 220 nm; HPLC/MS, m/z 313 [MH⁺]).

N⁶-[2-[4-(2,4-Dichloro-phenyl)-5-morpholin-4-ylmethyl-pyrimidin-2-ylamino]-ethyl]-3-nitro-pyridine-2,6-diamine (60j). Solid 2-chloro-5-nitro-6-aminopyridine (11 mg, 0.06 mmol) was added to a suspension of N¹-[4-(2,4-dichloro-phenyl)-5-morpholin-4-ylmethyl-pyrimidin-2-yl]-ethane-1,2-diamine, as its trifluoroacetate salt (see procedure below) (40 mg, 0.06), and cesium carbonate (160 mg, 0.50 mmol) in anhydrous THF (3 mL) at 25 °C. To the resulting mixture was heated at 70 °C for 18 h. The reaction mixture was filtered, concentrated under reduced pressure, and the residue purified by column chromatography (silica gel, 5% methanol/methylene chloride) to afford 191 mg (60%) of N⁶-[2-[4-(2,4-dichloro-phenyl)-5-morpholin-4-ylmethyl-pyrimidin-2-ylamino]-ethyl]-3-nitro-pyridine-2,6-diamine (**60j**) as a yellow solid (HPLC, 99% at 482 nm; HPLC/MS, m/z 519 [MH⁺]).

[2-[4-(2,4-Dichloro-phenyl)-5-formyl-pyrimidin-2-ylamino]-ethyl]-carbamic Acid tert-Butyl Ester. Using the method of Swern, a solution of {2-[4-(2,4-dichloro-phenyl)-5-hydroxymethyl-pyrimidin-2-ylamino]-ethyl}-carbamic acid *tert*-butyl ester (100 mg, 0.24 mmol) in anhydrous CH₂Cl₂ (3 mL) was added to a stirred solution of oxalyl chloride (31 μL, 0.36 mmol) and DMSO (52 μL, 0.73 mmol) in anhydrous CH₂Cl₂ (5 mL) at −78 °C. After stirring for an additional 30 min at −78 °C, TEA (202 μL, 1.45 mmol) was added. After 15 min, the resulting suspension was allowed to warm to room temperature. Water (1 mL) was added to the reaction and the layers separated. The aqueous layer was extracted with methylene chloride (1 × 3 mL), and the combined organic layers were dried (sodium sulfate) and filtered. The organic solution was concentrated at ~25–30 °C to afford {2-[4-(2,4-dichloro-phenyl)-5-formyl-pyrimidin-2-ylamino]-ethyl}-carbamic acid *tert*-butyl ester as a light-yellow foam. This product proved to be air sensitive and was used quickly without further manipulation (HPLC, 95% at 220 nm; HPLC/MS, m/z 411 [MH⁺]).

[2-[4-(2,4-Dichloro-phenyl)-5-morpholin-4-ylmethyl-pyrimidin-2-ylamino]-ethyl]-carbamic Acid tert-Butyl Ester. A solution of sodium cyanoborohydride (1 M in THF) (242 μL, 0.24 mmol) was added to a stirred solution of {2-[4-(2,4-dichloro-phenyl)-5-formyl-pyrimidin-2-ylamino]-ethyl}-carbamic acid *tert*-butyl ester (50 mg, 0.12 mmol), morpholine (62 mg, 0.72 mmol), and AcOH glacial (15 μL) in THF (5 mL) at room temperature. After 5 min, the mixture was heated to 70 °C for 18 h. Following slow addition of water (1 mL), the mixture was partitioned between ethyl acetate (50 mL) and satd aq citric acid solution (10 mL). The organic layer was discarded, and aqueous layer was carefully basified with sodium hydroxide (10 M) to pH 9 then extracted with ethyl acetate (2 × 25 mL). The combined organic layers were dried (sodium sulfate), concentrated under reduced pressure, and purified by column chromatography (silica gel, 10% methanol/methylene chloride) to afford 30 mg (52%) of {2-[4-(2,4-dichloro-phenyl)-5-morpholin-4-ylmethyl-pyrimidin-2-ylamino]-ethyl}-carbamic acid *tert*-butyl ester (HPLC, 95% at 482 nm; HPLC/MS, m/z 411 [MH⁺]).

N¹-[4-(2,4-Dichloro-phenyl)-5-morpholin-4-ylmethyl-pyrimidin-2-yl]-ethane-1,2-diamine. Using the conditions described above, {2-[4-(2,4-dichloro-phenyl)-5-morpholin-4-ylmethyl-pyrimidin-2-ylamino]-ethyl}-carbamic acid *tert*-butyl ester (30 mg, 0.06) was dissolved in anhydrous trifluoroacetic acid (2 mL) and stirred at room temperature for 2 h. Evaporation of the solvent afforded (40 mg, 0.06) of N¹-[4-(2,4-dichloro-phenyl)-5-morpholin-4-ylmethyl-pyrimidin-2-yl]-ethane-1,2-diamine, as its trifluoroacetate salt, in near quantitative yield (HPLC, 95% at 482 nm; HPLC/MS, m/z 382 [MH⁺]).

N-(2-(5-Nitropyridin-2-ylamino)ethyl)-4-(2,4-dichlorophenyl)-5-(1H-tetrazol-1-yl)pyrimidin-2-amine (60k). This compound was prepared by similar procedures as compound **60p**, with the exceptions that 1-(2,4-dichloro-phenyl)-2-tetrazol-1-yl-ethanone was used to obtain 0.156g (32%) N-(2-(5-nitropyridin-2-ylamino)ethyl)-4-(2,4-dichlorophenyl)-5-(1H-tetrazol-1-yl)pyrimidin-2-amine (**60k**) (HPLC, 99% at 220 nm; HPLC/MS, m/z 475 [MH⁺]).

N-[2-[2-(6-Amino-5-nitro-pyridin-2-ylamino)-ethylamino]-4-(2,4-dichloro-phenyl)-pyrimidin-5-yl]-acetamide (60m). A solution of N²-[2-(6-amino-5-nitro-pyridin-2-ylamino)-ethyl]-4-(2,4-dichloro-phenyl)-pyrimidine-2,5-diamine (**60a**) (400 mg, 0.9 mmol) in chloroform (2 mL) was coupled with 4-chloro-butryl chloride (194 mg, 1.3 mmol) in the presence of disodium hydrogen phosphate pentahydrate (857 mg, 3.6 mmol). After stirring for 2 days at room temperature, the reaction solution was washed with 1 N sodium hydroxide solution (1 mL), and the crude reaction was treated with sodium ethoxide (330 mg, 4.5 mmol) in ethanol (2 mL). After 1 h, the reaction mixture was neutralized with 1 N HCl (pH 7) concentrated in vacuo, diluted with water (10 mL), and extracted with ethyl acetate (30 mL). The aqueous layer was extracted again with ethyl acetate (3 × 10 mL), the combined organic fractions were dried over sodium sulfate, filtered, concentrated under reduced pressure, and purified by column chromatography eluting with 5% methanol/methylene chloride to obtain 275 mg (60%) of N-[2-[2-(6-amino-5-nitro-pyridin-2-ylamino)-ethylamino]-4-(2,4-dichloro-phenyl)-pyrimidin-5-yl]-acetamide (**60m**) (HPLC, 97% at 220 nm; HPLC/MS, m/z 504.3 [MH⁺]).

1-[2-[2-(6-Amino-5-nitro-pyridin-2-ylamino)-ethylamino]-4-(2,4-dichloro-phenyl)-pyrimidin-5-yl]-piperazin-2-one (**60n**). Starting from 2,4-dichlorophenacyl chloride (**21b**) and 3-oxo-piperazine-1-carboxylic acid *tert*-butyl ester in place of phthalimide, compound **60n** was synthesized in the same manner as **60a**. The Boc group was removed with TFA in CH_2Cl_2 to give 1-[2-[2-(6-amino-5-nitro-pyridin-2-ylamino)-ethylamino]-4-(2,4-dichloro-phenyl)-pyrimidin-5-yl]-piperazin-2-one (**60n**) in 36% overall yield (HPLC, 99% at 220 nm; HPLC/MS, m/z 518 $[\text{MH}^+]$).

Compound **60o** was synthesized by procedures similar to those used to produce **60n**, with the exception that the aniline of **60a** was reacted in sequence with bromoacetic acid, followed by bromine displacement by 2-methylamino-ethanol, which was cyclized through Mitsunobu employing Ph_3P and DIAD to give the final product. Identity and purity were minimally assessed by HPLC and HPLC/MS.

N^6 -{2-[4-(2,4-Dichloro-phenyl)-5-morpholin-4-yl-pyrimidin-2-ylamino]-ethyl}-3-nitro-pyridine-2,6-diamine (**60p**). A mixture of 1 mmol of 1-(2,4-dichloro-phenyl)-3-dimethylamino-2-morpholin-4-yl-propenone (see procedures below) (329 mg, 1 mmol), amino-2-[(6-amino-5-nitro(2-pyridyl)amino)ethyl]carboxamide (**32**), and Cs_2CO_3 (978 mg, 3 mmol) in DMF (10 mL) were stirred at 90 °C for 14 h. The reaction mixture was concentrated in vacuo, diluted with water (20 mL), and extracted with ethyl acetate (50 mL). The solution was extracted with ethyl acetate (3×25 mL) and dried over sodium sulfate, filtered, concentrated under reduced pressure, and purified by column chromatography eluting with 5% methanol/methylene chloride to obtain 0.404 g (80%) N^6 -{2-[4-(2,4-dichloro-phenyl)-5-morpholin-4-yl-pyrimidin-2-ylamino]-ethyl}-3-nitro-pyridine-2,6-diamine (**60p**) (HPLC, 99% at 220 nm; HPLC/MS, m/z 505 $[\text{MH}^+]$).

1-(2,4-Dichlorophenyl)-2-morpholin-4-ylethan-1-one. A solution of 2,4-dichlorophenacyl chloride (**21b**) (223 mg, 1 mmol) in DMF (10 mL) was added dropwise to a stirred solution of morpholine (871 mg, 10 mmol) in DMF (10 mL) at room temperature. After 14 h, the reaction mixture was concentrated in vacuo, diluted with water (10 mL), and extracted with ethyl acetate (30 mL). The solution was extracted with ethyl acetate (3×10 mL), dried over sodium sulfate, filtered, concentrated under reduced pressure, and purified by column chromatography eluting with 50% ethyl acetate and 50% hexane to obtain 0.164 g (60%) 1-(2,4-dichlorophenyl)-2-morpholin-4-ylethan-1-one (HPLC, 99% at 220 nm; HPLC/MS, m/z 274 $[\text{MH}^+]$).

1-(2,4-Dichloro-phenyl)-3-dimethylamino-2-morpholin-4-yl-propenone. A solution of 1-(2,4-dichlorophenyl)-2-morpholin-4-ylethan-1-one (435 mg, 1 mmol) in *N,N*-dimethylformamidedimethyl acetal (DMFDMA) (10 mL) was stirred at 80 °C for 6 h. The reaction mixture was concentrated in vacuo and purified by trituration with diethyl ether to obtain 0.316 g (96%) 1-(2,4-dichloro-phenyl)-3-dimethylamino-2-morpholin-4-yl-propenone (HPLC, 99% at 220 nm; HPLC/MS, m/z 329 $[\text{MH}^+]$).

N^6 -{2-[4-(2,4-Dichloro-phenyl)-5-piperazin-1-yl-pyrimidin-2-ylamino]-ethyl}-3-nitro-pyridine-2,6-diamine (**60q**). This compound was prepared by similar procedures as compound **60p**, with the exceptions that *tert*-butyl piperazinecarboxylate was used to make *tert*-butyl 4-[2-(2,4-dichlorophenyl)-2-oxoethyl]piperazinecarboxylate and the Boc protecting group was removed from the final product with aq HCl (3M) in MeOH at 60 °C over 1 h and then concentrated in vacuo to obtain 0.136 g (27%) of N^6 -{2-[4-(2,4-dichloro-phenyl)-5-piperazin-1-yl-pyrimidin-2-ylamino]-ethyl}-3-nitro-pyridine-2,6-diamine (**60q**) as an HCl salt (HPLC, 99% at 220 nm; HPLC/MS, m/z 504 $[\text{MH}^+]$).

N^6 -{2-[4-(2,4-Dichloro-phenyl)-5-(4-methyl-piperazin-1-yl)-pyrimidin-2-ylamino]-ethyl}-3-nitro-pyridine-2,6-diamine (**60r**). This compound was prepared by similar procedures as compound **60p**, with the exception that methylpiperazine was used to make 1-(2,4-dichlorophenyl)-2-(4-methylpiperazinyl)ethan-1-one to obtain 0.145 g (28%) of N^6 -{2-[4-(2,4-dichloro-phenyl)-5-(4-methyl-piperazin-1-yl)-pyrimidin-2-ylamino]-ethyl}-3-nitro-pyridine-2,6-diamine (**60r**) as a light-yellow powder (HPLC, 95% at 220 nm; HPLC/MS, m/z 518 $[\text{MH}^+]$).

N^6 -{2-[4-(2,4-Dichloro-phenyl)-5-pyridin-2-yl-pyrimidin-2-ylamino]-ethyl}-3-nitro-pyridine-2,6-diamine (**60s**). This compound was

prepared by similar procedures as compound **60p**, with the exception that 1-(2,4-dichloro-phenyl)-2-pyridin-2-yl-ethanone (prepared by the method of Buchwald et al.⁴⁷) was used to obtain 0.183 g (19.6%) of N^6 -{2-[4-(2,4-dichloro-phenyl)-5-pyridin-2-yl-pyrimidin-2-ylamino]-ethyl}-3-nitro-pyridine-2,6-diamine (**60s**) as a light-yellow powder (HPLC, 99% at 220 nm; HPLC/MS, m/z 497 $[\text{MH}^+]$). ^1H NMR (CDCl_3) δ 8.68 (s, 1H), 8.54 (d, 1H, $J = 6$ Hz), 8.02 (d, 1H, $J = 12$ Hz), 7.53 (t, $J = 9$ Hz, 1H), 7.28–7.38 (m, 2H), 7.18 (dd, $J = 6, 3$ Hz, 1H), 6.88 (d, $J = 9$ Hz, 1H), 3.84 (s, 4H), 3.70 (br s, 3H).

1-[2-[2-(6-Amino-5-nitro-pyridin-2-ylamino)-ethylamino]-4-(2,4-dichloro-phenyl)-pyrimidin-5-yl]-3-trifluoromethyl-1H-pyridin-2-one (**60t**). This compound was prepared by similar procedures as compound **25u**, with the exception that 3-trifluoromethyl-1H-pyridin-2-one with DIEA and **21b** was used to prepare 1-[2-(2,4-dichlorophenyl)-2-oxo-ethyl]-3-trifluoromethyl-1H-pyridin-2-one (2.9 g, 8.3 mmol), which was used to obtain 1.08 g (22%) 1-[2-[2-(6-amino-5-nitro-pyridin-2-ylamino)-ethylamino]-4-(2,4-dichloro-phenyl)-pyrimidin-5-yl]-3-trifluoromethyl-1H-pyridin-2-one (**60t**) as a light-yellow powder after prep HPLC purification (HPLC, 99% at 220 nm; HPLC/MS, m/z 581 $[\text{MH}^+]$).

Compounds **61a–u** were synthesized by procedures similar to those used to produce **36a**, with the exception that the correct 1-(substituted phenyl)-2-(1H-imidazol-2-yl)-ethanone (**30a**) was used to form the pyrimidine products. Identity and purity were minimally assessed by HPLC and HPLC/MS.

N^2 -(2-(4-(2-Bromo-4-chlorophenyl)-5-(1H-imidazol-2-yl)-pyrimidin-2-ylamino)ethyl)-5-nitropyridine-2,6-diamine (**61r**). Compound **61r** was synthesized by procedures similar to those used to produce **36b** with the exception that 1-(substituted phenyl)-2-(1H-imidazol-2-yl)-ethanone (**30a**) was used to form the pyrimidine (HPLC, 99% at 482 nm; HPLC/MS, m/z 530 $[\text{MH}^+]$). ^1H NMR ($\text{DMSO}-d_6$) δ 8.73 (d, $J = 22$ Hz, 1H), 8.42–8.23 (br m, 2H), 7.91 (dd, $J = 22, 9$ Hz, 2H), 7.75–7.49 (m, 5H), 7.63 (s, 1H), 5.95 (dd, $J = 22, 9$ Hz, 2H), 3.62–3.21 (br m, 4H). HRMS (FAB+): m/z calcd for $\text{C}_{20}\text{H}_{18}\text{BrCl}_2\text{N}_9\text{O}_2$ $[\text{MH}^+]$ 530.0449, found 530.0458.

Compounds **62a–g** were synthesized by procedures similar to those used to produce **1**, with the exception that the correct 1-(2,4-dichlorophenyl)-2-(4-methyl-1H-imidazol-2-yl)-ethanone (**30b**) was used to form the pyrimidine products. Identity and purity were minimally assessed by HPLC and HPLC/MS.

Kinases and Kinase Assays. ERK2, protein kinase C (PKC)- α , PKC- ζ , p90RSK2, AMPK, and pdk1 kinases were purchased from Upstate Biotechnology (Lake Placid, NY). DNA-PK was purified from HeLa cells as described previously.⁹⁶ Other recombinant human protein kinases were expressed in SF9 cells with glu- or hexahis-peptide tags. Glu-tagged proteins were purified as described previously,⁹⁷ and his-tagged proteins were purified according to the manufacturer's instructions (Qiagen, Valencia, CA). All kinase assays followed the same core protocol with variations in peptide substrate and activator concentrations described below. Polypropylene 96-well plates were filled with 300 μL /well buffer (50 mmol/L tris HCl, 10 mmol/L MgCl_2 , 1 mmol/L EGTA, 1 mmol/L dithiothreitol, 25 mmol/L β -glycerophosphate, 1 mmol/L NaF, 0.01% BSA, pH 7.5) containing kinase, peptide substrate, and any activators. Information on the kinase concentration, peptide substrate, and activator (if applicable) for these assays is as follows: GSK3- α (27 nmol/L and 0.5 $\mu\text{mol/L}$ biotin-CREB peptide); GSK3- β (29 nmol/L and 0.5 $\mu\text{mol/L}$ biotin-CREB peptide); CDC2 (0.8 nmol/L and 0.5 $\mu\text{mol/L}$ biotin histone H1 peptide); ERK2 (400 units/mL and myelin basic protein-coated Flash Plate [PerkinElmer]); PKC- α (1.6 nmol/L, 0.5 $\mu\text{mol/L}$ biotin-histone H1 peptide, and 0.1 mg/mL phosphatidylserine + 0.01 mg/mL diglycerides); PKC- ζ (0.1 nmol/L, 0.5 $\mu\text{mol/L}$ biotin-PKC-86 peptide, and 50 $\mu\text{g/mL}$ phosphatidylserine + 5 $\mu\text{g/mL}$ diacylglycerol); AKT1 (5.55 nmol/L and 0.5 $\mu\text{mol/L}$ biotin phospho-AKT peptide); p70 S6 kinase (1.5 nmol/L and 0.5 $\mu\text{mol/L}$ biotin-GGKKRR-LASLRA); p90 RSK2 (0.049 units/mL and 0.5 $\mu\text{mol/L}$ biotin-GGKKRRRLASLRA); Tie2 (1 $\mu\text{g/mL}$ and 200 nmol/L biotin-GGGGAPDLYKDFLT); flt1 (1.8 nmol/L and 0.25 $\mu\text{mol/L}$ KDRY1175 [B91616] biotin-GGGGQDGKDYIVLP1-NH₂); KDR (0.95 nmol/L and 0.25 $\mu\text{mol/L}$ KDRY1175 [B91616] biotin-

GGGGQDGGKDYIVLPI-NH₂); bFGF receptor tyrosine kinase (RTK; 2 nmol/L and 0.25 μ mol/L KD91175 [B91616] biotin-GGGGQD-GKDYIVLPI-NH₂); IGF1 RTK (1.91 nmol/L and 1 μ mol/L biotin-GGGGKKKSPGEYVNIEFG-amide); insulin RTK (using DG44 IR cells⁹⁸ AMP kinase (470 units/mL, 50 μ mol/L SAMS peptide, and 300 μ mol/L AMP); pdk1 (0.25 nmol/L, 2.9 nmol/L unactivated AKT, and 20 μ mol/L each of DOPC and DOPS + 2 μ mol/L PIP3); CHK1 (1.4 nmol/L and 0.5 μ mol/L biotin-CDC25 peptide); CK1- ϵ (3 nmol/L and 0.2 μ mol/L biotin-peptide); DNA PK⁹⁶ and phosphatidylinositol (PI) 3-kinase (5 nmol/L and 2 μ g/mL PI). Test compounds or controls were added in 3.5 μ L of DMSO, followed by 50 μ L of ATP stock to yield a final concentration of 1 μ mol/L ATP in all cell-free assays. After incubation, triplicate 100 μ L aliquots were transferred to Combiplate eight plates (LabSystems, Helsinki, Finland) containing 100 μ L/well 50 μ mol/L ATP and 20 nmol/L EDTA. After 1 h, the wells were rinsed five times with PBS, filled with 200 μ L of scintillation fluid, sealed, left 30 min, and counted in a scintillation counter. All steps were performed at room temperature. Inhibition was calculated as 100% (inhibited – no enzyme control)/(DMSO control – no enzyme control).

Enzyme and Receptor Panels. Selectivity against nonkinase enzymes was tested on the Cerep “Enzyme” panel, including acetylcholinesterase, adenylate cyclase, Na/K ATPase, cathepsin B and G, cyclooxygenase 1 and 2, ECE, epithelial growth factor receptor, elastase, guanylate cyclase, HIV-1 protease, inducible nitric oxide synthase, 5-lipoxygenase, monoamine oxidase A and B, phosphodiesterase I, II, III, and IV, PKC, phospholipase A2 and C, and tyrosine hydroxylase (Celle L’Evescault, France).

Selectivity against receptors was tested on the MDS “Profiling” panel, including adenosine A1, adrenergic (α 1 and α 2 nonselective and β 1 and β 2), calcium channel type L, dopamine D1 and D2, estrogen α , GABAA (agonist site and sodium channel), glucocorticoid, glutamate (NMDA/phencyclidine and nonselective), glycine (strychnine sensitive), histamine H1 (central), insulin, muscarinic M2 and M3, opiates δ , κ , and μ , phorbol ester, potassium channel, progesterone, serotonin (5-HT1 and 5-HT2/nonselective), sigma (nonselective), sodium channel (site 2), and testosterone (MDS Pharma Services, Bothell, WA).

GS Activity Assays. CHO-IR cells expressing human insulin receptor (provided by Hans Bos) were grown to 80% confluence in Hamm’s F12 medium with 10% fetal bovine serum and without hypoxanthine.⁹⁹ Trypsinized cells were seeded in 6-well plates at 1×10^6 cells/well in 2 mL of medium without fetal bovine serum. After 24 h, medium was replaced with 1 mL of serum-free medium containing GSK-3 inhibitor or control (final DMSO concentration 0.1%) for 30 min at 37 °C. Cells were lysed by freeze/thaw in 50 mmol/L Tris (pH 7.8) containing 1 mmol/L EDTA, 1 mmol/L DTT, 100 mmol/L NaF, 1 mmol/L phenylmethylsulfonyl fluoride, and 25 μ g/mL leupeptin (buffer A) and centrifuged 15 min at 4 °C/14000g. The activity ratio of GS was calculated as the GS activity in the absence of glucose-6-phosphate divided by the activity in the presence of 5 mmol/L glucose-6-phosphate, using the filter paper assay of Thomas et al.¹⁰⁰

Primary hepatocytes from male Sprague–Dawley rats that weighed 140 g were prepared at the Rice Liver Laboratory (San Francisco, CA) and used 1–3 h after isolation. Aliquots of 1×10^6 cells in 1 mL of DMEM/F12 medium plus 0.2% BSA and GSK-3 inhibitors or controls were incubated in 12-well plates on a low-speed shaker for 30 min at 37 °C in a CO₂-enriched atmosphere, collected by centrifugation, and lysed by freeze/thaw in buffer A plus 0.01% NP40; the GS assay was again performed using the method of Thomas et al.¹⁰⁰

Isolated Rat Skeletal Muscle Incubations. Overnight-fasted animals were anesthetized with pentobarbital sodium (50 mg/kg ip). Soleus muscles were dissected into strips (ca. 25 mg) and incubated for 1 h at 37 °C in 3 mL of oxygenated (95% O₂/5% CO₂) Krebs–Henseleit buffer with 8 mmol/L glucose, 32 mmol/L mannitol, and 0.1% BSA (radioimmunoassay grade; Sigma Chemical) with or without the indicated concentrations of insulin (Humulin R; Eli Lilly, Indianapolis, IN) or the GSK-3 inhibitor. Thereafter, the muscle was used to assess the activity ratio (activity in the absence of glucose-6-phosphate divided by the activity in the presence of 5 mmol/L

glucose-6-phosphate) of GS¹⁰⁰ or glucose transport activity, using 1 mmol/L 2-deoxyglucose.¹⁰¹

Animals. Female *db/db* mice were obtained from The Jackson Laboratories (Bar Harbor, ME) at 6 weeks and used when 8–9 weeks of age. Male ZDF rats were obtained from Genetic Models Inc. (Indianapolis, IN) at 8–9 weeks and used at 10–13 weeks of age. Animals were fed Purina 5008 laboratory chow, received water ad libitum, and were maintained on a 12 h light/dark cycle (6:00 A.M., 6:00 P.M.) at 22–24 °C.

Efficacy Models. Blood was obtained by shallow tail snipping at lidocaine-anesthetized tips. Blood glucose was measured directly (One-Touch Glucometer; LifeScan, San Jose, CA) or heparinized plasma was collected for measurement of glucose (Beckman Glucose Analyzer, Mountain View, CA) or insulin (Alpco Elisa, Windham, NH). Animals were prebled and randomized to vehicle control or GSK-3 inhibitor treatment groups. For glucose tolerance tests (GTTs), animals were fasted throughout the procedure with food removal early in the morning, 3 h before first prebled (*db/db* mice), or the previous night, 16 h before the bleed (ZDF rats). When the time course of plasma glucose and insulin changes in fasting ZDF rats was measured, food was removed ~16 h before test agent administration. The glucose challenges in the GTT were 1.35 g/kg ip (ipGTT) or 2 g/kg via oral gavage (oGTT). Test inhibitors were formulated as solutions in 20 mmol/L citrate-buffered 15% captisol (Cydex, Overland Park, KS) or as fine suspensions in 0.5% carboxymethylcellulose (CMC).

Statistical Analysis. The significance of differences between multiple groups was assessed by a factorial ANOVA with a post hoc Fisher’s protected least significant difference test (StatView version 5.0; SAS Institute Inc., Cary, NC). Differences between two groups were determined by an unpaired Student’s *t* test. *P* 0.05 was considered to be statistically significant. All data are reported as means \pm SE.

Purification of GSK3- β for Crystallization. Traditional techniques for generating co-structures with this family of aminopyrimidines, such as soaking of compounds into apo-crystals of GSK3- β or co-crystallizing the protein in the presence of the compound, failed to generate well-diffracting of the complex. In the former approach, exposure of the apo-crystals to even small quantities of the compound led to significant cracking and damage to the GSK3- β crystals and loss of atomic level diffraction despite the use of synchrotron X-ray sources. This crystal damage suggests that GSK3- β underwent significant structural changes during binding of the compound. In the latter approach, co-crystallization screens run in the presence of compounds failed to generate any co-crystals. To overcome these limitations, it was necessary to generate a ternary complex of GSK3- β bound to adenosine diphosphate (ADP) and a peptide derived from a client protein of GSK3- β . When crystallized, this complex was amenable to forming the cocrystal of a broad range of chemical scaffolds without suffering damage or reduction in resolution of the data.

A construct consisting of residues 37–384 of human GSK3- β and a C-terminal Glu-tag were expressed in SF-9 cells using a baculovirus expression system. Cell paste from 20 L of cell culture was washed with 100 mL of PBS buffer (10 mM NaPi, pH 7.5, 150 mM NaCl) and then resuspended in 300 mL of buffer A (20 mM Tris, 1 mM tungstate, 1 mM arsenate, 50 mM DTT, 10 μ g/mL leupeptin, 1 μ g/mL pepstatin A, 10% glycerol (w:v), 0.35% (w:v) octylglucoside, 1 mM Mg²⁺). The cells were then homogenized in a 100 mL of Douncer (20 strokes with pestle B). The homogenate was centrifuged in a Ti45 rotor at 45000 rpm for 35 min to remove cell debris and nuclei.

Following the centrifugation, the supernatant was carefully decanted and filtered through a 0.45 μ filter to remove cell debris. The filtrate was loaded on an S-fraction column (EM Science) equilibrated with buffer A supplemented with 50 mM DTT. The filtered cell filtrate was then loaded onto the column. After loading, the column was washed with 3 column volumes of buffer A containing 50 mM DTT and two column volumes of buffer A. The protein was then eluted with a linear gradient of 0 to 1 M NaCl in buffer A over 20 column volumes. Fractions containing GSK3- β were detected using anti-GSK antibody

(Santa Cruz Biotech). The Western-blot positive fractions were pooled and mixed with an equal volume of buffer B (20 mM Tris, pH 7.5, 10% (w:v) glycerol, 3.1 M NaCl) and filtered.

The filtrate was then loaded onto a phenyl-650 M column (Tosohass) equilibrated with buffer C (20 mM Tris, pH 7.5, 10% (w:v) glycerol, 1.6 M NaCl). After the loading was completed, the column was washed with 5 column volumes of buffer C and then eluted with a linear gradient of 0–100% of buffer A over 20 column volumes. Fractions containing GSK3- β were detected using anti-GSK antibody as in the previous purification step. Western-blot positive fractions were pooled.

The pooled fractions were then loaded onto a Affi-Gel 10 Glu-tag affinity column (BioRad) equilibrated with buffer D (20 mM Tris, pH 7.5, 20% (w:v) glycerol, 0.3 M NaCl, 0.2% (w:v) octylglucoside). The column was then washed with 5 column volumes of buffer D, and the protein subsequently was eluted with 100 mL of glu-tag peptide (at 100 μ g/mL) in buffer D. GSK3- β containing fractions were detected using SDS-PAGE and Coomassie Blue staining. These fractions were pooled and filtered into to buffer D. The pure protein was concentrated into buffer D using an Amicon concentrator using a 10 kDa MWCO YM10 membrane to a concentration of approximately 4.8 mg/mL. This concentrated material was used for crystallization.

Crystallization of GSK3- β Ternary Complex and Generation of GSK3- β :Compound 1 Co-structure. To form the ternary complex, a solution containing 100 mM of the seven-residue peptide H₂N-LSRRPS(P)Y-CO₂H (the sixth position is a phosphoserine), 20 mM ATP, 100 mM MgCl₂, and 100 mM Tris-HCl, pH 7.5, was mixed in a 1:10 (v:v) ratio with GSK3- β protein at 4.8 mg/mL in buffer D. The resulting solution was incubated on ice at 4 °C for 2 h. The purpose of this incubation was to allow the kinase to fully phosphorylate the client peptide and then subsequently form the ternary complex. Following the incubation period, crystallization trials were set up using the hanging drop vapor diffusion method. A two-dimensional grid of precipitant containing 7–12 (w:v) PEG 6000 and 5–8% MPD (v:v) was established using a 24-well Linbro plate. Then 2 μ L of the protein ternary complex solution was mixed with 2 μ L of the precipitant solution from the reservoir on a glass coverslip. The coverslip was then placed over the reservoir, and the coverslip and reservoir were sealed with vacuum grease. The crystals grew to a maximum size over the course of 4 days at room temperature. The resulting crystals crystallized in the *P*2₁ space group with a monomer of the ternary complex in the asymmetric unit and had the following approximate unit cell: *a* = 57.0 Å, *b* = 64.8 Å, *c* = 57.2 Å, $\alpha = \gamma = 90^\circ$, $\beta = 100.9^\circ$. This varied from crystal to crystal. The crystals were then harvested for soaking experiments.

To generate a co-structure, the ternary complex crystals were transplanted to a 5 μ L drop of soaking solution drawn from the reservoir precipitant solution and 1 mM of compound 1 for 12–24 h. During this time, the ADP was displaced and replaced by the compound. This displacement lowered the resolution of the crystal somewhat, but no visible cracking or damage was seen and atomic level resolutions could still be achieved using an in-house X-ray generator. The crystals were cryoprotected using a cryosolution consisting of 12% (w:v) PEG 6000, 11% (v:v) MPD, 0.1 M HEPES, pH 7.5, and 20% (w:v) glycerol, supplemented with 1 mM of compound 1. The crystals were then frozen in the LN₂, and X-ray crystal data was collected. This protocol also worked for all other chemical scaffolds tested, as well as for larger molecules, such as peptides.

X-ray Crystallography Data Collection and Processing. X-ray crystallographic data was collected in-house on a Rigaku RU-300 X-ray generator and a Rigaku R-Axis IIC area detector using Cu K α X-ray radiation. Two separate crystals were used, and data sets were collected for each. Data for these crystals were processed, merged, and scaled using DENZO/HKL2000. Data was collected to 2.6 Å.

Structure Solution and Refinement. The co-structure was solved using molecular replacement and a search model of GSK3- β solved previously. The structure was refined to convergence using COOT,¹⁰² BUSTER,¹⁰³ and the PHENIX suite¹⁰⁴ of programs. Data

collection and refinement statistics for all structures are listed in Table S1 (see Supporting Information).

■ ASSOCIATED CONTENT

§ Supporting Information

The Supporting Information is available free of charge on the ACS Publications website at DOI: 10.1021/acs.jmedchem.7b00922.

Copies of ¹H and ¹³C NMR spectra, HPLC and LCMS traces of representative compounds (PDF)

Molecular formula strings (CSV)

Accession Codes

Coordinates and structure factors for the GSK3:compound 1 costructure have been deposited in the Protein Data Bank (RCSB) under PDB accession code 6B8J. Authors will release the atomic coordinates and experimental data upon article publication.

■ AUTHOR INFORMATION

Corresponding Author

*Phone: (510) 879-9505. E-mail: dirksen.bussiere@novartis.com.

ORCID

Savithri Ramurthy: 0000-0002-2444-5309

Dirksen E. Bussiere: 0000-0002-5623-5648

Present Addresses

[‡]For A.S.W.: 3-V Biosciences, Inc., 3715 Haven Avenue, Suite 220, Menlo Park, California 94025, United States; allan.wagman@3vbio.com.

[§]For R.S.B.: Vermont Biosynthetics, LLC, 365 Glinnis Road, Northfield, Vermont 05663, United States.

^{||}For S.P.B.: Amgen Inc., One Amgen Center Drive, Thousand Oaks, California 91320, United States.

[⊥]For D.G.: 77 Markham Avenue, Redwood City, California 94063, United States.

[#]For V.P.L.: Information Technologies—Clinical Services, University of California—San Francisco, 1550 Bryan Street, Suite 650, San Francisco, California 94103, United States.

[∇]For B.H.L.: 2026 South Lincoln Avenue, Spokane, Washington 99203, United States.

[○]For S.C.N.: 311 Preakness Court, Walnut Creek, California 94597, United States.

[◆]For Z.J.N.: Acme Bioscience, Inc., 3941 East Bayshore Road, Palo Alto, California 94304, United States.

[¶]For J.M.N.: Oppilan Pharma, Ltd., 332 Encinitas Boulevard, Encinitas, California 92024, United States.

[□]For P.A.R.: Ironwood Pharmaceuticals, 301 Binney Street, Cambridge, Massachusetts 02142, United States.

[●]For D.B.R.: 2375 Cowper Street, Palo Alto, California 94301, United States.

[◇]For S.D.H.: Relypsa, Inc., 100 Cardinal Way, Redwood City, California 94063, United States.

[■]For K.W.J.: XOMA Limited, 2910 Seventh Street, Berkeley, California 94701, United States.

Author Contributions

The manuscript was written through the contributions of all of the authors. All authors have given approval to the final version of the manuscript. The authors declare no competing financial interests.

Notes

The authors declare the following competing financial interest(s): All authors are current or former employees of Novartis and/or Chiron Corporation.

[†]No longer at Novartis Institutes for BioMedical Research—Emeryville, formerly Chiron Corporation.

ACKNOWLEDGMENTS

We thank Weiping Jia and Gavin Dollinger for MS services, Alice Wang for compound purification, and Anu Sharma for collecting HPLC and LCMS data of several compounds. We thank Drs. Lewis T. Williams, Manoj Desai, Yumi Nakagawa, and Jacob Plattner for their advice and mentorship during the project.

ABBREVIATIONS USED

CHO-IR, Chinese hamster ovary transfected with human insulin receptor; CMC, critical micelle concentration; DIEA, *N,N*-diisopropylethylamine; DMA, dimethylacetamide; DMF, dimethylformamide; DMSO, dimethyl sulfoxide; DTT, dithiothreitol; HPLC, high performance liquid chromatography; LCMS, liquid chromatography–mass spectrometry; NIDDM, noninsulin dependent diabetes mellitus; NMP, *N*-methyl-2-pyrrolidone; NMR, nuclear magnetic resonance; oGTT, oral glucose tolerance test; SAR, structure–activity relationship; THF, tetrahydrofuran; TFA, trifluoroacetic acid; TMSOTf, trimethylsilyl trifluoromethanesulfonate; ZDF, Zucker diabetic fatty

REFERENCES

- (1) *IDF Diabetes Atlas*, 7th ed.; International Diabetes Foundation: Brussels, 2015.
- (2) Turner, R. C.; Cull, C. A.; Frighi, V.; Holman, R. R. Glycemic control with diet, sulfonylurea, metformin, or insulin in patients with type 2 diabetes mellitus: progressive requirement for multiple therapies (UKPDS 49). *JAMA* **1999**, *281* (21), 2005–2012.
- (3) UK Prospective Diabetes Study (UKPDS) Group. Intensive blood-glucose control with sulphonylureas or insulin compared with conventional treatment and risk of complications in patients with type 2 diabetes (UKPDS 33). *Lancet* **1998**, *352* (9131), 837–853.
- (4) Hauner, H. Managing type 2 diabetes mellitus in patients with obesity. *Treat. Endocrinol.* **2004**, *3* (4), 223–232.
- (5) Davidson, J. A.; Holland, W. L.; Roth, M. G.; Wang, M.; Lee, Y.; Yu, X.; McCorkle, S. K.; Scherer, P. E.; Unger, R. H. Glucagon therapeutics: Dawn of a new era for diabetes care. *Diabetes/Metab. Res. Rev.* **2016**, *32* (7), 660–665.
- (6) Rotella, D. P. Novel “second-generation” approaches for the control of type 2 diabetes. *J. Med. Chem.* **2004**, *47* (17), 4111–4112.
- (7) Woodgett, J. R. Physiological roles of glycogen synthase kinase-3: potential as a therapeutic target for diabetes and other disorders. *Curr. Drug Targets: Immune, Endocr. Metab. Disord.* **2003**, *3* (4), 281–290.
- (8) Jope, R. S.; Johnson, G. V. W. The glamour and gloom of glycogen synthase kinase-3. *Trends Biochem. Sci.* **2004**, *29* (2), 95–102.
- (9) Nikoulina, S. E.; Ciaraldi, T. P.; Mudaliar, S.; Mohideen, P.; Carter, L.; Henry, R. R. Potential role of glycogen synthase kinase-3 in skeletal muscle insulin resistance of type 2 diabetes. *Diabetes* **2000**, *49* (2), 263–271.
- (10) Nikoulina, S. E.; Ciaraldi, T. P.; Mudaliar, S.; Carter, L.; Johnson, K.; Henry, R. R. Inhibition of glycogen synthase kinase 3 improves insulin action and glucose metabolism in human skeletal muscle. *Diabetes* **2002**, *51* (7), 2190–2198.
- (11) Ciaraldi, T. P.; Carter, L.; Mudaliar, S.; Henry, R. R. GSK-3 β and control of glucose metabolism and insulin action in human skeletal muscle. *Mol. Cell. Endocrinol.* **2010**, *315* (1–2), 153–158.
- (12) Tanti, J. F.; Gual, P.; Grémeaux, T.; Gonzalez, T.; Barrès, R.; Le Marchand-Brustel, Y. Alteration in insulin action: role of IRS-1 serine phosphorylation in the retroregulation of insulin signalling. *Ann. Endocrinol.* **2004**, *65* (1), 43–48.
- (13) Kirwan, J. P.; del Aguila, L. F. Insulin signalling, exercise and cellular integrity. *Biochem. Soc. Trans.* **2003**, *31* (6), 1281–1285.
- (14) Qiao, L. Y.; Goldberg, J. L.; Russell, J. C.; Sun, X. J. Identification of enhanced serine kinase activity in insulin resistance. *J. Biol. Chem.* **1999**, *274* (15), 10625–10632.
- (15) Tanti, J. F.; Grémeaux, T.; van Obberghen, E.; Le Marchand-Brustel, Y. Serine/threonine phosphorylation of insulin receptor substrate 1 modulates insulin receptor signaling. *J. Biol. Chem.* **1994**, *269* (8), 6051–6057.
- (16) Wagman, A. S.; Johnson, K. W.; Bussiere, D. E. Discovery and development of GSK3 inhibitors for the treatment of type 2 diabetes. *Curr. Pharm. Des.* **2004**, *10* (10), 1105–1137.
- (17) Jope, R. S.; Cheng, Y.; Lowell, J. A.; Worthen, R. J.; Sitbon, Y. H.; Beurel, E. Stressed and inflamed, can GSK3 be blamed? *Trends Biochem. Sci.* **2017**, *42* (3), 180–192.
- (18) McCubrey, J. A.; Rakus, D.; Gizak, A.; Steelman, L. S.; Abrams, S. L.; Lertpiriyapong, K.; Fitzgerald, T. L.; Yang, L. V.; Montalto, G.; Cervello, M.; Libra, M.; Nicoletti, F.; Scalisi, A.; Torino, F.; Fenga, C.; Neri, L. M.; Marmiroli, S.; Cocco, L.; Martelli, A. M. Effects of mutations in Wnt/ β -catenin, hedgehog, Notch and PI3K pathways on GSK-3 activity—Diverse effects on cell growth, metabolism and cancer. *Biochim. Biophys. Acta, Mol. Cell Res.* **2016**, *1863* (12), 2942–2976.
- (19) Zeidan-Chulia, F.; Moreira, J. C. F. Targeting the GSK3 β / β -catenin signaling to treat Alzheimer's disease: Plausible or utopic? In *Drug Design and Discovery in Alzheimer's Disease*; Bentham Science: Sharjah, 2014; Vol. 6, pp 623–642.
- (20) Golpich, M.; Amini, E.; Hemmati, F.; Ibrahim, N. M.; Rahmani, B.; Mohamed, Z.; Raymond, A. A.; Dargahi, L.; Ghasemi, R.; Ahmadiani, A. Glycogen synthase kinase-3 beta (GSK-3 β) signaling: Implications for Parkinson's disease. *Pharmacol. Res.* **2015**, *97*, 16–26.
- (21) Beurel, E.; Grieco, S. F.; Jope, R. S. Glycogen synthase kinase-3 (GSK3): Regulation, actions, and diseases. *Pharmacol. Ther.* **2015**, *148*, 114–131.
- (22) Seira, O.; Del Río, J. A. Glycogen synthase kinase 3 beta (GSK3 β) at the tip of neuronal development and regeneration. *Mol. Neurobiol.* **2014**, *49* (2), 931–944.
- (23) Takahashi-Yanaga, F. Activator or inhibitor? GSK-3 as a new drug target. *Biochem. Pharmacol.* **2013**, *86* (2), 191–199.
- (24) Osolodkin, D. L.; Palyulin, V. A.; Zefirov, N. S. Glycogen synthase kinase 3 as an anticancer drug target: novel experimental findings and trends in the design of inhibitors. *Curr. Pharm. Des.* **2013**, *19* (4), 665–679.
- (25) Ghaderi, S.; Alidadiani, N.; Dilaver, N.; Heidari, H. R.; Parvizi, R.; Rahbarghazi, R.; Soleimani-Rad, J.; Baradaran, B. Role of glycogen synthase kinase following myocardial infarction and ischemia–reperfusion. *Apoptosis* **2017**, *22* (7), 887–897.
- (26) Ko, R.; Lee, S. Y. Glycogen synthase kinase 3 β in Toll-like receptor signaling. *BMB Rep.* **2016**, *49* (6), 305–310.
- (27) McLauchlan, H.; Elliott, M.; Cohen, P. The specificities of protein kinase inhibitors: an update. *Biochem. J.* **2003**, *371* (1), 199–204.
- (28) Bain, J.; Plater, L.; Elliott, M.; Shpiro, N.; Hastie, C. J.; McLauchlan, H.; Klevernic, I.; Arthur, J. S. C.; Alessi, D. R.; Cohen, P. The selectivity of protein kinase inhibitors: a further update. *Biochem. J.* **2007**, *408* (3), 297–315.
- (29) Davies, S. P.; Reddy, H.; Caivano, M.; Cohen, P. Specificity and mechanism of action of some commonly used protein kinase inhibitors. *Biochem. J.* **2000**, *351* (1), 95–105.
- (30) Maeda, Y.; Nakano, M.; Sato, H.; Miyazaki, Y.; Schweiker, S. L.; Smith, J. L.; Truesdale, A. T. 4-Acylamino-6-arylfuro[2,3-d]-pyrimidines: potent and selective glycogen synthase kinase-3 inhibitors. *Bioorg. Med. Chem. Lett.* **2004**, *14* (15), 3907–3911.
- (31) Tavares, F. X.; Boucheron, J. A.; Dickerson, S. H.; Griffin, R. J.; Preugschat, F.; Thomson, S. A.; Wang, T. Y.; Zhou, H.-Q. N-Phenyl-4-pyrazolo[1,5-b]pyridazin-3-ylpyrimidin-2-amines as potent and selec-

tive inhibitors of glycogen synthase kinase 3 with good cellular efficacy. *J. Med. Chem.* **2004**, *47* (19), 4716–4730.

(32) Wan, Y.; Hur, W.; Cho, C. Y.; Liu, Y.; Adrian, F. J.; Lozach, O.; Bach, S.; Mayer, T.; Fabbro, D.; Meijer, L.; Gray, N. S. Synthesis and target identification of hymenialdisine analogs. *Chem. Biol.* **2004**, *11* (2), 247–259.

(33) Nuss, J. M.; Renhowe, P. A. Advances in solid-supported organic synthesis methods, 1998 to 1999. *Curr. Opin. Drug Discovery Dev.* **1999**, *2* (6), 631–650.

(34) Schultz, P.; Ring, D. B.; Harrison, S. D.; Bray, A. M. Preparation of Purines as Inhibitors of Glycogen Synthase Kinase 3 (GSK3). Patent 97-US19472 19971010, 1998.

(35) Desai, M. C.; Nuss, J. M.; Spear, K. L.; Singh, R.; Renhowe, P. A.; Brown, E. G.; Richter, L.; Scott, B. O. Combinatorial Libraries of Substrate-Bound Cyclic Organic Compounds. U.S. Patent 5,958,792, 1999.

(36) Norman, T. C.; Gray, N. S.; Koh, J. T.; Schultz, P. G. A structure-based library approach to kinase inhibitors. *J. Am. Chem. Soc.* **1996**, *118* (31), 7430–7431.

(37) Nuss, J. M.; Harrison, S. D.; Ring, D. B.; Boyce, R. S.; Brown, S. P.; Goff, D.; Johnson, K.; Pfister, K. B.; Ramurthy, S.; Renhowe, P. A.; Seely, L.; Subramanian, S.; Wagman, A. S.; Zhou, X. A. Inhibitors of Glycogen Synthase Kinase 3. U.S. Patent 6,489,344 B1, 2002.

(38) Atwal, K. S.; Rovnyak, G. C.; Schwartz, J.; Moreland, S.; Hedberg, A.; Gougoutas, J. Z.; Malley, M. F.; Floyd, D. M. Dihydropyrimidine calcium channel blockers: 2-heterosubstituted 4-aryl-1,4-dihydro-6-methyl-5-pyrimidinecarboxylic acid esters as potent mimics of dihydropyridines. *J. Med. Chem.* **1990**, *33* (5), 1510–1515.

(39) Wagman, A. S.; Wang, L.; Nuss, J. M. Simple and efficient synthesis of 3,4-dihydro-2-pyridones via novel solid-supported aza-annulation. *J. Org. Chem.* **2000**, *65* (26), 9103–9113.

(40) Bedford, C. D.; Howd, R. A.; Dailey, O. D.; Miller, A.; Nolen, H. W.; Kenley, R. A.; Kern, J. R.; Winterle, J. S. Nonquaternary cholinesterase reactivators. 3. 3(5)-Substituted 1,2,4-oxadiazol-5(3)-aloximes and 1,2,4-oxadiazole-5(3)-thiocarbohydroximates as reactivators of organophosphonate-inhibited eel and human acetylcholinesterase in vitro. *J. Med. Chem.* **1986**, *29* (11), 2174–2183.

(41) Sakurai, S.; Ogawa, N.; Suzuki, T.; Kato, K.; Ohashi, T.; Yasuda, S.; Kato, H. Synthesis of [[(benzenesulfonamido)alkyl]phenyl]-alkanoic acid derivatives containing pyridyl or imidazolyl groups and their thromboxane A2 receptor antagonistic and thromboxane A2 synthase inhibitory activities. *Chem. Pharm. Bull.* **1996**, *44* (8), 1510–1520.

(42) Bastiaansen, L. A. M.; Macco, A. A.; Godefroi, E. F. 2-(2-Imidazolyl)acetophenones via arylation of N-substituted 2-methyl-imidazoles. *J. Chem. Soc., Chem. Commun.* **1974**, 36.

(43) Macco, A. A.; Godefroi, E. F.; Drouen, J. J. M. 2-(2-Imidazolyl)acetophenones. Preparation and some reactions. *J. Org. Chem.* **1975**, *40* (2), 252–255.

(44) Knölker, H.-J.; Boese, R.; Hitzemann, R. Imidazole derivatives. Part II. Synthesis of imidazo[1,2-a]pyridin-5-ones. *Heterocycles* **1989**, *29* (8), 1551–1558.

(45) Lipshutz, B. H.; Morey, M. C. An approach to the cyclopeptide alkaloids (phencyclopeptides) via heterocyclic diamide/dipeptide equivalents. Preparation and N-alkylation studies of 2,4(5)-disubstituted imidazoles. *J. Org. Chem.* **1983**, *48* (21), 3745–3750.

(46) Groa, M.; McKervey, M. A.; Nieuwenhuyzen, M. Synthesis of amino acid-derived imidazoles from enantiopure N-protected α -amino glyoxals. *Tetrahedron Lett.* **2000**, *41*, 1275–1278.

(47) Palucki, M.; Buchwald, S. L. Palladium-catalyzed α -arylation of ketones. *J. Am. Chem. Soc.* **1997**, *119* (45), 11108–11109.

(48) Galante, R. J. Method of synthesizing sterically hindered 5-substituted-1H-tetrazoles from nitriles using a Lewis acid and an azide. U.S. Patent 5,502,191, 1996.

(49) Stiefl, N.; Gedeck, P.; Chin, D.; Hunt, P.; Lindvall, M.; Spiegel, K.; Springer, C.; Biller, S.; Buenemann, C.; Kanazawa, T.; Kato, M.; Lewis, R.; Martin, E.; Polyakov, V.; Tommasi, R.; van Drie, J.; Vash, B.; Whitehead, L.; Xu, Y.; Abagyan, R.; Rausch, E.; Totrov, M. FOCUS-Development of a global communication and modeling platform for

applied and computational medicinal chemists. *J. Chem. Inf. Model.* **2015**, *55* (4), 896–908.

(50) Gedeck, P.; Lu, Y.; Skolnik, S.; Rodde, S.; Dollinger, G.; Jia, W.; Berellini, G.; Vianello, R.; Faller, B.; Lombardo, F. Benefit of retraining pK_a models studied using internally measured data. *J. Chem. Inf. Model.* **2015**, *55* (7), 1449–1459.

(51) Aoki, M.; Yokota, T.; Sugiura, I.; Sasaki, C.; Hasegawa, T.; Okumura, C.; Ishiguro, K.; Kohno, T.; Sugio, S.; Matsuzaki, T. Structural insight into nucleotide recognition in tau-protein kinase I/ glycogen synthase kinase 3 β . *Acta Crystallogr., Sect. D: Biol. Crystallogr.* **2004**, *60* (3), 439–446.

(52) Kim, K. S.; Tarakeshwar, P.; Lee, J. Y. Molecular clusters of π -systems: Theoretical studies of structures, spectra, and origin of interaction energies. *Chem. Rev.* **2000**, *100* (11), 4145–4186.

(53) McGaughey, G. B.; Gagné, M.; Rappé, A. K. π -Stacking interactions. Alive and well in proteins. *J. Biol. Chem.* **1998**, *273* (25), 15458–15463.

(54) Sinnokrot, M. O.; Sherrill, C. D. Substituent effects in π - π Interactions: Sandwich and T-shaped configurations. *J. Am. Chem. Soc.* **2004**, *126* (24), 7690–7697.

(55) Bullock, A. N.; Russo, S.; Amos, A.; Pagano, N.; Bregman, H.; Debreczeni, J. E.; Lee, W. H.; von Delft, F.; Meggers, E.; Knapp, S. Crystal structure of the PIM2 kinase in complex with an organoruthenium inhibitor. *PLoS One* **2009**, *4* (10), e7112.

(56) Guimarães, C. R. W.; Rai, B. K.; Munchhof, M. J.; Liu, S.; Wang, J.; Bhattacharya, S. K.; Buckbinder, L. Understanding the impact of the P-loop conformation on kinase selectivity. *J. Chem. Inf. Model.* **2011**, *51* (6), 1199–1204.

(57) Müller, S.; Chaikuad, A.; Gray, N. S.; Knapp, S. The ins and outs of selective kinase inhibitor development. *Nat. Chem. Biol.* **2015**, *11* (11), 818–821.

(58) Pettersen, E. F.; Goddard, T. D.; Huang, C. C.; Couch, G. S.; Greenblatt, D. M.; Meng, E. C.; Ferrin, T. E. UCSF Chimera-A visualization system for exploratory research and analysis. *J. Comput. Chem.* **2004**, *25* (13), 1605–1612.

(59) Ring, D. B.; Johnson, K. W.; Henriksen, E. J.; Nuss, J. M.; Goff, D.; Kinnick, T. R.; Ma, S. T.; Reeder, J. W.; Samuels, I.; Slabiak, T.; Wagman, A. S.; Hammond, M.-E. W.; Harrison, S. D. Selective glycogen synthase kinase 3 inhibitors potentiate insulin activation of glucose transport and utilization in vitro and in vivo. *Diabetes* **2003**, *52* (3), 588–595.

(60) Cohen, P.; Goedert, M. GSK3 inhibitors: development and therapeutic potential. *Nat. Rev. Drug Discovery* **2004**, *3* (6), 479–487.

(61) Henriksen, E. J.; Kinnick, T. R.; Teachey, M. K.; O'Keefe, M. P.; Ring, D.; Johnson, K. W.; Harrison, S. D. Modulation of muscle insulin resistance by selective inhibition of GSK-3 in Zucker diabetic fatty rats. *Am. J. Physiol. - Endocrinol. Metab.* **2003**, *284* (5), E892–E900.

(62) Eldar-Finkelman, H.; Krebs, E. G. Phosphorylation of insulin receptor substrate 1 by glycogen synthase kinase 3 impairs insulin action. *Proc. Natl. Acad. Sci. U. S. A.* **1997**, *94* (18), 9660–9664.

(63) Smith, L. K.; Rice, K. M.; Garner, C. W. The insulin-induced down-regulation of IRS-1 in 3T3-L1 adipocytes is mediated by a calcium-dependent thiol protease. *Mol. Cell. Endocrinol.* **1996**, *122* (1), 81–92.

(64) Welsh, G. I.; Wilson, C.; Proud, C. G. GSK3: a SHAGGY frog story. *Trends Cell Biol.* **1996**, *6* (7), 274–279.

(65) Kolterman, O. G.; Insel, J.; Saekow, M.; Olefsky, J. M. Mechanisms of insulin resistance in human obesity: evidence for receptor and postreceptor defects. *J. Clin. Invest.* **1980**, *65* (6), 1272–1284.

(66) Reaven, G. M. Role of insulin resistance in human disease (syndrome X): an expanded definition. *Annu. Rev. Med.* **1993**, *44* (1), 121–131.

(67) Shulman, G. I. Cellular mechanisms of insulin resistance. *J. Clin. Invest.* **2000**, *106* (2), 171–176.

(68) Embi, N.; Rylatt, D. B.; Cohen, P. Glycogen synthase kinase-3 from rabbit skeletal muscle. Separation from cyclic-AMP-dependent protein kinase and phosphorylase kinase. *Eur. J. Biochem.* **1980**, *107* (2), 519–527.

- (69) Fisher, J. S.; Nolte, L. A.; Kawanaka, K.; Han, D.-H.; Jones, T. E.; Holloszy, J. O. Glucose transport rate and glycogen synthase activity both limit skeletal muscle glycogen accumulation. *Am. J. Physiol. Endocrinol. Metab.* **2002**, *282* (6), E1214–E1221.
- (70) Fioderek, F. T. Rodent genetic models for obesity and non-insulin-dependent diabetes mellitus. *Diabetes Mellit.* **1996**, 604–618.
- (71) Ionescu, E.; Sauter, J. F.; Jeanrenaud, B. Abnormal oral glucose tolerance in genetically obese (*fa/fa*) rats. *Am. J. Physiol.* **1985**, *248* (5 Pt 1), E500–E506.
- (72) Terrettaz, J.; Assimacopoulos-Jeannet, F.; Jeanrenaud, B. Severe hepatic and peripheral insulin resistance as evidenced by euglycemic clamps in genetically obese *fa/fa* rats. *Endocrinology* **1986**, *118* (2), 674–678.
- (73) Muñoz, M. C.; Barberà, A.; Domínguez, J.; Fernández-Alvarez, J.; Gomis, R.; Guinovart, J. J. Effects of tungstate, a new potential oral antidiabetic agent, in Zucker diabetic fatty rats. *Diabetes* **2001**, *50* (1), 131–138.
- (74) Sparks, J. D.; Phung, T. L.; Bolognino, M.; Cianci, J.; Khurana, R.; Peterson, R. G.; Sowden, M. P.; Corsetti, J. P.; Sparks, C. E. Lipoprotein alterations in 10- and 20-week-old Zucker diabetic fatty rats: hyperinsulinemic versus insulinopenic hyperglycemia. *Metab. Clin. Exp.* **1998**, *47* (11), 1315–1324.
- (75) Anai, M.; Funaki, M.; Ogihara, T.; Terasaki, J.; Inukai, K.; Katagiri, H.; Fukushima, Y.; Yazaki, Y.; Kikuchi, M.; Oka, Y.; Asano, T. Altered expression levels and impaired steps in the pathway to phosphatidylinositol 3-kinase activation via insulin receptor substrates 1 and 2 in Zucker fatty rats. *Diabetes* **1998**, *47* (1), 13–23.
- (76) Brozinick, J. T.; Misener, E. A.; Ni, B.; Ryder, J. W.; Dohm, G. L. Impaired insulin signaling through GSK3 in insulin resistant skeletal muscle. *Diabetes* **2000**, *49* (5), A326–A326.
- (77) Luo, J.; Quan, J.; Tsai, J.; Hobensack, C. K.; Sullivan, C.; Hector, R.; Reaven, G. M. Nongenetic mouse models of non-insulin-dependent diabetes mellitus. *Metab. Clin. Exp.* **1998**, *47* (6), 663–668.
- (78) Cline, G. W.; Johnson, K.; Regittnig, W.; Perret, P.; Tozzo, E.; Xiao, L.; Damico, C.; Shulman, G. I. Effects of a novel glycogen synthase kinase-3 inhibitor on insulin-stimulated glucose metabolism in Zucker diabetic fatty (*fa/fa*) rats. *Diabetes* **2002**, *51* (10), 2903–2910.
- (79) Ali, A.; Hoefflich, K. P.; Woodgett, J. R. Glycogen synthase kinase-3: Properties, functions, and regulation. *Chem. Rev.* **2001**, *101* (8), 2527–2540.
- (80) Polakis, P. Wnt signaling in cancer. *Cold Spring Harbor Perspect. Biol.* **2012**, *4* (5), a008052–a008052.
- (81) Polakis, P. The many ways of Wnt in cancer. *Curr. Opin. Genet. Dev.* **2007**, *17* (1), 45–51.
- (82) Polakis, P. Wnt signaling and cancer. *Genes Dev.* **2000**, *14* (15), 1837–1851.
- (83) Harada, N.; Tamai, Y.; Ishikawa, T.; Sauer, B.; Takaku, K.; Oshima, M.; Taketo, M. M. Intestinal polyposis in mice with a dominant stable mutation of the beta-catenin gene. *EMBO J.* **1999**, *18* (21), 5931–5942.
- (84) Coghlan, M. P.; Culbert, A. A.; Cross, D. A.; Corcoran, S. L.; Yates, J. W.; Pearce, N. J.; Rausch, O. L.; Murphy, G. J.; Carter, P. S.; Roxbee Cox, L.; Mills, D.; Brown, M. J.; Haigh, D.; Ward, R. W.; Smith, D. G.; Murray, K. J.; Reith, A. D.; Holder, J. C. Selective small molecule inhibitors of glycogen synthase kinase-3 modulate glycogen metabolism and gene transcription. *Chem. Biol.* **2000**, *7* (10), 793–803.
- (85) Cohen, Y.; Chetrit, A.; Cohen, Y.; Sirota, P.; Modan, B. Cancer morbidity in psychiatric patients: influence of lithium carbonate treatment. *Med. Oncol. Tumor Pharmacother.* **1998**, *15* (1), 32–36.
- (86) Kratz, J. E.; Stearns, D.; Huso, D. L.; Slunt, H. H.; Price, D. L.; Borchelt, D. R.; Eberhart, C. G. Expression of stabilized β -catenin in differentiated neurons of transgenic mice does not result in tumor formation. *BMC Cancer* **2002**, *2* (1), 33.
- (87) Johnson, C. D.; Puntis, M.; Davidson, N.; Todd, S.; Bryce, R. Randomized, dose-finding phase III study of lithium gamolenate in patients with advanced pancreatic adenocarcinoma. *Br. J. Surg.* **2001**, *88* (5), 662–668.
- (88) Gould, T. D.; Gray, N. A.; Manji, H. K. Effects of a glycogen synthase kinase-3 inhibitor, lithium, in adenomatous polyposis coli mutant mice. *Pharmacol. Res.* **2003**, *48* (1), 49–53.
- (89) Cross, D. A.; Culbert, A. A.; Chalmers, K. A.; Facci, L.; Skaper, S. D.; Reith, A. D. Selective small-molecule inhibitors of glycogen synthase kinase-3 activity protect primary neurones from death. *J. Neurochem.* **2001**, *77* (1), 94–102.
- (90) Harada, N.; Miyoshi, H.; Murai, N.; Oshima, H.; Tamai, Y.; Oshima, M.; Taketo, M. M. Lack of tumorigenesis in the mouse liver after adenovirus-mediated expression of a dominant stable mutant of beta-catenin. *Cancer Res.* **2002**, *62* (7), 1971–1977.
- (91) Zhang, Y.; Welzig, C. M.; Picard, K. L.; Du, C.; Wang, B.; Pan, J. Q.; Kyriakis, J. M.; Aronovitz, M. J.; Claycomb, W. C.; Blanton, R. M.; Park, H.-J.; Galper, J. B. Glycogen synthase kinase-3 inhibition ameliorates cardiac parasympathetic dysfunction in type 1 diabetic Akita mice. *Diabetes* **2014**, *63* (6), 2097–2113.
- (92) Weikel, K. A.; Cacicedo, J. M.; Ruderman, N. B.; Ido, Y. Knockdown of GSK3 increases basal autophagy and AMPK signalling in nutrient-laden human aortic endothelial cells. *Biosci. Rep.* **2016**, *36* (5), e00382–e00382.
- (93) Marchand, B.; Tremblay, I.; Cagnol, S.; Boucher, M.-J. Inhibition of glycogen synthase kinase-3 activity triggers an apoptotic response in pancreatic cancer cells through JNK-dependent mechanisms. *Carcinogenesis* **2012**, *33* (3), 529–537.
- (94) Bock, A. S.; Leigh, N. D.; Bryda, E. C. Effect of Gsk3 inhibitor CHIR99021 on aneuploidy levels in rat embryonic stem cells. *In Vitro Cell. Dev. Biol.: Anim.* **2014**, *50* (6), 572–579.
- (95) Buikema, J. W.; Zwetsloot, P.-P. M.; Doevendans, P. A.; Sluijter, J. P. G.; Domian, I. J. Expanding Mouse Ventricular Cardiomyocytes Through GSK-3 Inhibition. In *Current Protocols in Cell Biology*; John Wiley & Sons, Inc.: Hoboken, NJ, 2013; Vol. 61, pp 23.9.1–23.9.10.
- (96) Carter, T.; Vancurová, I.; Sun, I.; Lou, W.; DeLeon, S. A DNA-Activated Protein Kinase from HeLa Cell Nuclei. *Mol. Cell. Biol.* **1990**, *10* (12), 6460–6471.
- (97) Rubinfeld, B.; Munemitsu, S.; Clark, R.; Conroy, L.; Watt, K.; Crosier, W. J.; McCormick, F.; Polakis, P. Molecular cloning of a GTPase activating protein specific for the Krev-1 protein p21rap1. *Cell* **1991**, *65* (6), 1033–1042.
- (98) Klein, H. H.; Kowalewski, B.; Drenckhan, M.; Neugebauer, S.; Matthaei, S.; Kotzke, G. A Microtiter well assay system to measure insulin activation of insulin receptor kinase in intact human mononuclear cells. Decreased insulin effect in cells from patients with NIDDM. *Diabetes* **1993**, *42* (6), 883–890.
- (99) Osterop, A. P.; Medema, R. H.; Bos, J. L.; vd Zon, G. C.; Müller, D. E.; Flier, J. S.; Möller, W.; Maassen, J. A. Relation between the insulin receptor number in cells, autophosphorylation and insulin-stimulated Ras.GTP formation. *J. Biol. Chem.* **1992**, *267* (21), 14647–14653.
- (100) Thomas, J. A.; Schlender, K. K.; Larner, J. A Rapid filter paper assay for UDPglucose-glycogen glucosyltransferase, including an improved biosynthesis of UDP-14C-glucose. *Anal. Biochem.* **1968**, *25* (1), 486–499.
- (101) Henriksen, E. J.; Halseth, A. E. Early alterations in soleus GLUT-4, glucose transport, and glycogen in voluntary running rats. *J. Appl. Physiol.* **1994**, *76* (5), 1862–1867.
- (102) Emsley, P.; Lohkamp, B.; Scott, W. G.; Cowtan, K. Features and development of Coot. *Acta Crystallogr., Sect. D: Biol. Crystallogr.* **2010**, *66* (4), 486–501.
- (103) Bricogne, G.; Blanc, E.; Brandl, M.; Flensburg, C.; Keller, P.; Paciorek, W.; Roversi, P.; Sharff, A.; Smart, O. S.; Vonnrhein, C.; Womack, T. O. *BUSTER*; Global Phasing Ltd: Cambridge, UK, 2016.
- (104) Adams, P. D.; Afonine, P. V.; Bunkóczi, G.; Chen, V. B.; Davis, I. W.; Echols, N.; Headd, J. J.; Hung, L.-W.; Kapral, G. J.; Grosse-Kunstleve, R. W.; McCoy, A. J.; Moriarty, N. W.; Oeffner, R.; Read, R. J.; Richardson, D. C.; Richardson, J. S.; Terwilliger, T. C.; Zwart, P. H. PHENIX: A comprehensive Python-based system for macromolecular structure solution. *Acta Crystallogr., Sect. D: Biol. Crystallogr.* **2010**, *66* (2), 213–221.